Concepts and Science for Coastal Erosion Management

CONSCIENCE

Specific Targeted Research Project

Thematic priority: Forecasting and developing innovative policies for sustainability in the medium and long term

Modelling of sandy beach and dune erosion

Date **March 2010**

Deliverable number **D 13c**
Revision status final

Task Leader Leo van Rijn

CONSCIENCE is co-funded by the European Community Sixth Framework Programme for European Research and Technological Development (2002-2006) Start date March 2007, duration 3 Years		
Document Dissemination Level		
PU	Public	**PU**
PP	Restricted to other programme participants (including the Commission Services)	
RE	Restricted to a group specified by the consortium (including the Commission Services)	
CO	Confidential, only for members of the consortium (including the Commission Services)	

Co-ordinator: Deltares, the Netherlands
Project Contract No: 044122
Project website: www.conscience-eu.net

Modelling of sandy beach and dune erosion

Deliverable:	D13c
Project:	Concepts and Science for Coastal Erosion Management
EC Contract:	044122

Document Information

Title:	Modelling of sandy beach and dune erosion
Lead Author:	Leo C. van Rijn
Client:	European Commission
Contract No.:	044122
Reference:	Deliverable D13c

Document History

Date	Version	Author	Reviewed by	Notes
31-03-2010	2.0	Leo van Rijn		
01-01-2008	1.0	Leo van Rijn		

Acknowledgements
The work described in this report was supported by the Commission of the European Communities under Contract number 044122, Concepts and Science for Coastal Erosion, Conscience.

Contents

1 Introduction

Beach and dune erosion and associated mitigation measures are the most classical coastal engineering problems that are existing and have been studied extensively by many researchers (**Dean 1973, Vellinga 1986, Kriebel et al. 1991, Dette and Ulicska 1987, Kraus et al. 1991, Steetzel, 1993, Larson et al., 2004**).

Field experience over a long period of time in the coastal zone has led to the notion that storm waves cause sediment to move offshore while fair-weather waves and swell return the sediment shoreward. During high-energy conditions with breaking waves (storm cycles), the mean water level rises due to tide-induced forces, wind- and wave-induced setup and the beach and dune zone of the coast are heavily attacked by the incoming waves, usually resulting in erosion processes. When storm waves arrive at the beach, the crests break frequently, resulting in large volumes of water running up the beach face (see **Figure 1.1**). Sand is dragged down the slope by the downrush causing erosion of the beach and dune faces and undermining of the dune toe. Part of the dune face may collapse when the the local dune slope angle is larger than the equilibrium slope and lumps of sediment slide downwards (see **Figure 1.3**) where it can be eroded again by wave-induced processes. The mass of sediment-laden water returning to the sea will drop its load at deeper water to form a bar. The sediments are carried in seaward direction by wave-induced near-bed return currents (undertow) and in longshore direction by wave-, wind- and tide-induced currents, which may feed locally generated rip currents. The undertow currents bring the sediments to the nearshore breaker bar systems, whereas the rip currents carry the sediments over longer distances to the edge of the surf zone. Three-dimensional flow patterns are dominant in the inner surf zone, whereas vertical circulations are dominant in the outer surf zone. These processes proceed relatively fast, as indicated by relatively large short-term variations (on the scale of events) of shoreline recession, formation of breaker bars and rip channels. During conditions with low non-breaking waves, onshore-directed transport processes related to wave-asymmetry and wave-induced streaming are dominant, usually resulting in accretion processes in the beach zone. A characteristic feature in the swash zone during low-energy conditions is the zig-zag movement of the sediment particles which is also known as beach drifting. In case of oblique wave incidence, the swash will run up the beach in the direction of wave propagation, but the backwash will move down the steepest slope under the influence of gravity. This latter movement usually is at right angle to the shore. Sediment particles being moved by the swash and backwash will follow a zig-zag pattern along the shore parallel to the front of the breaking waves. The water carried in the uprush percolates partly through the sediment surface down to the water table at about mean sea level. This percolation reduces the volume of downwash, so causing the sand carried up to be deposited partly on the beach face. This build-up of the beach continues during low-energy conditions.

Herein, the attention is focussed on dune erosion processes during major storm events with relatively high surge levels. Observations during recent dune erosion experiments in the large-scale Deltaflume of **Delft Hydraulics** show the dominance of four processes (see also **Figure 1.1**):

1) strong wave impact forces at the steep dune face generating relatively strong bed-shear stresses and hence erosion of sediment,
2) large-scale turbulence due to the impact (wave collision) of incoming breaking waves and reflected broken waves generating fountains of water (see **Figure 1.2**) and sediment resulting in a significant increase of the sediment carrying capacity of the offshore-directed return flows in the surf zone in front the dune,
3) the generation of low frequency waves in the surf zone (surf beat) due to spatial and temporal variation of the breaking point of the irregular high-frequency waves resulting in a spatial and temporal variation of the the wave-induced set-up and
4) the regular sliding of the dune face when its has become too steep and the formation of a small bar at the dune face toe (see **Figure 1.3**).

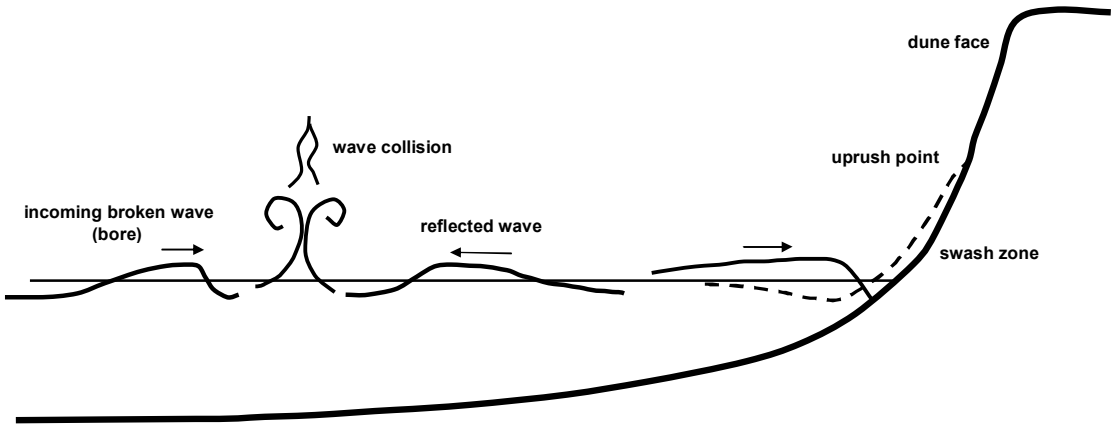

Figure 1.1 *Wave processes in shallow surf zone in front of dune*

Figure 1.2 *Impact of incoming and outgoing (reflected) waves in Deltaflume*

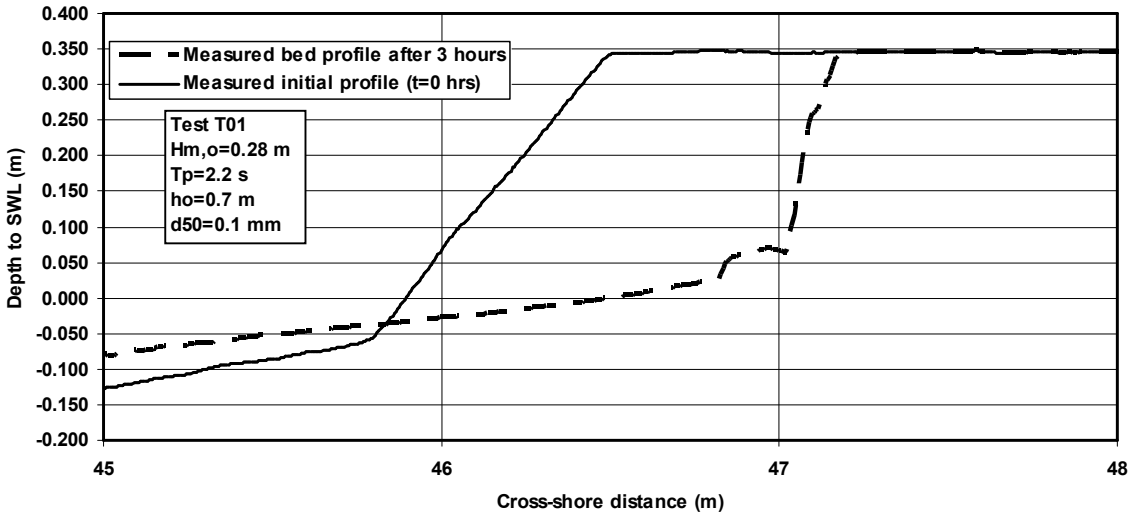

Figure 1.3 *Bed profile after 3 hours in small-scale flume; dune slumping in front of dune*

An overview of existing empirical models to estimate dune erosion is given by **Larson et al. (2004)** and will not be repeated herein. A semi-empirical model (S-beach) has been proposed by **Larson and Kraus (1989)**. This model is based on equilibrium theory with limited description of the physical processes. A beach profile is assumed to attain an equilibrium shape if exposed to constant wave conditions for a sufficiently long time. An equilibrium profile ($h=Ax^{2/3}$ with x=cross-shore coordinate and A=shape paramer depending on bed material diameter) dissipates incident wave energy without significant net change in shape. The transport rate is related to the difference between the actual wave energy dissipation and the equilibrium wave energy dissipation along the equilibrium profile. The transport direction is determined from an empirical criterion. **Steetzel (1993)** has proposed a process-based mathematical model based on cross-shore wave propagation, wave shoaling, wave refraction and wave breaking. The output of the wave model is used to compute the local cross-shore sand transport rate. Bed level changes are determined from cross-shore gradients of the transport rate in a numerical loop system. A crucial process is the erosion of sand in the dune face zone, which is done by the use of a function which relates the relative magnitude of the transport rate in this zone to its position and level with respect to the last grid point of the wave model. Low-frequency effects (surf beat), the production of extra turbulence due to collapsing and colliding waves as well as dune face sliding are not taken into account explicitly. The model of **Steetzel (1993)** has been calibrated using measured data from experiments in the large-scale Deltaflume of Delft Hydraulics. Varies field cases have been used to demonstrate the validity of the model.

This study by **Prof. Dr. L.C. van Rijn** of **Delft Hydraulics** focuses on three topics:

- analysis of scaling laws for dune erosion and re-analysis of earlier model experiments (**Chapter 2**);
- development of simple engineering dune erosion rule (**Chapters 2 and 5**);
- mathematical modelling of dune erosion processes using process-based cross-shore profile model (**CROSMOR**- model), (**Chapters 3 and 4**);

2 Scaling laws for beach and dune erosion

2.1 Definitions

Physical scale models of sandy (quartz) materials have been used frequently to study coastal engineering problems. Scaling laws for coastal movable bed models of are welll established (**Le Méhauté, 1970**; **Noda, 1972; Kamphuis, 1972, 1982; Hughes, 1993**), but the errors due to scale effects are less well understood.

The basic philosophy for movable-bed models can be formulated as ensuring that the relative magnitudes of all dominant processes are the same in model and prototype. Preferably, the scale model should be validated using field (prototype) data, but often this is not feasible and large-scale model results are used as prototype data. For coastal scale models the most relevant requirement is to attain similarity of the cross-shore equilibrium bed profiles between prototype and model, particularly in the surf zone (**Hughes and Fowler, 1990**). This means that the dimensionless parameters describing equilibrium profile behaviour should be the same in model and prototype. The most dominant mode of transport being either bed load or suspended load (depending on wave conditions and bed material) should be represented correctly. Both undistorted models and distorted models have been used in scale modelling. Ensuring similarity in a undistorted model is less complicated than in a distorted model. **Dean (1985)** reasoned that, in an undistorted model with a sand bed, the fall trajectory of a suspended particle must be geometrically similar to the equivalent prototype trajectory and fall with a time proportional to the prototype fall time. This can be accomplished by ensuring similarity of the fall velocity parameter between the prototype and the model, which is only feasible in an undistorted model. Distorted models can be used when the reproduction of the bulk erosion volume (dune erosion volume; **Vellinga, 1986**) is most important, while the precise reproduction of the equilibrium profile in the entire surf zone is less important.

In physical scale modelling the basic parameters (wave height, length, orbital velocity, etc.) are generally much smaller than the corresponding values in nature. The ratio of the value in nature (prototype) and in the laboratory model is generally expressed by the scale parameter $n=p_p/p_m$ with p_p=parameter value in prototype and p_m=parameter value in laboratory model. Thus, $n>1$.

Correct representation of the physical processes in nature requires that the dimensionless numbers (Froude number, Reynolds number, etc.) characterizing these processes are the same in nature and in the laboratory model. Examples of these numbers are: the Froude number (subcritical or supercritical flow), the Reynolds' number (laminar of turbulent flow), the surf similarity parameter (type of breaking), the Suspension parameter (bed load or suspended load transport), the Shields parameter (intensity of sediment transport and type of bed forms). Often, it is sufficient for correct scale modelling that these dimensionless numbers are in a certain range rather than imposing a fixed value. For example, it is often sufficient that the flow is turbulent in the laboratory model which is satisfied if the Reynolds' number is larger than about 1000.

Scaling problems
The design of movable-bed scale models involve various problems related to the selection of the appropriate scales, as follows:

- the scale model depth should not be so small that the flow (unidirectional and/or oscillatory) is no longer in the fully turbulent regime or that surface tension effects become dominant;
- the scale model shear stress should be sufficiently large that it is significantly beyond the critical bed-shear stress for initiation of motion; this requirement often implies a scale distortion in bed roughnes (ripples in model; sheet flow in prototype);
- the scale model sediment should not be small that cohesive properties become important;
- the scale model distortions should not be so large that the type of sediment transport (either dominant bed load or suspended load) in the spatial domain of interest (either offshore or inshore) is incorrect; as scale distortion is controversial (contradictory views) it should be kept to a minimum value.

The physical processes dominating beach and dune erosion are: wave breaking and wave-driven flows (undertow), generation of surf beat (long waves), sediment suspension, dune face slumping, etc.

2.2 Wave dynamics

Correct representation of the wave dynamics requires (see **Vellinga, 1986**):

$$n_u=n_T=(n_L)^{0.5}=(n_H)^{0.5}=(n_h)^{0.5} \qquad (2.1)$$

with: u=orbital velocity, T= wave priod, H=wave height, L=wave length, h=water depth.
Generally, **Equation (2.1)** is known as Froude scaling.

2.3 Wave breaking

The type of wave breaking is generally characterized by the surf similarity parameter, expressed as: $\xi=\tan(\beta)/(H/L)^{0.5}$, with tan(β)=local bed slope(=Δh/Δl). Spilling breaking occurs for $\xi<0.4$, plunging waves for $0.4<\xi<2.3$ and surging waves for >2.3
Correct representation of wave breaking requires: $n_\xi=1$ or $n_h/n_l=(n_H/n_L)^{0.5}$

Using: $n_H=n_h$ and $n_L=(n_T)^2$ from **Equation (2.1)** it follows that: $n_T=(n_h)^{0.5}(n_l/n_h)$ (2.2)

Equation (2.2) is known as the distorted Froude scaling. The ratio n_l/n_h expresses the distortion scale. Generally, it is required that $n_l>n_h$ to fit the relatively long cross-shore profile in the laboratory model. **Equation (2.2)** shows that correct representation of the wave dynamics including wave breaking can only be represented in a non-distorted model ($n_l=n_h$). In a distorted model ($n_l/n_h>1$) with a steeper bed slope, the waves should be shorter (at the same wave height) to obtain the same surf similarity parameter. In practice this latter parameter is not so important as long as the waves are breaking and are in a certain breaking range (either spilling or plunging). More intense spilling of more intense plunging is not so important. Hence, in most

cases the waves are scaled using the Froude scaling (Equation (2.1)) rather than the distorted Froude scaling (Eqaution (2.2)).

2.4 Undertow

The erosion processes at the beach during wave attack are mainly governed by the transport capacity of the undertow (wave-driven flow). Correct representation of the undertow velocity requires that: $n_{ur}/n_{cw}=1$, with u_r=undertow velocity and c_w=wave celerity. Based on linear wave theory in shallow water (mass flux theory), the undertow is proportional to: $u_r \approx gH^2/(c_w h)$. Thus, $u_r/c_w \approx gH^2/(c_w^2 h)$.

From $n_{ur}/n_{cw}=1$, it follows that: $(n_T)^2(n_H)^2=n_h(n_L)^2$, which results in: $n_T=(n_h)^{0.5}$ (2.3)

Equation (2.3) is similar to **Equation (2.1)**; Froude scaling.

2.5 Wave runup along dune face

The wave runup along the dune face can be represented by:

$$RU=\alpha\, g^{0.5}\, T\, H^{0.5} \tan(\beta) \tag{2.4}$$

with: RU=wave runup (vertical level above still water level) exceeded by 2% of the waves, α=coefficient ($\cong$0.7), tan(β)=local bed slope.
This yields:

$$n_{RU}=n_T\,(n_H)^{0.5}\,(n_h/n_l)=n_h\,(n_h/n_l) \tag{2.5a}$$

The wave runup scale is only equal to the vertical depth scale in the case of a non-distorted model ($n_l/n_h=1$).
When a distorted model (with $n_l>n_h$) is used, the runup scale will be overestimated in the model, which may result in overestimation of the erosion. Assuming that $n_l/n_h=(n_h)^{0.28}$ (see **Equation 2.14h**), it follows that:

$$n_{RU}=(n_h)^{0.72} \tag{2.5b}$$

This means that the runup scale will a factor $(n_h)^{0.28}$ too large in a distorted model based on $n_l/n_h=(n_h)^{0.28}$. For example, $n_h=6$ and $n_l/n_h=(6)^{0.28}=1.65$, then $n_{RU}=(6)^{0.72}=3.6$. Ideally, the runup scale should actually be equal to 6. The runup scale is thus a factor 6/3.6= 1.65 ($=6^{0.28}$) too large in a distorted model.

2.6 Suspension parameter

Dune and beach erosion in breaking wave conditions (surf zone) over a sandy bed is largely controlled by suspension processes, characterized by the dimensionless number $H/(w_sT)$, which should be the same in nature in the model. The dimensionless fall velocity parameter $H/(w_sT)$ was popularized by **Dean (1973, 1985).** This parameter represents the time taken by a sediment particle to travel a vertical distance equal to the wave height. Suspended load dominates for $H/(w_sT)<<1$. Similar results have been obtained by **Le Méhauté (1970)** based on the similarity of ratio U/w_s with U=horizontal peak obrital velocity and w_s= fall velocity.

Thus: $n_H=n_{ws}\, n_T$ or $n_T=n_h/n_{ws}$. (2.6)

Combining **Equations (2.6)** and **(2.2)**, yields:

$$n_l/n_h=(n_h)^{0.5}/n_{ws} \quad (2.7a)$$

or,

$$n_{ws}=(n_h)^{0.5}\,(n_l/n_h)^{-1} \quad (2.7b)$$

Using $n_{ws}=n_{d50}$ for sediments of 0.1 to 0.5 mm, it follows that: $n_{d50}=(n_h)^{0.5}\,(n_l/n_h)^{-1}$ (2.7c)

Equation (2.7a) gives a scale relationships for distorted models. The value of n_l can be found after selecting n_h and n_{ws}.

By using **Equation (2.7a,b,c)** the modelling of wave breaking and suspension processes is fairly correct, but no information is available on the morfological time scale involved. This latter parameter can only be determined by considering the transport rates at the toe of the beach and or dune in comparison to the amount of sediment eroded from the beach and/or dune face.

Similarity of sedimentation processes in quiescent areas (trough zone landward of the bar crest) can be obtained by assuming that the horizontal suspended transport gradient is approximately equal to the vertical deposition flux at the bed:

$$d(h\,u\,c)/dx=w_s\,c \quad (2.7d)$$

Equation (2.7d) applies to both the prototype and the scale model. Similarity is preserved, if:

$$n_{ws}=n_u\,(n_l/n_h)^{-1}=(n_h)^{0.5}\,(n_l/n_h)^{-1} \quad (2.7e)$$

Equation (2.7e) is the same as Equation (2.7b).

2.7 Mobility parameter

Correct representation of the bed forms and bed-load transport in nature and model requires that the sediment mobility parameter $f(U_{max})^2/[(s-1)gd_{50}]$ is equal in both cases (f=friction factor). Thus:

$$n_{mob}=1 \text{ or } (n_u)^2=n_{s-1}\,n_{d50}\,(n_f)^{-1} \quad (2.8a)$$

Based on linear wave theory: $U_{max}=\pi HT^{-1}\sinh(kh)$ with $k=2\pi/L$. In shallow water: $\sinh(kh)=kh$. Thus:

$$U_{max}=2\pi^2 HhT^{-1}L^{-1} \quad (2.8b)$$

Using $n_H=n_L=n_h$ and Eq.(2.2): $n_T=(n_h)^{0.5}(n_l/n_h)$, it follows that: $n_U=(n_h)^{0.5}(n_l/n_h)$ (2.8c)

Combining **Equations (2.8a)** and **(2.8c)**, yields: $(n_u)^2=n_h\,(n_l/n_h)^2\,n_{d50}\,(n_f)^{-1}$ or,

$$n_{d50}= n_h\ n_f\,(n_{s-1})^{-1}\,(n_l/n_h)^{-2} \tag{2.8d}$$

Using sand in a non-distorted model, if follows that:

$$n_{d50}= n_h\ n_f \tag{2.8e}$$

The friction factor scale generally is much smaller than 1 ($n_f<<1$) for storm conditions (flat bed in prototype and ripples in model; $f_p\cong0.01$ and $f_m\cong0.05$ or $n_f\cong0.2$). This behaviour is favourable for modelling purposes as it leads to less fine model sediment. For example: $n_h=25$, $n_f=0.2$ and thus $n_{d50}=5$. Preferably, regular waves should not be used in a scale model because the ripples may induce offshore-directed sand transport against the wave direction (in case of non-breaking waves).

As regards fully developed sand transport, it essential that the dimensionless excess shear stress or excess velocity (U_{max}-U_{cr}) is reproduced correctly (U_{cr}=critical orbital velocity for initiation of motion). This requires that the $f(U_{max}-U_{cr})^2/[(s-1)gd_{50}]$ is equal in both model and prototype or:

$$(n_{u-ucr})^2=n_{s-1}\ n_{d50}\ (n_f)^{-1} \tag{2.8f}$$

Scale effects will be relatively small as long as $U>>U_{cr}$ in the scale model and relatively large for $U\cong U_{cr}$ or $U<U_{cr}$ in the scale model. In the latter case no sediment motion will occur in the model. This may occur when relatively coarse sand is used in the scale model. These scale errors generally are largest outside the surf zone (offshore slope of outer bar). Scale conditions close to initiation of motion should be avoided as much as possible.

The mobility parameter is most important in shoaling waves with dominant sand transport close to the bed. This parameter is less important in the surf zone with strongly breaking waves.

2.8 Suspended transport at toe of beach or dune and morphological time scale

The suspended transport rate in the surf zone is given by: $q_s=huc$ with q_s=transport rate in m^2/s, h= water depth, u=undertow velocity and c=concentration. It is assumed that the concentration is fairly constant over the depth in the inner surf and swash zone.

The suspended sediment concentration just above the near-bed zone is assumed to be proportional to:

$$c \approx \frac{(U)^a\,(SL)^b}{(T)^c\,(d_{50})^d\,(s-1)^e} \tag{2.9a}$$

with: U= peak orbital velocity, SL=bed slope, T= wave period, d_{50}=median sediment size of bed material, s=relative density ($=\rho_s/\rho_w$).
From basic sediment research in laboratory flumes it is known that approximately (**Van Rijn, 1993, 2006**):

$$c \approx U^3,\ c \approx 1/(T)^{1\ to\ 2},\ c \approx 1/(d_{50})^{1\ to\ 2} \text{ and } c \approx 1/(s\text{-}1).$$

The effects of bed slope on the depth-averaged concentration is less well known, but it is herein assumed that c increases (in some way; b=0.5 to 2) with increasing bed slope ($c \approx SL^{0.5\ to\ 2}$). Thus, a= 2 to 3, b=0.5 to 2, c=1 to 2, d=1 to 2 and e=1.

Using $n_U=(n_h)^{0.5}$, $n_T=(n_h)^{0.5}$ and $n_{SL}=n_h/n_l$, the suspended sand concentration scale n_c can be represented as:

$$n_c=(n_h)^{0.5a-0.5c}\,(n_{d50})^{-d}\,(n_{s-1})^{-e}\,(n_l/n_h)^{-b} \tag{2.9b}$$

The suspended transport scale ($n_{qs}=n_h n_u n_c$) can be represented as:

$$n_{qs}=(n_h)^{1.5+0.5a-0.5c}\,(n_{d50})^{-d}\,(n_{s-1})^{-e}\,(n_l/n_h)^{-b} \tag{2.9c}$$

The transport rate at the seward toe of the beach or dune is also equal to:

$$q_s=A_e/T_m \tag{2.10}$$

with: A_e= erosion area and T_m=time scale to erode the beach or dune face.

The scale relationship related to **Equation (2.10)** is:

$$n_{qs}=(n_h)(n_l)/n_{Tm}=(n_l/n_h)(n_h)^2/(n_{Tm}) \tag{2.11}$$

From **Equations (2.11)** and **(2.9c)**, it follows that:

$$n_{Tm}=(n_l/n_h)^{b+1}\,(n_{d50})^{d}\,(n_{s-1})^{e}\,(n_h)^{0.5-0.5a+0.5c} \tag{2.12a}$$

The morfological time scale can be expressed as: $n_{Tm}=n_h^{\alpha}$ (2.12b)

Using α=0.5, the morfological time scale is equal to wave period time scale :$n_{Tm}=n_T=n_h^{0.5}$ (2.12c)

2.9 Proposed scaling laws for suspension-dominated surf zone

Using **Equations (2.12c)** and **(2.12a)**, it follows that:

$$(n_l/n_h)^{b+1}=(n_{d50})^{-d}\,(n_{s-1})^{-e}(n_h)^{\alpha-0.5+0.5a-0.5c} \tag{2.13}$$

Equation (2.13) can be used to determine the distortion model scale.

Using α=0.5, a=3, b=1, c=1, d=2, e=1, yields: $(n_l/n_h)=(n_{d50})^{-1}\,(n_{s-1})^{-0.5}(n_h)^{0.5}$ (2.14a)
Using α=0.5, a=2, b=1, c=1, d=2, e=1, yields: $(n_l/n_h)=(n_{d50})^{-1}\,(n_{s-1})^{-0.5}(n_h)^{0.25}$ (2.14b)
Using α=0.5, a=3, b=1, c=2, d=2, e=1, yields: $(n_l/n_h)=(n_{d50})^{-1}\,(n_{s-1})^{-0.5}(n_h)^{0.25}$ (2.14c)

Using α=0.56, a=2, b=1, c=1, d=2, e=1, yields: $(n_l/n_h)=(n_{d50})^{-1}\,(n_{s-1})^{-0.5}(n_h)^{0.28}$ (2.14d)
Using α=0.6, a=2, b=1, c=1, d=2, e=1, yields: $(n_l/n_h)=(n_{d50})^{-1}\,(n_{s-1})^{-0.5}(n_h)^{0.3}$ (2.14e)
Using α=1.0, a=2, b=1, c=1, d=2, e=1, yields: $(n_l/n_h)=(n_{d50})^{-1}\,(n_{s-1})^{-0.5}(n_h)^{0.5}$ (2.14f)

Using α=0.5, a=2, b=1, c=1, d=1, e=1, yields: $(n_l/n_h)=(n_{d50})^{-0.5}\,(n_{s-1})^{-0.5}(n_h)^{0.25}$ (2.14g)
Using α=0.56, a=2, b=1, c=1, d=1, e=1, yields: $(n_l/n_h)=(n_{d50})^{-0.5}\,(n_{s-1})^{-0.5}(n_h)^{0.28}$ (2.14h)
Using α=0.6, a=2, b=1, c=1, d=1, e=1, yields: $(n_l/n_h)=(n_{d50})^{-0.5}\,(n_{s-1})^{-0.5}(n_h)^{0.30}$ (2.14i)

Summarizing, if α is in the range 0.5 to 1.0, it follows that:

$$(n_l/n_h)=(n_{d50})^{-0.5\text{ to }-1}\,(n_{s-1})^{-0.5}(n_h)^{0.25\text{ to }0.50} \quad (2.14j)$$

Equation (2.9a) can also be formulated in terms of the fall velocity of the sediments (w_s) in stead of the median sediment diameter (d_{50}). Using $w_s \approx d_{50}$ for fine sand and α=0.5 to 1.0, this yields:

$$(n_l/n_h)=(n_{ws})^{-0.5\text{ to }-1}\,(n_{s-1})^{-0.5}(n_h)^{0.25\text{ to }0.50} \quad (2.14k)$$

Using sand with density of 2650 kg/m^3, it follows that: n_{s-1}=1. If the same sand is used in model and prototype (or n_{d50}=1), it follows that:

$$(n_l/n_h)=(n_h)^{0.25\text{ to }0.50} \quad (2.14l)$$

Based on analysis of many scale model results on dune erosion (sand with n_{d50}=1; same sand in model and prototype), **Van de Graaff (1977)** has proposed:

$$(n_l/n_h)=(n_h)^{0.28} \quad (2.14m)$$

Equation (2.14j) is very close to **Equation (2.14d)**.

The concentration scale is proposed to be based on **Eq.(2.9a)** : $n_c=(n_h)^{0.5}\,(n_{d50})^{-1\text{ to }2}\,(n_{s-1})^{-1}\,(n_l/n_h)^{-1}$ (2.15)

Based on analysis of the dune erosion tests of **Vellinga (1986)**, the best overall results are obtained by using **Equation (2.14h)**, see **Section 2.10**.

2.10 Analysis of scale model results and errors for dune erosion

Experimental data of scale tests on dune erosion has been collected by **Vellinga (1986)** and **Delft Hydraulics (2004, 2006a,b)**. The basic experimental data are given in **Tables 2.2** and **2.3**. The experimental data typically represent beach and dune erosion conditions along the Dutch North Sea coast during a very severe storm (design storm), which is herein defined as the Reference Case, see **Table 2.1**. The

median sediment diameter along the Dutch coast is assumed to be 225 μm. The high storm surge level (SSL) of 5 m above MSL is assumed to be constant over a duration of 5 hours during the peak of the storm. This equivalent duration of 5 hours yields approximately the same overall dune erosion volume as a complete storm cycle with growing and waning phases (**Vellinga, 1986**). The offshore significant wave height is assumed to have a constant value of $H_{s,o}$= 7.6 m and the peak wave period is T_p=12 s.

Using a depth scale of n_h=5, the offshore wave height in the Deltaflume is about 1.5 m. The measured offshore wave height during the large-scale tests in the Deltaflume of **Vellinga (1986)** appeared to be somewhat larger (1.8 m) than originally intended (1.5 m), see page 103 and 133 of **Steetzel (1993)**. Given the depth scale of n_h=5, this results in a deep water wave height of $H_{s,o}$=9 m. This latter value was used in later tests.

Parameter	**Prototype conditions used by Vellinga (1986)**	**Prototype conditions used by Delft Hydraulics (2004, 2006a,b)**
Offshore wave height (m)	7.6 (Pierson and Moskowitz spectrum)	9.0 (Pierson and Moskowitz spectrum)
Offshore wave period (s)	12	12, 15, 18
Offshore water depth (m)	21 m	27 m
Storm surge level above MSL (m)	+5 m NAP during 5 hours	+5 m NAP during 5 hours
Median sediment diameter (μm)	225	225
Median fall velocity (m/s)	0.0267	0.0267
Water temperature (^oC)	10	10
Cross-shore profile	a) dune height at +15 m NAP, b) dune face with slope of 1 to 3 down to a level of +3 m NAP, c) slope of 1 to 20 between +3m and 0 m NAP, d) slope of 1 to 70 between 0 and -3 m NAP, e) slope of 1 to 180 seaward of -3 m NAP line	a) dune height at +15 m NAP, b) dune face with slope of 1 to 3 down to a level of +3 m NAP, c0 slope of 1 to 20 between +3m and 0 m NAP, d) slope of 1 to 70 between 0 and -3 m NAP, e) slope of 1 to 180 seaward of -3 m NAP line

(Remark: Mean Sea Level (MSL) is about equal to NAP)

Table 2.1 *Parameters of Dutch coastal profile; Reference Case*

Test	d_{50} (μm)	Te (^oC)	w_s (m/s)	$H_{s,o}$ (m)	T_p (s)	h_{toe} (m)	n_{d50} (-)	n_h (-)	n_l/n_h (-)
111	225	12.5	0.0276	0.091	1.31	0.461	1	84	3.9
115	225	13	0.0278	0.091	1.31	0.461	1	84	2.71
112	150	12.5	0.016	0.091	1.31	0.461	1.5	84	2.93
116	150	13	0.0161	0.091	1.31	0.461	1.5	84	1.89
113	130	12.5	0.013	0.091	1.31	0.461	1.730769	84	2.09
117	130	13	0.0132	0.091	1.31	0.461	1.730769	84	1.44
114	95	12.5	0.0082	0.091	1.31	0.461	2.368421	84	2
118	95	13	0.0083	0.091	1.31	0.461	2.368421	84	1.18
101	225	15.5	0.0287	0.163	1.76	0.585	1	47	3.5
105	225	15	0.0285	0.163	1.76	0.585	1	47	2.45
102	150	15.5	0.0168	0.163	1.76	0.585	1.5	47	2.44
106	150	15	0.0167	0.163	1.76	0.585	1.5	47	1.79
103	130	15.5	0.0138	0.163	1.76	0.585	1.730769	47	2.02
107	130	15	0.0137	0.163	1.76	0.585	1.730769	47	1.62
104	95	15.5	0.0087	0.163	1.76	0.585	2.368421	47	1.73
108	95	15	0.0086	0.163	1.76	0.585	2.368421	47	1.4
121	225	10.5	0.0269	0.292	2.35	0.806	1	26	3.08
125	225	9.5	0.0265	0.292	2.35	0.806	1	26	1.95
122	150	10.5	0.0154	0.292	2.35	0.806	1.5	26	2.3
126	150	9.5	0.0152	0.292	2.35	0.806	1.5	26	1.48
123	130	10.5	0.0125	0.292	2.35	0.806	1.730769	26	1.62
127	130	9.5	0.0123	0.292	2.35	0.806	1.730769	26	1.1
124	95	10.5	0.0079	0.292	2.35	0.806	2.368421	26	1.32
128	95	9.5	0.00078	0.292	2.35	0.806	2.368421	26	1.04
Dflume	225	7.5	0.027	1.5-1.7*	5.4	4.2	1	5	2

Te= water temperature, w_s= fall velocity, $H_{s,o}$= deep water wave height, T_p= wave period, h_{toe}= water depth at toe of dune, n_{d50}=ratio of sediment diameter in prototype (=225 μm) and model, n_h= water depth scale, n_l= length scale

* actual wave height was 1.7 m rather than 1.5 m (see Table 6.2 of Steetzel, 1993)

Table 2.2A *Scale test data of Vellinga (1986) based on prototype conditons of Table 2.1.*

Test	$A_{t=0.3\ hours}$ (m^2)	$A_{t=1\ hours}$ (m^2)	$A_{t=3\ hours}$ (m^2)	$A_{t=6\ hours}$ (m^2)	$A_{t=10.5\ hours}$ (m^2)	$A_{t=16\ hours}$ (m^2)
111	0.0132	0.0148	0.0158	0.015	0.0174	0.0206
115	0.0082	0.0059	0.0051	0.0037	0.0032	0.0036
112	0.0104	0.0162	0.0176	0.0176	0.0249	0.0313
116	0.0056	0.0066	0.0072	0.0095	0.0117	0.0145
113	0.0056	0.0091	0.0095	0.0116	0.017	0.0193
117	0.0047	0.0055	0.0076	0.0101	0.0145	0.0191
114	0.0049	0.0085	0.0148	0.0191	0.032	0.0389
118	0.0025	0.0058	0.0095	0.0165	0.0242	0.0312
101	0.0449	0.051	0.06	0.0651	0.0765	0.0872
105	0.0331	0.0366	0.0395	0.0419	0.0468	0.0523
102	0.0571	0.0636	0.0776	0.0865	0.0975	0.1153
106	0.032	0.0415	0.0478	0.0529	0.0603	0.0753
103	0.0469	0.054	0.0634	0.0754	0.0903	0.1093
107	0.0261	0.0336	0.0396	0.0448	0.0547	0.0703
104	0.0473	0.0646	0.0956	0.13	0.1648	0.2151
108	0.0266	0.0411	0.0552	0.0739	0.0995	0.1314
121	0.1838	0.225	0.2914	0.323	0.3623	0.3916
125	0.1852	0.1107	0.1265	0.1265	0.1265	0.1328
122	0.1751	0.2207	0.267	0.267	0.2688	0.2747
126	0.1015	0.1293	0.1634	0.169	0.1677	0.1728
123	0.1543	0.2345	0.3129	0.3463	0.3624	0.3836
127	0.0779	0.1435	0.1964	0.2253	0.23	0.247
124	0.161	0.2781	0.3891	0.4644	0.5183	0.5369
128	0.1175	0.1898	0.2673	0.3108	0.3943	0.4538
Dflume	3.92	7.08	11.07	13.3	14.8	-

A= Erosion area above storm surge level (in m^3/m)

Table 2.2B *Dune erosion volumes of Vellinga (1986) based on prototype conditons of Table 2.1*

Test	d_{50} (μm)	Te (^oC)	w_s (m/s)	$H_{s,o}$ (m)	T (s)	h_{toe} (m)	n_{d50} (-)	n_h (-)	n_l/n_h (-)
Sflume 2004-T03	95	9.5	0.006	0.3	1.83	0.7	2.368421	30	1.68
Sflume 2004-T01	95	9.5	0.006	0.3	2.19	0.7	2.368421	30	1.68
Sflume 2004-T02	95	9.5	0.006	0.3	2.59	0.7	2.368421	30	1.68
Dflume 2006-T01	200	8	0.023	1.5	4.9	4.5	1.125	6	2
Dflume 2006-T02	200	8	0.023	1.5	6.12	4.5	1.125	6	2
Dflume 2006-T03	200	8	0.023	1.5	7.35	4.5	1.125	6	2

Te= water temperature, w_s= fall velocity, $H_{s,o}$= deep water wave height, T= wave period, h_{toe}= water depth at toe of dune, n_{d50}=ratio of sediment diameter in prototype (=225 μm) and model, n_h= water depth scale, n_l= length scale

Table 2.3A *Scale test data of Delft Hydraulics (2004, 2006a,b).*

Test	$A_{t=0.3\ hours}$ (m^2)	$A_{t=1\ hours}$ (m^2)	$A_{t=2.04\ hours}$ (m^2)	$A_{t=3\ hours}$ (m^2)	$A_{t=6\ hours}$ (m^2)	$A_{t=8\ hours}$ (m^2)
Sflume 2004-T03	0.048	0.149		0.246	0.337	
Sflume 2004-T01	0.061	0.171		0.289	0.394	
Sflume 2004-T02	0.061	0.193		0.328	0.419	
Dflume 2006-T01	2.13	4.23	5.88			8.6
Dflume 2006-T02	2.29	4.58	6.32			9.57
Dflume 2006-T03	2.48	5.31	7.1			9.85

A= Erosion area above storm surge level (in m^3/m)

Table 2.3B *Dune erosion volumes of Delft Hydraulics (2004, 2006a,b).*

The median sediment diameter of the scale test series was varied in the range of 95 to 225 μm; thus: n_{d50}=2.4 to 1. The vertical scale is in the range between n_h=84 and n_h=5. Large scale tests with n_h=5 and 6 were performed in the Deltaflume (length of 233 m, depth of 7m, width of 5 m) of **Delft Hydraulics (2006a,b)**.

The data of **Vellinga (1986**) have been used to find the proper scale relationship, applying the following approach:

1. select a scaling law from **Equations (2.14a) to (2.14h)**;
2. compute the steepness scale n_l/n_h and the length scale n_l by using the selected scaling law;

3. compute the ratio R of steepness scale used in each test and the steepness scale based on scaling law used;
4. select those tests from **Table 2.2A** which have a ratio of about R≅1 (in range of 0.8 to 1.2) with $R=(n_l/n_h)_{used}/(n_l/n_h)_{scaling\ law}$;
5. convert the measured erosion area A_d (above storm surge level) at each time to prototype erosion values using the scale rule $n_A=n_h\ n_l$;
6. convert the time value at which the erosion area has been measured to a prototype time value using **Equation (2.12b)**: $n_{Tm}=n_h^{\alpha}$ with α in range of 0.5 to 1 depending on selected scaling law (**Equation (2.14a) to (2.14h)**);
7. make a plot of the erosion area as a function of time (prototype values);
8. if the applied scaling law is perfect, all curves will collapse on one single curve (minimum scatter);
9. repeat procedure for all available scaling scaling laws.

It is noted that the data of some tests with very small water depths (n_h=84) have been neglected (in this study) due to the presence of scale effects. Some of the tests with very small depths (n_h=84) and relatively coarse sediment (225 μm) show decreasing erosion values in time probably due to onshore transport effects. The combination of very small waves and coarse sediment (n_h=84 and 225 μm) may easily lead to onshore bed load transport rather than offshore suspended load transport (as present in prototype conditions). The combination of very small waves and fine sediment (n_h=84 and 95 μm) may lead to hydraulically smooth flow conditions. In the latter case the fine sediment particles are buried in the laminar sublayer leading to much larger critical shear stresses (left limb of the Shields curve) and hence reduction of the transport rate.

Figure 2.1 shows a plot of the dune erosion area (data of **Vellinga, 1986**) as a function of time based on **Equation (2.14h)**, showing minimum scatter. The data point related to the Deltaflume was corrected because the steepness ratio R was much too large (R=1.28).

Table 2.4 shows the measured dune erosion areas of the tests of **Vellinga (1986)** at three times (t=5, 10 and 20 hours) based on **Equations (2.14h), (2.14e), (2.14i), (2.14g)** and **(2.14k)**. The scatter is minimum for **Equations (2.14h)** and (**2.14i)**.

Based on analysis of all results, it is found that the scaling law according to **Equation (2.14h)** produces the least scatter. **Equation (2.14h)** yields:

$$n_l/n_h=(n_{d50})^{-0.5}\ (n_{s-1})^{-0.5}(n_h)^{0.28}$$

$$n_{Tm}=(n_h)^{0.56}$$

$$n_{Tm}=(n_l/n_h)^2(n_{d50})\ (n_{s-1})$$

These expressions are in line with earlier findings of **Vellinga (1986)**.

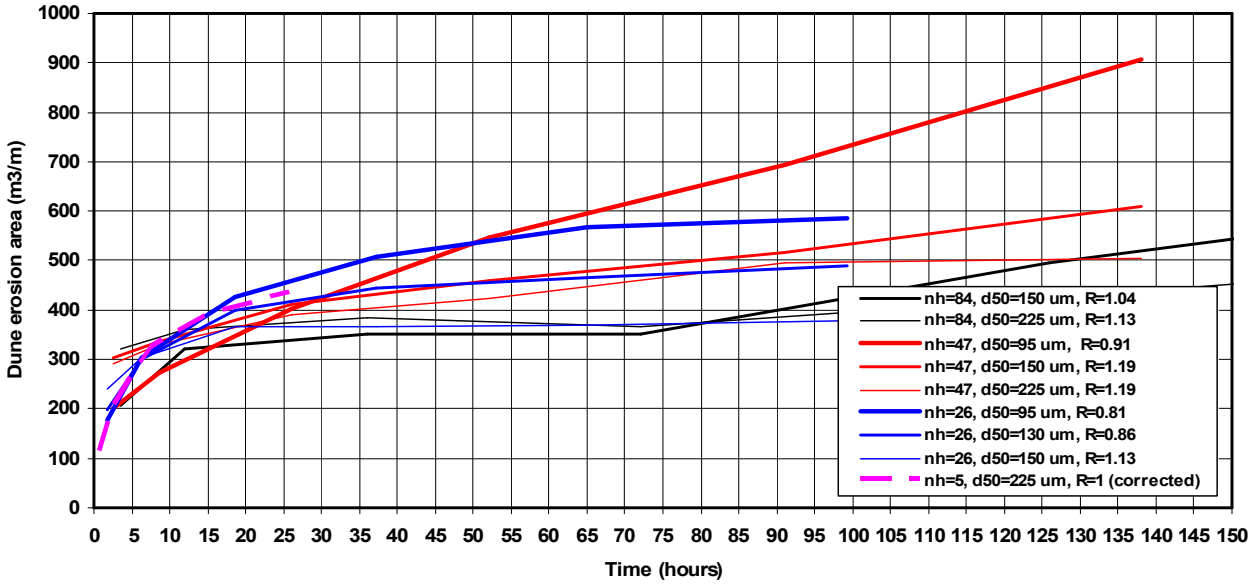

Figure 2.1 *Dune erosion area as function of time (prototype values) based on data of Vellinga (1986) and based on Equation (2.14h)*

Scaling laws - length scale - time scale	**Dune erosion area (m^3/m) after t=5 hours**	**Dune erosion area (m^3/m) after t=10 hours**	**Dune erosion area (m^3/m) after t=20 hours**
Equation (2.14h): $n_l/n_h=(n_{d50})^{-0.5}$ $(n_{s-1})^{-0.5}(n_h)^{0.28}$ $n_{Tm}=(n_h)^{0.56}$	250±100	350±100	450±100
Equation (2.14e): $n_l/n_h=(n_{d50})^{-1}$ $(n_{s-1})^{-0.5}(n_h)^{0.30}$ $n_{Tm}=(n_h)^{0.6}$	230±130	290±170	350±210
Equation (2.14i): $n_l/n_h=(n_{d50})^{-0.5}$ $(n_{s-1})^{-0.5}(n_h)^{0.30}$ $n_{Tm}=(n_h)^{0.6}$	270±100	370±100	450±100
Equation (2.14g): $n_l/n_h=(n_{d50})^{-0.5}$ $(n_{s-1})^{-0.5}(n_h)^{0.25}$ $n_{Tm}=(n_h)^{0.5}$	250±140	310±160	350±200
Equation (2.14k): $n_l/n_h=(n_{ws})^{-0.5}$ $(n_{s-1})^{-0.5}(n_h)^{0.28}$ $n_{Tm}=(n_h)^{0.56}$	230±130	300±160	350±200

Table 2.4 *Dune erosion area at three times (prototype values) based on data of Vellinga (1986) and based on Equations (2.14h), (2.14e), (2.14i), (14g) and (14k)*

Figure 2.2 shows the dune erosion area at t=5 hours as a function of the ratio R of the model steepness used and scaling law steepness (based on **Equation 2.14h**). The dune erosion area is determined by using the length scale from the scaling law (black dots) and from the the values used in the tests (open dots). The dune erosion area above SSL is about 250 m^3/m for a ratio R=1. For R>1 the dune erosion area increases with R. The fitted curve can be used to correct the dune erosion area for tests with a ratio R larger than 1. The scale analysis results show that the scale tests should be done at a distorted scale to properly represent the wave breaking and wave runup processes. Ideally, the distorted scale used in the tests should always be the same as the distorted scale according to the scaling law (R=ratio=1). This is not always feasible. For example, the distortion scale of the tests in the Deltaflume is $n_l/n_h=2$ to accomodate the reference cross-shore profile in the Deltaflume test. Using **Equation (2.14h)**, the ideal distortion scale is 1.56 resulting in R=1.28. Hence, the steepness in the Deltaflume is too large compared with the scaling law. **Figure 2.2** based on many test data shows that the dune erosion area increases with increasing steepness ratio R. This curve has been used to correct the data point of the delta flume test (see Figure 2.1), which has a ratio of R=1.28. For R=1 the dune erosion area after 5 hours is about 70% of that for R=1.28.

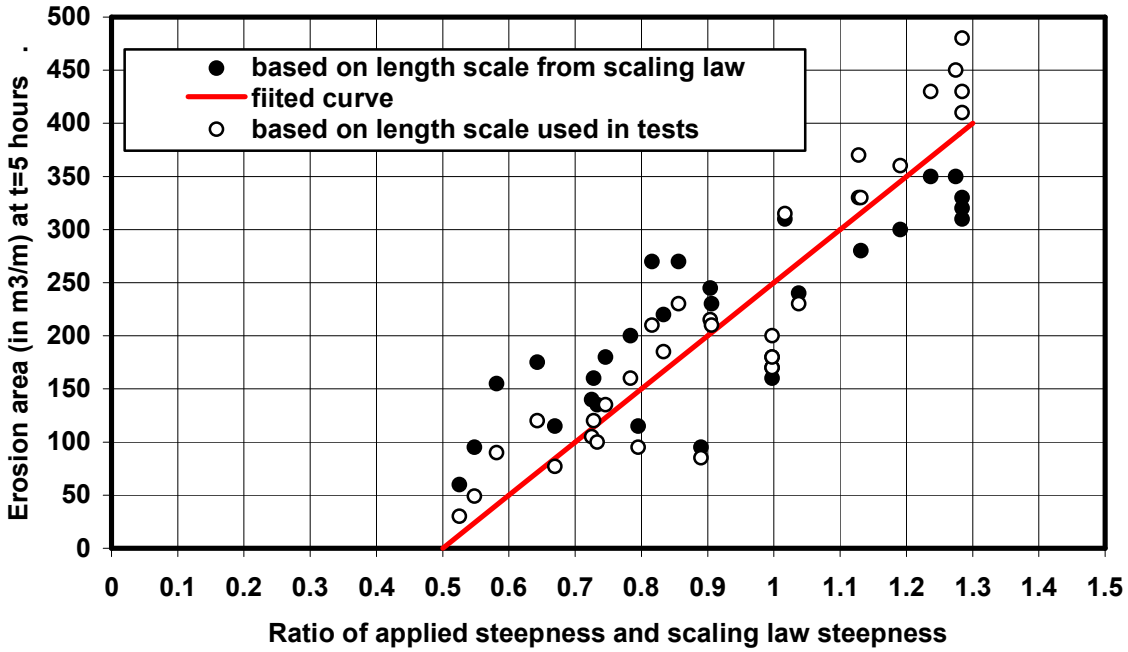

Figure 2.2 *Dune erosion area (above SSL) at t=5 hours as function of the steepness ratio R (data of Vellinga, 1986).*

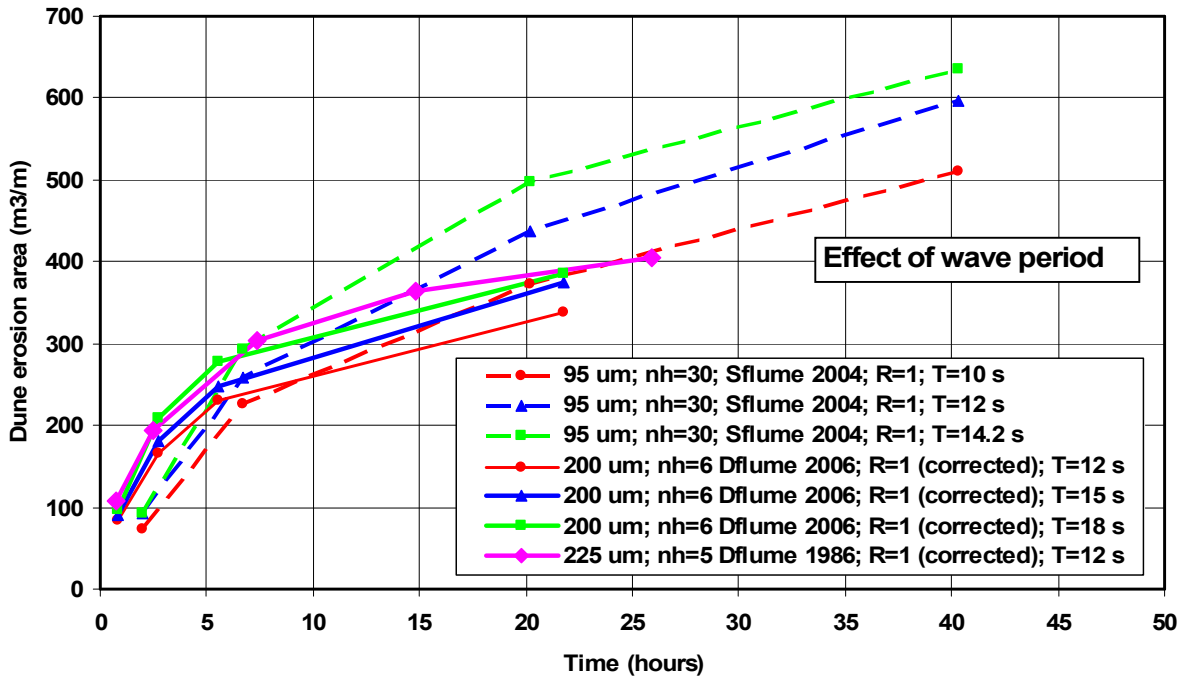

Figure 2.3 *Dune erosion area (above SSL) as a function of time;*
Data of tests with scales of 30, 6 and 5 and wave periods between 10 and 18 s
(Delft Hydraulics, 2004, 2006a,b)

Figure 2.3 shows the data of the small-scale and large-scale flume tests performed at **Delft Hydraulics (2004, 2006a,b)** focussing on the effect of the wave period. The wave period was varied in the range of 12 to 18 s. The offshore wave height was slightly modified to 9 m (compared to 7.6 m used by **Vellinga (1986)**). The small scale tests had a steepness ratio of R=1, but the steepness ratio of the Deltaflume tests was R=1.28 (Deltaflume was not long enough). As a result, the dune erosion areas obtained in the Deltaflume tests are somewhat too large and have been corrected using a correction factor of 0.7 based on **Figure 2.2**.

Figure 2.3 shows that the dune erosion area above storm surge level after 5 hours increases with increasing wave period (about 18% for T increasing from 12 to 18 s). Scale effects can also be observed as the (corrected) dune erosion area after 5 hours is much larger in the Deltaflume (about 25%) than that in the small scale flume. The scale effects are largest during the first 5 hours (at prototype scale) and seem to fade away at larger time scale (10 hours). The large scale Deltaflume test of **Vellinga (1986)** shows slightly larger erosion areas (about 5% to 10%) after 5 and 10 hours than that of **Delft Hydraulics (2006a,b)**.
The dune erosion after 5 hours (in prototype values) is **approximately 250 m^3/m**, which is somewhat smaller (15%) than the **value of 300 m^3/m** obtained by **Vellinga (1986)** for the Reference Case.

Scale-related errors
A basic question related to the results of the laboratory dune erosion tests is the applicability of the scale relations to field storm conditions.

To address this topic, the measured dune erosion volumes along Dutch coast caused by the February 1953 storm can be used. Field data for this event are available for a coastal section (Delfland section; length of about 17 km) between The Hague and Rotterdam. The data comprise of cross-shore bed profiles measured a few days after the storm event (post-storm profiles) and bed profiles measured before the storm (pre-storm profiles measured about 3 to 6 months before the storm). The water level during the storm increased from +1.5 m to +3.9 m (above NAP; approx. mean sea level) over a period of about 15 hours. The maximum wave height is about $H_{s,o}$= 6.3 m. The local beach grain size is about 0.225 mm. The measured dune erosion area above the maximum storm surge level of +3.9 m varies in the range of 60 to 150 m^3/m with a mean value of about 90 m^3/m (**Vellinga, 1986** and **Steetzel, 1993**).

Based on the available empirical scaling laws (using depth scale of 3.3 and a length scale of 4.6), the February 1953 storm including the time-varying storm surge level was simulated by **Vellinga (1986)** in the Deltaflume of Delft Hydraulics. The dune erosion volume for this (distorted) laboratory test is about 120 m^3/m, which is about 30% larger than the mean observed value of 90 m^3/m for field conditions. These results may indicate that the scaling laws based on (distorted) 2D laboratory tests produce values which are somewhat too large for 3D field conditions. Given the lack of data for extreme storm conditions, a firm conclusion on the scale errors cannot yet be given.

2.11 Summary of scaling laws for beach and dune erosion by storm waves

Based on analysis of scale model results for dune erosion, the final set of scaling laws proposed by the present author (Van Rijn; this study) is:

$$(n_l/n_h)= (n_h)^{0.28} (n_{d50})^{-0.5} (n_{s-1})^{-0.5} \quad (2.16a)$$

$$n_A=n_l\, n_h \quad (2.16b)$$

$$n_{Tm}=(n_h)^{0.56} \quad (2.16c)$$

Using Eq. (2.16c) in (2.16a) yields: $n_{Tm}==(n_l/n_h)^2 (n_{d50})^1 (n_{s-1})^1$ (2.16d)

According to **Vellinga (1986)**, the scaling laws for dune erosion read as:

$$(n_l/n_h)=(n_h)^{0.28} (n_w)^{-0.56} \quad (2.17a)$$

$$n_A=n_l\, n_h \quad (2.17b)$$

$$n_{TM}=(n_h)^{0.5} \quad (2.17c)$$

Using Eq. (2.17c) in (2.17a) yields: $n_{TM}=(n_l/n_h) (n_h)^{0.22} (n_w)^{0.56}$ (2.17d)

with: n_w=fall velocity scale, n_{TM}=morphological time scale, n_A= erosion area scale.
The practical ranges are: n_l/n_h=1 to 2; n_h=1 to 50; n_{d50}=1 to 5 and n_{ws}=1 to 5.
Using Equation (2.16d) or (2.17d), the parameters n_l/n_h, n_h and n_{d50} (or n_{ws}) can be chosen freely within the given practical ranges and the time scale is fixed. Hence, three scale parameters are free.

Using the time scale according to Eq.(2.16c) or (2.17c), the distortion scale, the depth scale or the sediment scale follows from Eq. (2.16a) or (2.17a) and cannot be violated. Hence, only two scale parameters are free.

To design a physical scale model, the following methods are possible:

Method 1 (two free parameters)

1. select depth scale and distortion scale;
2. find the grain size scale (or the fall velocity scale) from **Eq. (2.16a)** or **(2.17a);**
3. find the time scale from **Eq. (2.16c)** or **(2.17c);**
4. translate the measured results to prototype values using the applied depth and length scale (n_h and n_l).

Example

Given: $n_h=5$, $n_l/n_h=2$, $n_l=10$, $n_{s-1}=1$ (sand)
Van Rijn: $n_{d50}=0.61$, $n_{Tm}=2.5$ and $n_A=n_l\ n_h=5x10=50$
Vellinga: $n_w=0.6$, $n_{Tm}=2.2$ and $n_A=n_l\ n_h=5x10=50$
The results are almost similar.

Often, **Equation (2.16a)** or **(2.17a)** cannot be fully matched because of the given flume dimensions (flume not long enough to fit cross-shore profile in flume) and the available sediment material (finer or coarser than required). Then, method 2A or 2B should be used

Method 2A (three free parameters)

1. select depth scale, distortion scale and sediment size scale (or fall velocity scale);
2. find the time scale from **Eq.(2.16d)** or **(2.17d);**
3. translate the measured results to prototype values using the applied depth scale (n_h and n_l).

Example

Given: $n_h=5$, $n_l/n_h=2$, $n_l=10$, $n_{d50}=1$, $n_w=1$, $n_{s-1}=1$ (sand)
Van Rijn: Method 2A: $n_{Tm}=(n_l/n_h)^2\ (n_{d50})^1\ (n_{s-1})^1=4$ and $n_A=5x10=50$
Vellinga: Method 2A: $n_{Tm}=(n_l/n_h)\ (n_h)^{0.22}\ (n_w)^{0.56}=2\ x\ (5)^{0.22}\ x\ 1=2.84$ and $n_A=5x10=50$

Method 2B (three free parameters)

1. select depth scale, distortion scale and sediment size scale (or fall velocity scale);
2. find the time scale from **Eq.(2.16c)** or **(2.17c);**
3. find the morphological length $n_{l,s}$ scale from **Eq.(2.16a)** of **(2.17a);**
4. translate the measured results to prototype values using the applied depth scale n_h and the morphological length scale $n_{l,s}$; the ratio $\gamma=n_{l.s}/n_l$ can be seen as the scale effect ($A_{proto}=\gamma\ n_h\ n_l\ A_{model}$) with $\gamma<1$ for very distorted models and $\gamma>1$ for undistorted models.

Example

Given: $n_h=5$, $n_l/n_h=2$, $n_l=10$, $n_{d50}=1$, $n_w=1$, $n_{s-1}=1$ (sand)
Van Rijn: Method 2B: $n_{Tm}=(n_h)^{0.56}=2.5$ and $n_{l,s}=(n_h)^{1.28}\ (n_{d50})^{-0.5}\ (n_{s-1})^{-0.5}=8.5$ and $n_A=5x8.5=42.5$

Vellinga: Method 2B: $n_{Tm}=(n_h)^{0.5}=2.2$ and $n_{l,s}=(n_h)^{1.28}\ (n_w)^{-0.56}=7.85$ and $n_A=5x7.85=39$

The focus of the present study is on dune erosion by storm waves. To check the validity of the proposed scaling laws for the beach erosion regime, other scaling laws as found in the literature are discussed hereafter.

Noda (1972) has performed various beach erosion experiments in scale models (distorted and undistorted) with relatively low regular waves focussing on relatively coarse sand (>0.5 mm; initial slope of 1 to 25). Based on analysis of quasi-equilibrium bed profiles, he proposed the following scaling laws:

$$n_{d50}=(n_h)^{0.55} \quad (2.18a)$$

$$n_l/n_h=(n_h)^{0.32} \quad (2.18b)$$

Ito and Tsuchiya (1984, 1986, 1988) and **Ito et al. (1995)** have done detailed studies of beach erosion profiles in quasi-equilibrium conditions under low and high waves. They have used small-scale and large-scale physical models (undistorted) with regular waves and initial slopes of 1 to 15 and 1 to 30. Similitude between bed profiles of different scales is defined to exist when the difference is less than twice the experimental error (based on repeated tests). The low-wave cases show onshore transport with the formation of a swash bar at the upper end of the beach slope (1 to 30), while the high-wave cases show offshore transport with the formation of a breaker bar at the lower end of the beach slope (1 to 15). The prototype bed profiles are obtained from the results measured in large-scale wave flumes (offhore depth of 1 to 4.3 m; wave periods of 3 to 11 s).

The scaling laws derived from these undistorted scale model (regular waves) series are:

$$n_{d50}=(n_h)^{0.83} \quad \text{for } n_h<2.2 \quad (2.19a)$$

$$n_{d50}=1.7(n_h)^{0.2} \quad \text{for } n_h\geq 2.2 \quad (2.19b)$$

$$n_{Tm}=(n_h)^{0.5} \quad (2.19c)$$

These scaling laws were applied to a storm-induced beach erosion event (14-18 March 1981) on the Ogata coast facing the Pacific Ocean (Japan). The significant wave height increased from 0.5 m to about 4 m in about one day, remained constant for the following day and decreased again after that. The storm-induced set-up was about 0.3 m. The beach sediments varied in the range of 0.2 mm in the offshore zone to about 0.4 mm at the beach. The depth scale was set to $n_h=50$, the grain size scale was set to $n_{d50}=3.7$ based on Equation (2.19b). Two model sands were used to represent the beach material variation in the prototype. The wave height variation during the storm event was represented by schematizing it into three regular wave cases, each with constant but different wave height and period.

The beach profile changes observed in the prototype are reproduced very well when the mean wave height is used as the representative wave height in the prototype and slightly less good when the significant wave height is used. Similar conclusions are given by **Ito et al. (1995)**.

Wang et al. (1990) have proposed:

$$n_l/n_h=[(n_h)(n_{s-1})^{-2}(n_{ws})^{-2}]^{\alpha} \quad (2.21)$$

with:

Method A: $\alpha=0.5$ for $n_T=n_{TM}=(n_h)^{0.5}(n_l/n_h)$
method B: $\alpha=0.25$ for $n_T=(n_h)^{0.5}(n_l/n_h)$ and $n_{TM}=(n_h)^{0.5}$

They have found that Method B yields better agreement in terms of the morphological time scale and that the similarity of the wave breaking process (surf similarity parameter) and the fall velocity parameter are the most important considerations for correct modelling of beach processes.

Hughes (1993) has proposed a distorted model time scale which is similar to the preservation of the surf similarity parameter (see Equation (2.2 and 2.7b)). Thus: $n_T=n_{TM}=(n_h)^{0.5}(n_l/n_h)$

Hughes and Fowler (1990) have performed small-scale model experiments (undistorted) aimed at reproducing large-scale experiments in the GWK (Grosser Wellen Kanal, Hannover); the latter being defined as the prototype. The prototype sediment is $d_{50}=0.33$ mm and $w_s=0.0447$ m/s. The depth at the toe of the initial profile is 5 m for the prototype and 0.67 m for the scale model. The wave period is 6 s for the prototype and 2.2 s for the scale model. Using an undistorted model, the applied scaling laws are (see Equation 2.7):

$$n_{ws}=(n_h)^{0.5} \quad (2.20a)$$
$$n_{Tm}=(n_h)^{0.5} \quad (2.20b)$$

Given a depth scale of $n_h=7.5$, the fall velocity scale is $n_{ws}=2.73$ (scale model sand of 0.13 mm, $w_s=0.0164$ m/s). In the prototype experiments, sand with a median diameter of 0.33 mm was placed in front of a concrete structure with a slope of 1 to 4. The initial sand slope was also 1 to 4. Both regular and irregular (Jonswap) wave tests were done. In the case of regular waves (H=1.5 m for prototype and 0.2 m for scale model) the model erosion at the upper end of the beach was slightly (10%) under-estimated. Almost perfect agreement was obtained by increasing the wave height by about 10%. Comparing test results of irregular waves ($H_{1/3}=1.5$ and 0.2 m; Tp=6 and 2.2 s for prototype and scale model) in the prototype and in the scale model, the agreement was found to be very good, see **Figure 2.4**.

Comparable profile development can be achieved between regular waves in the scale model and irregular waves in the prototype when the value of significant wave height is used as the regular wave heigth in the scale model. Profile development is found to be approximately twice as fast in the scale model with regular waves. Hence, only half the number of waves is required to obtain the same quasi-equilibrium bed profile (at corresponding times). In all tests the (offshore) slope at the toe of the beach was much steeper in the prototype (0.33 mm) than in the scale model (0.15 mm), see Figure 2.4. Probably, there was relatively large onshore transport at this location (shoaling waves) in the prototype (GWK, Hannover) causing a steeper slope.

Dette and Uliczka (1986) have compared beach profiles of the GWK (Hannover) with similar tests performed at scale of 1 to 10 (n_h=10). The scale model sand (0.33 mm) was similar to that used in the GWK. The best agreement of the beach profiles in the surf zone was found when the scaling laws of Vellinga (see Equation (2.17)) were used. In the offshore zone where bed-load transport is dominant the scaled-up model results were substantially too shallow (less steep profiles in scale model).

Ranieri (2007) has made the most recent contribution to the scaling laws of beach profiles. Test results of the GWK (Hannover) have been defined as the prototype results. A series of undistorted scale models (n_h in the range of 10 to 45; Froude scaling) has been executed to determine the scale effects. He has proposed to correct the scale errors based on a distortion coefficient (α_{surf}) to be applied only to the surf zone between the bar crest and the water line. The erosion volume in the prototype (A_p) can be computed by:

$$A_p=\alpha_{surf}\, n^2\, A_m \tag{2.21a}$$

with: A_m= erosion volume of scale model; $n=n_h=n_l$= length scale of undistorted model and $\alpha_{surf}=n_{l,s}/n_h$=correction factor in the range of 1 to 2.5 acting in surf zone only (approximately between bar crest and water line)

The α_{surf} is found to depend on:

$$\alpha_{surf} = -1.42 + 1.12 \ln(n_\phi/n_k) \quad \text{for } n_\phi>5 \tag{2.21b}$$
$$\alpha_{surf} = 1 \quad \text{for } n_\phi\leq 5 \tag{2.21c}$$

with: $n_\phi=n/(n_{s-1}\ n_{d50})$ and $n_k=(\Phi_{95}-\Phi_5)/(2.44(\Phi_{75}-\Phi_{25}))$, with: $\Phi_i={}^2\log(d_i)$ and d_i=particle size.

The scale models used by Ranieri have been initially set up as undistorted models using Froude scaling. The correction coefficient acting on the horizontal scale has been obtained by requiring optimum agreement between the quasi-equilibrium profiles of the scale model and the prototype. Correction has been applied only to the surf zone between approximately the bar crest and the water line. This method allows to design very small undistorted models and then to correct the results by using the α_{surf}-coefficient.

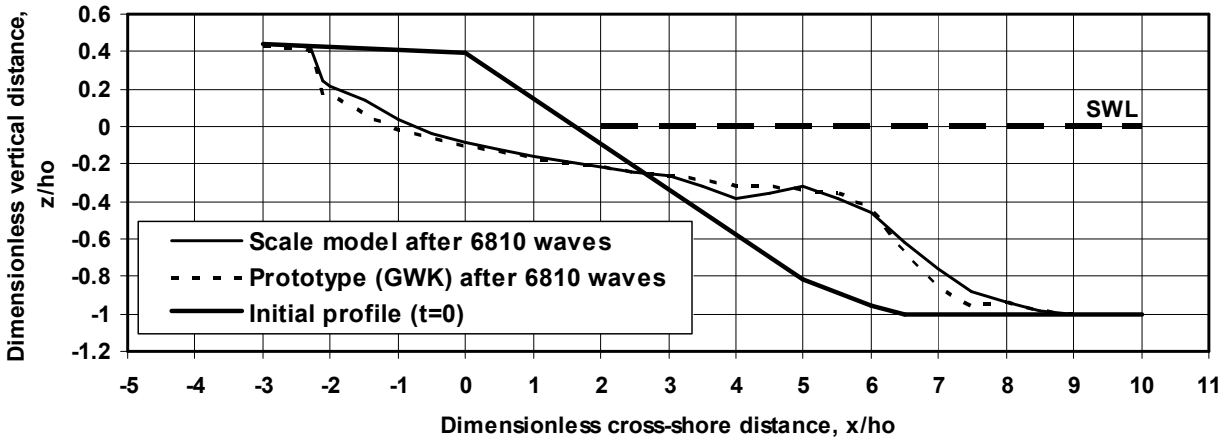

Figure 2.4 *Comparison of cross-shore bed profiles of scale model and prototype (irregular waves)*

Assuming fine model sand in the range of 0.1 to 0.5 mm ($n_{d50} \cong n_{ws}$) and undistorted models, the various grain size scaling laws are plotted in **Figure 2.5**. The scaling laws of **Ito and Tsuchiya (1984, 1986, 1988)** deviates considerably from the other three scaling laws.

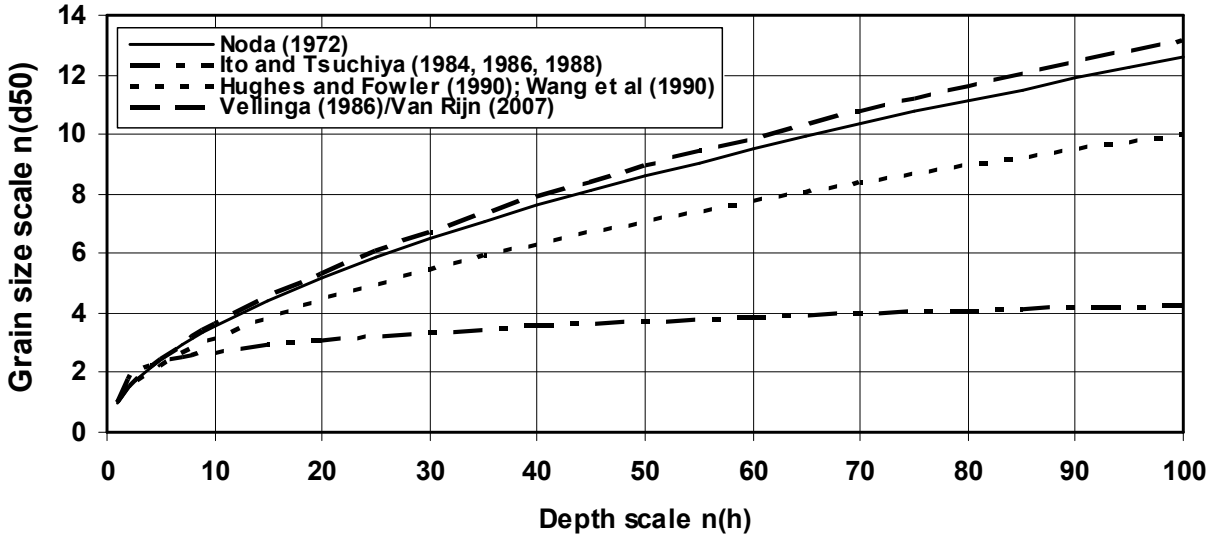

Figure 2.5 *Grain size scale as function of depth scale for various methods*

2.12 Empirical dune erosion prediction methods

Vellinga (1986) has developed the DUROS-model, which is being used as the standard dune erosion rule for the Dutch coast. This model is based on the following assumptions:

- the shape of the erosion profile is defined by a parabolic function which is independent of the initial profile; the most seaward position of the erosion profile is determined by the offshore wave height and the beach grain size.

- the dune erosion volume above storm surge level is determined by shifting this profile horizontally until the erosion volume is equal to the deposition volume (per unit width).

The DUROS model yields an erosion volume of about 300 m^3/m for the Dutch Reference Case, see Table 2.1.

Recently, the DUROS-model has been improved to include the offshore wave period resulting in the DUROS+ model (**Delft Hydraulics, 2007**).

3 Cross-shore model for dune erosion (CROSMOR2007)

3.1 Introduction

The **CROSMOR2007**-model is an updated version of the **CROSMOR2004**-model (**Van Rijn, 1997, 2006, 2007d**). The model has been extensively validated by **Van Rijn et al. (2003)**. **Figure 3.1** shows a definition sketch.

The propagation and transformation of individual waves (wave by wave approach) along the cross-shore profile is described by a probabilistic model (**Van Rijn and Wijnberg, 1994, 1996**) solving the wave energy equation for each individual wave. The individual waves shoal until an empirical criterion for breaking is satisfied. The maximum wave height is given by $H_{max}=\gamma_{br}$ h with γ_{br}= breaking coefficient and h=local water depth. The default wave breaking coefficient is represented as a function of local wave steepness and bottom slope. The default breaking coefficient varies between 0.4 for a horizontal bottom and 0.8 for a very steep sloping bottom. The model can also be run a with a constant breaking coefficient (input value). Wave height decay after breaking is modelled by using an energy dissipation method. Wave-induced set-up and set-down and breaking-associated longshore currents are also modelled. Laboratory and field data have been used to calibrate and to verify the model. Generally, the measured $H_{1/3}$-wave heights are reasonably well represented by the model in all zones from deep water to the shallow surf zone. The fraction of breaking waves is reasonably well represented by the model in the upsloping zones of the bottom profile. Verification of the model results with respect to wave-induced longshore current velocities has shown reasonably good results for barred and non-barred profiles (**Van Rijn et al., 2003; Van Rijn and Wijnberg, 1994, 1996**).

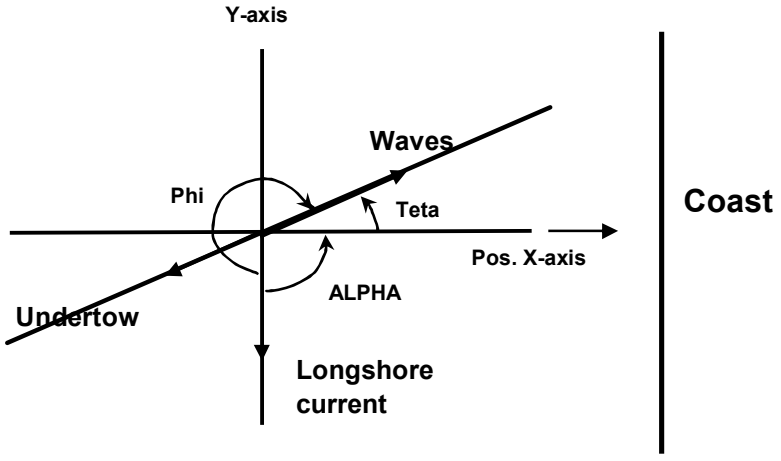

Figure 3.1 *Definition sketch of cross-shore profile model*
Teta= angle between wave direction and positive x-axis
Phi= angle between wave and current direction
Alpha= angle between longshore current direction and positive y-axis
(v_{long}<0 m/s; alfa=270^o and v_{long}>0 m/s; alfa=90^o)

The application of a numerical cross-shore profile model to compute the erosion of the beach and duneface poses a fundamental problem which is related to the continuous decrease of the water depth to zero in the swash zone at the runup point on the dune face. The numerical modelling of the (highly non-linear) wave-related processes in the swash zone with decreasing water depths is extremely complicated and is in an early stage of development. In the CROSMOR-model the numerical method is applied up to a point (last grid point) just seaward of the downrush point, where the mean water depth is of the order of 0.1 to 0.25 m. The complicated wave mechanics in the swash zone is not explicitly modelled, but taken into account in a schematized way. The limiting water depth in the last (process) grid point is set by the user of the model (input parameter; typical values are 0.1 m for small-scale laboratory conditions; 0.25 m for large-scale laboratory conditions and field conditions). Based on the input value, the model determines the last grid point by interpolation after each time step (variable number of grid points).

3.2 Wave orbital velocity and asymmetry

Kroon (1994) and **Wolf (1997)** have shown that the available theories for non-linear wave motion are not accurate in describing the asymmetry of the near-bed orbital velocity in field conditions. Generally, the wave velocity asymmetry in the surf zone is considerably overestimated by most non-linear wave theories. **Grasmeijer and Van Rijn (1998)** and **Grasmeijer (2002)** have shown that the semi-empirical method of **Isobe and Horikawa (1982)** with modified coefficients (based on data fitting using field data series from various coastal sites) produces very reasonable esimates of the peak orbital velocities in shallow water. This method which is a parameterisation of fifth-order Stokes wave theory and third-order cnoidal wave theory, can be used over a wide range of wave conditions. It is the standard method for computation of the wave velocity asymmetry of the **CROSMOR**-model and reads as:

$$U_{w,on}=U_{w,max}[0.5+(r_{max}-0.5)\tanh((r_a-0.5)/(r_{max}-0.5)) \quad (3.1a)$$

$$U_{w,off}=U_{w,max}-U_{w,on} \quad (3.1b)$$

$$U_{w,max}=2r\,U_w \quad (3.1c)$$

$$U_{w,on}=0.65U_{w,max} \text{ if } U_{w,on}<0.65U_{w,max} \text{ and } h<3h_L \quad (3.1d)$$

with:

$r=-0.4(H_s/h)+1$

$A_1=-0.0049(T_1)^2-0.069T_1+0.2911$

$T_1=T_p(g/h)^{0.5}$

$r_a= -5.25-6.1\tanh(A_1U_1-1.76)$; $r_a=0.5$ if $r_a<0.5$

$r_{max}= -2.5(h/L)+0.85$; $r_{max}=0.75$ if $r_{max}>0.75$ and $r_{max}=0.62$ if $r_{max}<0.62$

$U_1=U_{w,max}/(gh)^{0.5}$

with: U_w=peak orbital velocity near the bed based on linear wave theory (based on H_s and T_p), H_s=significant wave height, L= wave length, T_p=peak wave period, h=water depth, h_L=water depth in last grid point

The instantaneous velocities during the forward and the backward phase of the cycle are assumed to have a sinusoidal distribution. The duration period of each phase is corrected to obtain zero net flow over the full cycle ($T_{for} + T_{back} = T$).

3.3 Longuet Higgins streaming

The cross-shore sand transport rate in the near-bed region of shallow waters (near the coast) is strongly affected by small residual (net) currents induced by the wave motion. This was clearly observed by **Bijker et al. (1974)** who measured streaming velocities over the full depth at the toe of a sloping beach. Above a smooth bed they have found that the measured streaming is in reasonable agreement with the streaming predicted by using the conduction-solution of **Longuet-Higgins (1953)**. However, when the same incident waves propagate above a flat sand-roughened bed, the near-bed streaming, while still being in the onshore direction, is greatly reduced in magnitude. When the bed is rippled, the near-bed streaming is further reduced to approximately zero, while the streaming just above the bottom boundary layer is directed offshore.

The onshore-directed streaming (u_b) in the wave boundary layer over a flat bed given by **Longuet-Higgins (1953)** for Eulerian streaming due to viscous diffusion reads as: $u_b = \frac{3}{4} U_w^2/C$ with U_w= near-bed peak orbital velocity and C=L/T= phase velocity.
Davies and Villaret (1997, 1998, 1999) have reviewed the available experimental data sets of streaming velocities in the near-bed region. The data sets have been classified by using the relative bed roughness parameter (A_w/k_w) as discriminating parameter, with: A_w=peak orbital excursion near the bed, k_w=wave-related bed roughness height. Very rough rippled beds can be defined as conditions with $A_w/k_{s,w}<10$, rough plane beds as conditions with $A_w/k_w=10$ to 1000 and smooth plane beds as $A_w/k_w>1000$.

Analysis of the data sets shows that the wave-induced streaming at the edge of the wave boundary layer is negative (against wave propagation direction) or positive as a function of relative roughness A_w/k_w (**Davies and Villaret, 1999**). The streaming velocities at the edge of wave boundary layer become more negative for decreasing relative roughness values (A_w/k_w).

Some values are: $u_b=\beta(U_w)^2/c$ with β= -0.2 for A_w/k_w= 5, β= -1 for A_w/k_w= 1, β=-1.5 for A_w/k_w=0.5. Using β=0.75 (**Longuet-Higgins**) for $A_{\delta,w}/k_s>100$, these results can roughly be approximated by:

$$u_b=(-1+0.875\log(A_w/k_w))(U_w^2/C) \quad \text{for } 1<A_w/k_w<100 \quad (3.2a)$$
$$u_b=0.75(U_w^2/C) \quad \text{for } A_w/k_w\geq 100 \quad (3.2b)$$
$$u_b=-(U_w^2/C) \quad \text{for } A_w/k_w\leq 1 \quad (3.2c)$$

This expression yields:

$u_b = 0.75(U_w)^2/C$ for $A_w/k_w\geq 100$ (in line with Longuet-Higgins, 1953).

$u_b = 0$ for $A_w/k_w=13.9$

$u_b = -0.125(U_w)^2/C$ for $A_w/k_w=10$

$u_b = -(U_w)^2/C$ for $A_w/k_w=1$

3.4 Undertow

The depth-averaged return current (u_r) under the wave trough of each individual wave (summation over wave classes) is derived from linear mass transport and the water depth (h_t) under the trough. The mass transport is given by 0.125 g H^2/C with C= (g h)$^{0.5}$ = phase velocity in shallow water. This yields:

$$u_r = - \alpha \, g^{0.5} \, H^2/(h^{0.5} \, h_t) \qquad (3.3)$$

with α = 0.125, h_t = (0.95 - 0.35(H/h)) and h = water depth to MSL, based on the analysis of field data (**Kroon, 1994**). This approach implies a local response of the return current to the wave energy, which may not be a good representation of the physics involved. The return current is driven by a seaward-directed pressure gradient generated by the radiation stress-induced set-up of the water surface, which may lead to a delayed response of the return current. The non-local response in cross-shore direction is modelled by averaging the wave height and water depth over a short distance (equal to the wave length) seaward of the location x. The contribution of the rollers of broken waves to the mass transport and to the generation of longshore currents (**Svendsen, 1984; Dally and Osiecki, 1994**) can also be taken into account (input switch), see **Grasmeijer (2002)**. The vertical distribution of the undertow velocity is modelled by schematizing the water depth into three layers with a logarithmic distribution in the lower two layers and a third power distribution in the upper layer, yielding velocities which approach to zero at the water surface.

3.5 Low-frequency waves

Low-frequency waves are generated in the surf zone due to spatial and temporal variation of the wave breaking point resulting in spatial and temporal variation of the wave-induced set-up creating low-frequency waves (surf beat). This involves a transfer of energy in the frequency domain: from the high frequency to low frequency waves. The total velocity variance (total wave energy) consists of high-frequency and low-frequency contributions ($U^2_{rms}=U^2_{hf,rms}+U^2_{lf,rms}$).

Figure 3.2 shows high-frequency and low-frequency velocity values (U_{rms}) measured in the Deltaflume of Delft Hydraulics during dune erosion experiments in 2005 and 2006 (**Delft Hydraulics 2006b**; **Van Thiel de Vries et al., 2006**). The low-frequency waves have a period of about $4T_{p,hf}$. The low-frequency velocity ($U_{lf,rms}$) in the Deltaflume is about 0.25 m/s at the edge of the inner surf zone (x=170 m) and increases to about 0.7 m/s at the end of the swash zone (x=205 m). The high-frequency velocity gradually increases from about 0.5 m/s to 0.7 m/s.

Basically, accurate modelling of low-frequency waves requires the application of a long-wave model approach on the wave group time scale (**Van Thiel de Vries et al., 2006**). Such an approach is beyond the present scope of work. Herein, a more pragmatic approach is introduced to crudely represent the low-frquency effects.
The low-frequency significant wave height is modelled as:

$$H_{s,lf}=(\gamma-\gamma_{tr})^{\alpha} \, H_{s,hf} \qquad (3.4a)$$

$$U_{lf}=0.5 \, (H_{s,lf}/h)(gh)^{0.5} \qquad (3.4b)$$

with: $H_{s,lf}$= low-frequency significant wave height, $\gamma=H_{s,hf}/h$=relative significant high-frequency wave height, γ_{tr}= threshold value (=0.5), h= water depth, $H_{s,hf}$= significant high-frequency wave height, α=0.3, U_{lf}= peak velocity of low-frequency waves. The α-exponent is found to be 0.3 based on the data of the Deltaflume experiment (**Figure 3.2**). The long wave velocity is computed from long wave theory. Using this approach, long wave motion (surf beat) is generated under strongly breaking waves (plunging waves) in the surf zone.

Figure 3.3 shows measured and computed values of low-frequency waves. The measured significant low-frequency velocity is related to the measured rms-value of the low-frequency velocity: $U_{lf}=1.4U_{lf,rms}$. Reasonable agreement between measured and computed values can be observed. The peak velocity of the low-frequency waves is added to the peak velocity of the high-frequency waves: $U^2_w=U^2_{hf}+U^2_{lf}$, with: U_{hf}= peak velocity of high-frequency waves near the bed and U_{lf}= peak-velocity of low frequency waves. The total velocity (U^2_w) is used to compute the bed-shear stress.

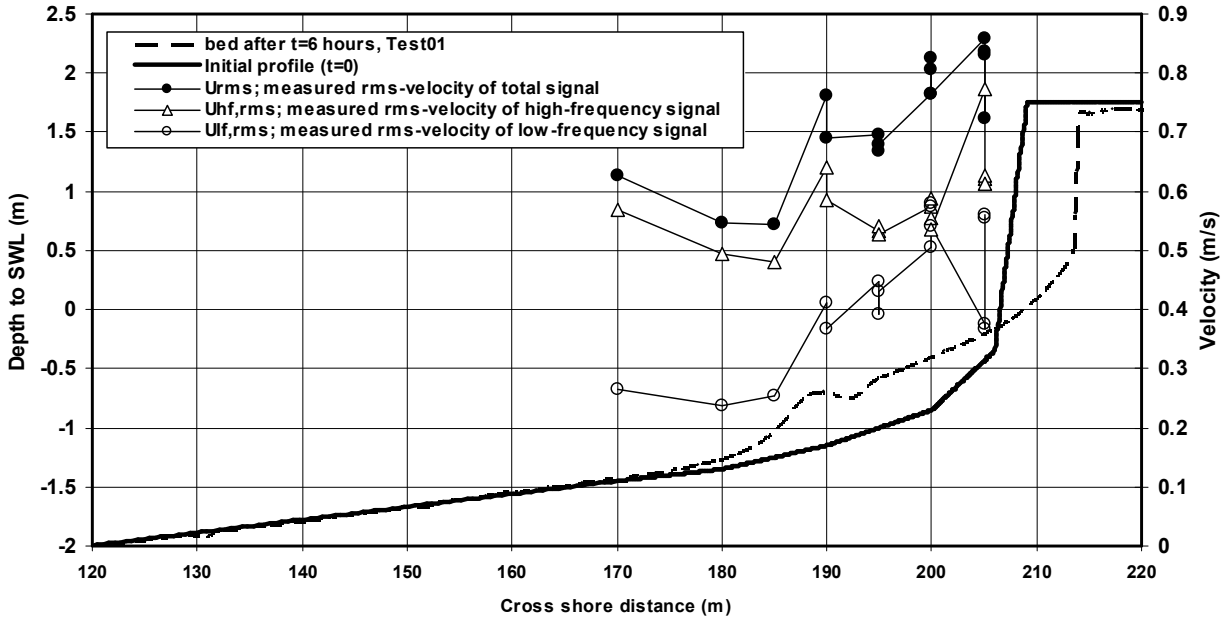

Figure 3.2 *Measured rms-velocities of high-frequency and low-frequency waves in surf zone of Deltaflume experiment on dune erosion (Test T01)*

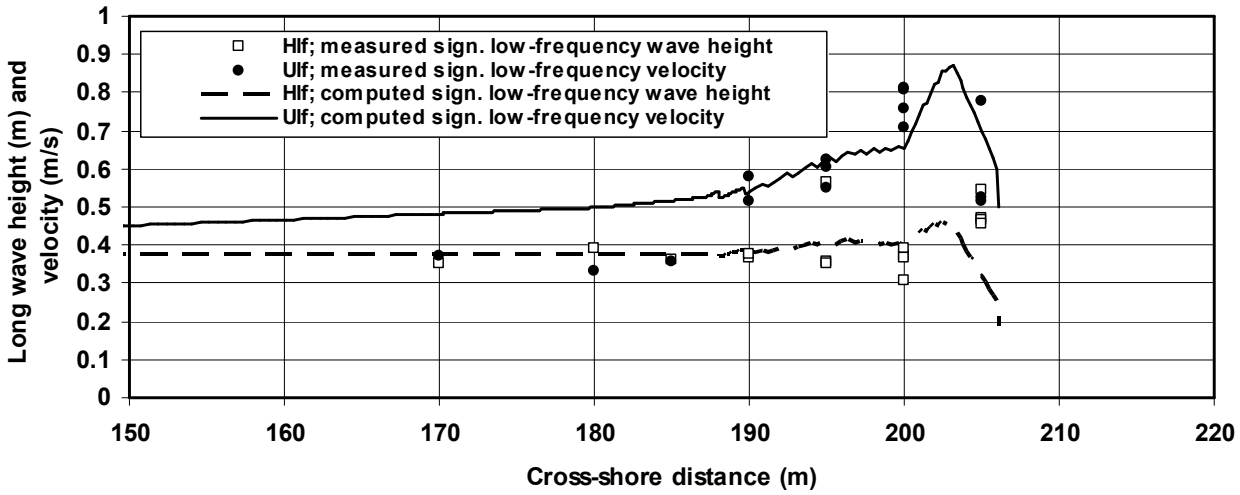

Figure 3.3 *Low-frequency wave height and velocity in surf zone of Deltaflume experiment on dune erosion (Test T01)*

3.6 Cross-shore tidal velocity

The cross-shore depth-averaged current velocity due to the rise and fall of the tide is taken into account by an expression based on continuity, assuming that the water surface is horizontal over a relatively short distance.

3.7 Sand transport

The **CROSMOR2007**-model is based on the **TRANSPOR2004** sand transport formulations (**Van Rijn, 2006, 2007a,b,c,d**). The effect of the local cross-shore bed slope on the transport rate is taken into account by (see **Van Rijn, 1993, 2006**).
The sand transport rate is determined for each wave (or wave class), based on the computed wave height, depth-averaged cross-shore and longshore velocities, orbital velocities, friction factors and sediment parameters. The net (averaged over the wave period) total sediment transport is obtained as the sum of the net bed load (q_b) and net suspended load (q_s) transport rates. The net bed-load transport rate is obtained by time-averaging (over the wave period) of the instantaneous transport rate using a formula-type of approach.

The net suspended load transport is obtained as the sum ($q_s = q_{s,c} + q_{s,w}$) of the current-related and the wave-related transport components (**Van Rijn, 1993; 2006**). The current-related suspended load transport ($q_{s,c}$) is defined as the transport of sediment particles by the time-averaged (mean) current velocities (longshore currents, rip currents, undertow currents). The wave-related suspended sediment transport ($q_{s,w}$) is defined as the transport of sediment particles by the oscillating fluid components (cross-shore orbital motion). The oscillatory or wave-related suspended load transport ($q_{s,w}$) has been implemented in the model, using the approach given by **Houwman and Ruessink (1996)**. The method is described by **Van Rijn (2006, 2007a,b,c,d)**. Computation of the wave-related and current-related suspended load transport components requires information of the time-averaged current velocity profile and sediment concentration profile. The convection-diffusion equation is applied to

compute the equilibrium time-averaged sediment concentration profile for current-related and wave-related mixing. The bed-boundary condition is applied as a prescribed reference concentration based on the time-averaged bed-shear stress due to current and wave conditions. A calibration factor (sef-factor=suspension enhancement factor) acting on the time-averaged bed-shear stress and hence on the reference concentration in the shallow surf zone (dune erosion zone) in front of the dune face has been used to calibrate the the model; sef=1 yields the default model settings; a sef-value in the range of 2 to 3 is found (based on Deltaflume experiments 2005; see later) to be valid for the shallow surf zone in front of the dune face. The sef-factor is used to simulate the effects of wave collision and breaking in the shallow surf zone on the bed-shear stress and the mixing capacity (increased turbulence) of the system resulting in a significant increase of the sand transport capacity. The shallow dune erosion zone is defined as the zone with a length scale of a few meters (of the order of the dune face length scale). To ensure a gradual transition from sef=1 outside the dune rosion zone, a linear transition is assumed to be present seaward of it.

3.8 Erosion in swash zone

The dune erosion zone in front of the relatively steep dune face is defined as the zone up to the run-up level which is dominated by breaking bores (swash motions). Herein, the length of the dune erosion zone (L_s) is determined as the maximum value of two length scales. Hence, $L_s=\max(L_{s1}, L_{s2})$ with:

1) $L_{s1}=6h_{L,m}$ with: $h_{L,m}$ =average water depth of last, five computational grid points. The last computational point is set by the model user by specifying a minimum water depth h_L (input value). This value should be approximately 0.1 times the dune face length ($h_L \cong 0.1L_d$);
2) $L_{s2}=x_R-x_L$ with: x_R=horizontal coordinate of run-up point and x_L=horizontal coordinate of last computational point.

Both approaches produce similar results. The length of the dune erosion zone is in the range of 0.5 to 1 times the dune face length (L_d, see Figure 3.4) above the still water level (SWL). The dune face length is in the range of L_d=1 to 3 m for large-scale laboratory conditions (Deltaflume) and L_d=3 to 5 m for field conditions.

Many run-up formulae are available in the literature. Most of these formulae are only valid for natural beaches with relatively flat slopes (dissipative beaches). To model dune erosion correctly, a run-up formula is required which is valid for steep slopes (up to 70^o).

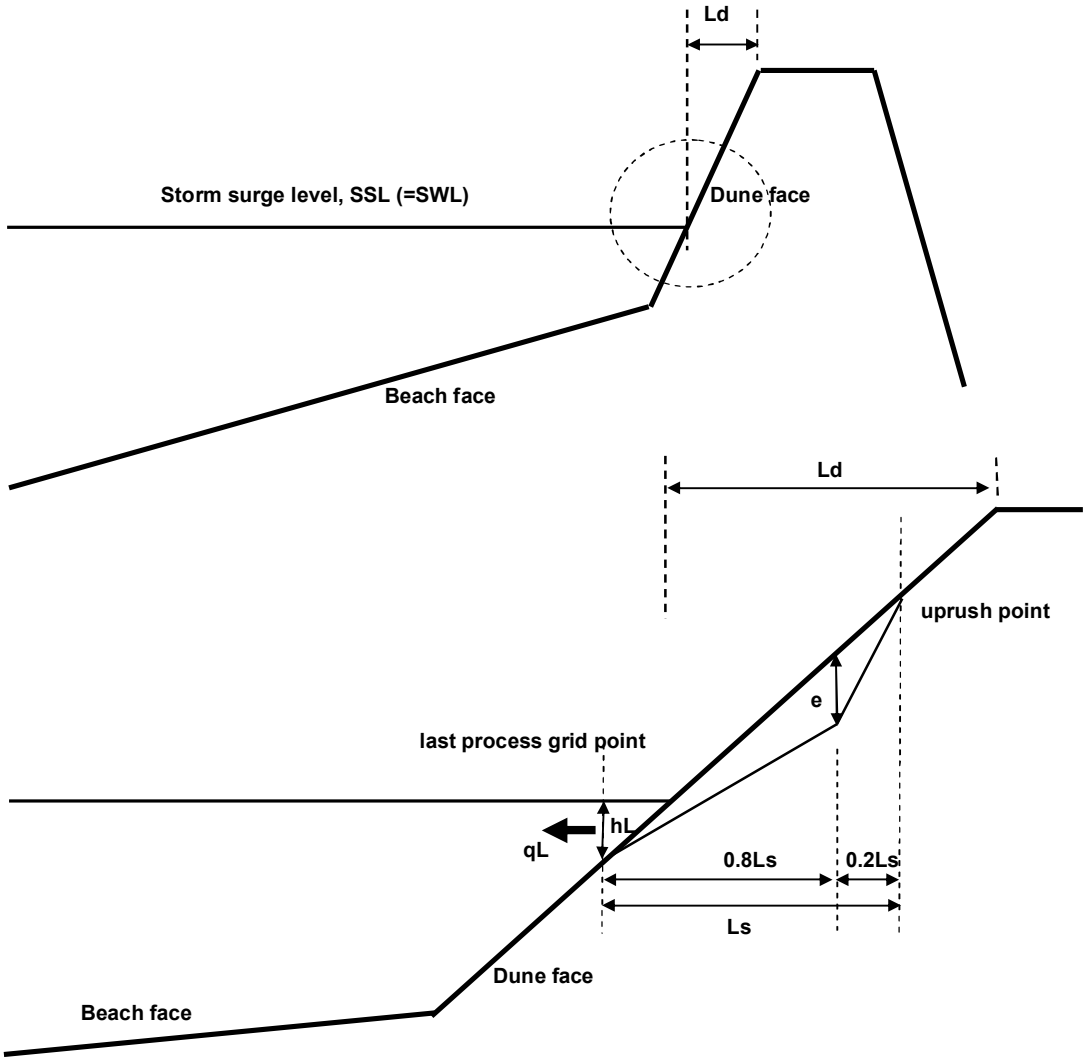

Figure 3.4 *Definition sketches of bed level changes in swash zone*
Top: Beach and dune face
Bottom: Erosion in swash zone at dune face

The runup level (above SWL plus set-up) associated with significant waves is estimated by (default approach):

$$R_s = 0.4\, H_{s,o} \tanh(3.4\zeta_o) \qquad (3.5a)$$

with: R_s=run-up level exceeded by 33% of the waves, $H_{s,o}$ =significant wave height at deep water, ζ_o=surf similarity parameter=tanβ $(H_{s,o}/L_{s,o})^{-0.5}$, $L_{s,o}$= wave length at deep water, tanβ=beach slope.

Equation (3.5a) yields a value of ζ_o=5 and R_s=3 m for $H_{s,o}$ =7.6 m, T_p=12 s, $L_{s,o}$=175 m (wave length at depth of 30 m), tanβ=1 (assuming a dune toe angle of about 45^o).

Van Gent (2001) has presented maximum run-up data for dikes with shallow foreshores based on local parameters rather than on deep water parameters. The experimental results can be represented by:

$$R_{2\%}/H_{s,toe}=2.3(\zeta)^{0.3} \quad \text{for } 1<\zeta<30 \tag{3.5.b}$$

with: $R_{2\%}$= run-up level exceeded by 2% of the waves, $\zeta=\tan\beta/[(2\pi/g)H_{s,toe}/T^2]^{0.5}$=surf similarity parameter, $H_{s,toe}$=significant wave height at toe of the structure, T = wave period, β=slope angle of structure, $L_o=T^2g/(2\pi)$.

Using: h_{toe}=2 m (dune toe at +3 m and water level at +5 m), $H_{s,toe}$=1.5 m, T=12 s, $\tan\beta$=1 (dune toe angle of 45^o), it folllows that ζ=12 and $R_{2\%}=2.3(\zeta)^{0.3}$ $H_{s,toe}$=7 m. Assuming $R_s=0.7$ $R_{2\%}$=5 m (for wave-induced erosion the R_s-value rather than the $R_{2\%}$-value should be used).

Larson et al. (2004) have analyzed typical dune erosion experiments in large–scale flumes and proposed:

$$R_s=0.158\,(H_{s,o}\,L_{s,o})^{0.5} \tag{3.5c}$$

Equation (3.5c) yields: R_s=6 m for $H_{s,o}$ =7.6 m and $L_{s,o}$ =175 m.

Based on **Equations (3.5a,b,c)**, the run-up level exceeded by 33% of the waves is roughly in the range of 3 to 6 m for a steep dune front.

The total erosion area (A_E) over the length of the dune erosion zone is defined as:

$$A_E=q_L\,\Delta t/((1-p)\rho_s) \tag{3.6a}$$

with: q_L=cross-shore transport computed at last grid point, Δt=time step, p=porosity factor of bed material, ρ_s=sediment density. The cross-shore transport generally is offshore directed during high energy (storm) conditions and onshore directed during low energy conditions. The erosion profile in the dune erosion zone with length L_s is assumed to have a triangular shape (see **Figure 3.4**), yielding $A_E=0.5eL_s$, with e=maximum erosion depth. The maximum erosion depth in the swash zone is:

$$e= 2q_L\,\Delta t/(L_s(1-p)\rho_s) \tag{3.6b}$$

In the case of onshore-directed transport (q_L) at the last grid point, the same procedure is followed resulting in accretion with a triangular shape (swash bar generation). This may occur during low-energy events (post storm conditions).

3.9 Bed level changes

Bed level changes are described by:

$$\rho_s(1-p)\partial z_b/\partial t + \partial(q_t)/\partial x = 0 \tag{3.7a}$$

with: z_b= bed level to datum, q_t= q_b + q_s= volumetric total load (bed load plus suspended load) transport, ρ_s= sediment density, p= porosity factor.

In discrete notation:

$$\Delta z_{b,x,t} = -[(q_{t,})_{x-\Delta x} - (q_t)_{x+\Delta x}]\ [\Delta t/(2\ \Delta x(1-p)\rho_s] \quad (3.7b)$$

with: Δt= time step, Δx= space step, $\Delta z_{b,i,x,t}$ = bed level change at time t (positive for decreasing transport in positive x-direction, yielding deposition).
The new bed level at time t is obtained by applying an explicit Lax-Wendorf scheme, as follows:

$$z_{b,x,t} = z_{b,x,t-\Delta t} + \Delta z_{b,x,t} + \gamma_b[1/2(z_{b,x-\Delta x,t-\Delta t} + z_{b,x+\Delta x,t-\Delta t}) - z_{b,x,t-\Delta t}] \quad (3.7c)$$

with: γ_b= smoothing factor (between 0.001 and 0.1).
The numerical solution method of the bed level computation introduces numerical errors. The total numerical error (ΔA) after a time step Δt can be evaluated from the following expression:

$$\Delta A = [(1/((1-p)\rho_s)\int(q_{t,x=0}-q_{t,x=L})dt]-[\int(z_{b,t+\Delta t}-z_{b,t})dx] \quad (3.7d)$$

with: ΔA= numerical error (in m^2) of total bed level change accumulated along the profile, Δt= time interval, p= porosity factor of bed material, ρ_s= sediment density, $q_{t,x=0}$= total load transport at x=0, $q_{t,x=L}$= total load transport at x=L, $z_{b,t+\Delta t}$= bed level at time $t+\Delta t$, $z_{b,t}$= bed level at time t.

The numerical error ΔA is zero, if the total volume of sediment per unit width entering or leaving the section with length L during the time interval Δt is equal to the total bed level change along the section over the time interval Δt. Generally, the numerical error is non-zero and should be removed from the profile. The total numerical error is evaluated after each time step Δt and is distributed along the profile in proportion to the local bed level changes and these "error"-bed level changes are subtracted from the actual bed levels.

3.10 Bed sliding at steep slopes

The bed level in the swash zone at the dune face may become so steep due to wave-induced erosion and other undermining processes that the local bed becomes unstable resulting in local bed failure. A wedge-shaped part of the dune face will slide downward to settle at the toe of the dune face (see **Figure 1.3**), where it can be eroded again by wave-induced processes (**Van Thiel de Vries et al., 2007**). The sliding procedure is a post-processing procedure after each time step, which is repeated until the bed is stable everywhere along the profile.
The local bed is assumed to slide out, if (see **Figure 3.5**):

$$\tan(\beta) > \tan(\alpha_x) \quad (3.8a)$$

with: $\tan(\alpha_x)=(z_{bo,i+1}-z_{bo,i})/(x_{i+1}-x_i)$ and β=maximum bed slope angle (input parameter), $z_{bo,i+1}$=old bed level at point i+1, $z_{bo,i}$=old bed level at point i

The new bed level at point x_{i+1} will become:

$$z_{bn,i+1}=z_{bo,i}+(x_{i+1}-x_i)\tan(\beta) \quad (3.8b)$$

The bed level difference b (see **Figure 3.5**) is:

$$b=z_{bo,i+1}-z_{bn,i+1} \quad (3.8c)$$

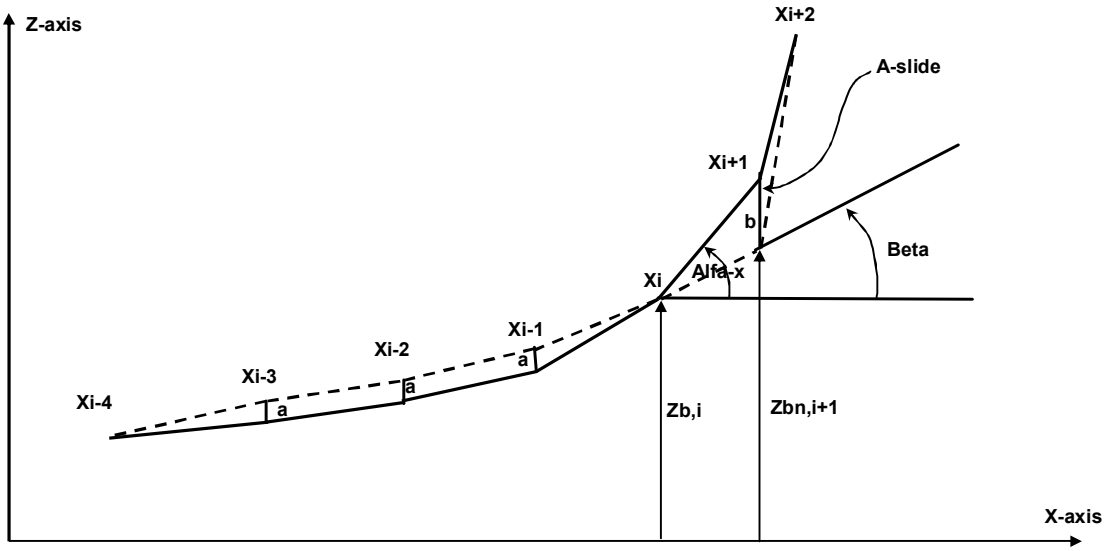

Figure 3.5 *Definition sketch of local bed sliding due to soil mechanical failure*

The sliding area is defined as the area between the new bed levels (after sliding) and the old bed levels between the points i+2 and i:

$$A_{slide}=0.5(z_{bo,i+1}-z_{bn,i+1})(x_{i+2}-x_i) \quad (3.8d)$$

This sliding area is assumed to be deposited between the grid points i and i-4. The deposition values at points i-1,i-2 and i-3 are assumed to be equal and are defined as (deposition area is equal to sliding area):

$$a=2A_{slide}/(x_i+x_{i-1}-x_{i-3}-x_{i-4}) \quad (3.8e)$$

The bed levels at the points i-1, i-2 and i-3 become:

$$\begin{aligned} z_{bn,i-1}&=z_{bo,i-1}+a \\ z_{bn,i-2}&=z_{bo,i-2}+a \\ z_{bn,i-3}&=z_{bo,i-3}+a \end{aligned} \quad (3.8f)$$

The bed profile in the zone around the last grid point is slightly smoothed (10%) after each time step to reduce bed irregularities (small bars) in this zone dus to the sliding process, by using the following scheme:

$$z_{bn}=z_{bn}+0.1(z_{bn,i+1}-2z_{bn,i}+z_{bn,i-1}) \quad (3.8g)$$

4 Modelling results of large-scale and small-scale laboratory data

4.1 Modelling of large-scale Deltaflume data

4.1.1 Experimental results

New experiments have been carried out in the Deltaflume (length of 233 m, width of 5 m and depth of 7 m) of **Delft Hydraulics** in the period October 2005 to March 2006, focussing on the effect of the wave period and type of wave spectrum on the dune erosion volumes. The data of the tests considered herein are shown in **Table 4.1**. Additional data is given by **Delft Hydraulics (2006a,b)**.

Test number	Offshore wave height (m)	Wave period (s)	Type of wave spectrum
T01/T06	1.5	4.9	single-topped
T02	1.5	6.1	single-topped
T03/T05	1.5	7.4	single-topped
T16	1.5	7.4 (largest value)	double-topped

Table 4.1 *Data of dune erosion tests in Deltaflume of Delft Hydraulics (2005 and 2006a,b)*

The initial bed profile (of all tests, see **Figure 4.1**) consists of five linear sections:

- transition section (length of 45 m) with slope of 1 to 25;
- shoreface (length of 124 m) with slope of 1 to 90, foreshore (length of 17.5 m) with slope of 1 to 35;
- beach (length of 5 m) with slope of 1 to 10, and
- dune (length of 3 m) with slope of 1 to 1.5.

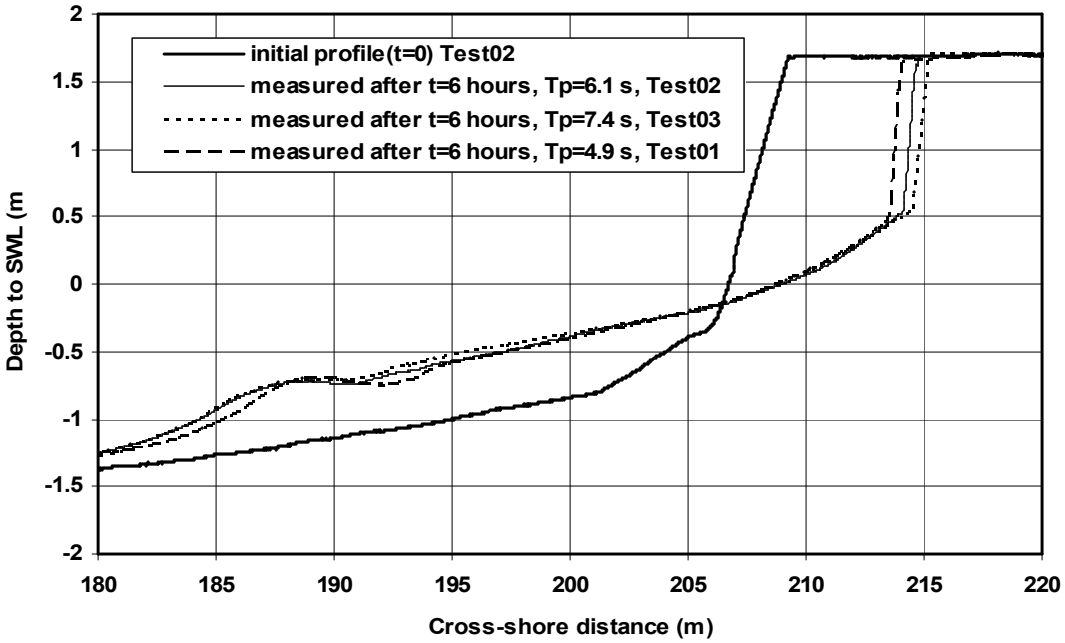

Figure 4.1 *Measured bed profiles after 6 hours for Tests T01, T02 and T03*

The bed material used is marine sand with d_{10}=0.142 mm, d_{50}= 0.2 mm and d_{90}= 0.286 mm. The fall velocity of the bed material has been determined by tests in a settling tube resulting in: w_s=0.023 m/s at a temperature of 9 ^{o}C. The still water level (SWL) representing the storm surge level (SSL) is set at 4.5 m above the original flume bottom. Irregular waves with a single topped Pierson-Moskowitz spectrum (single-topped) have been generated during 6 hours at the entrance of the flume during most tests. A double topped wave spectrum has been used in Test T16. Most tests have been repeated twice to perform detailed process measurements during the second test. The initial profile of all tests with respect to the still water level (SWL) is shown in **Figure 4.1**; the eroded profiles after t=6 hours are shown in **Figures 4.2** and **4.3**. The dune shows erosion above a level of -0.2 m (to SWL); deposition can be observed offshore of the -0.2 m bed level over a length of about 30 m. The erosion area increases by about 15% (based on T01 and T03) in the case of a larger wave period (from 4.9 s to 7.4 s), see also **Figure 4.1**. The erosion area decreases slightly by about 10% in the case of a double-topped spectrum (based on T03 and T16), see also **Figure 4.2**.

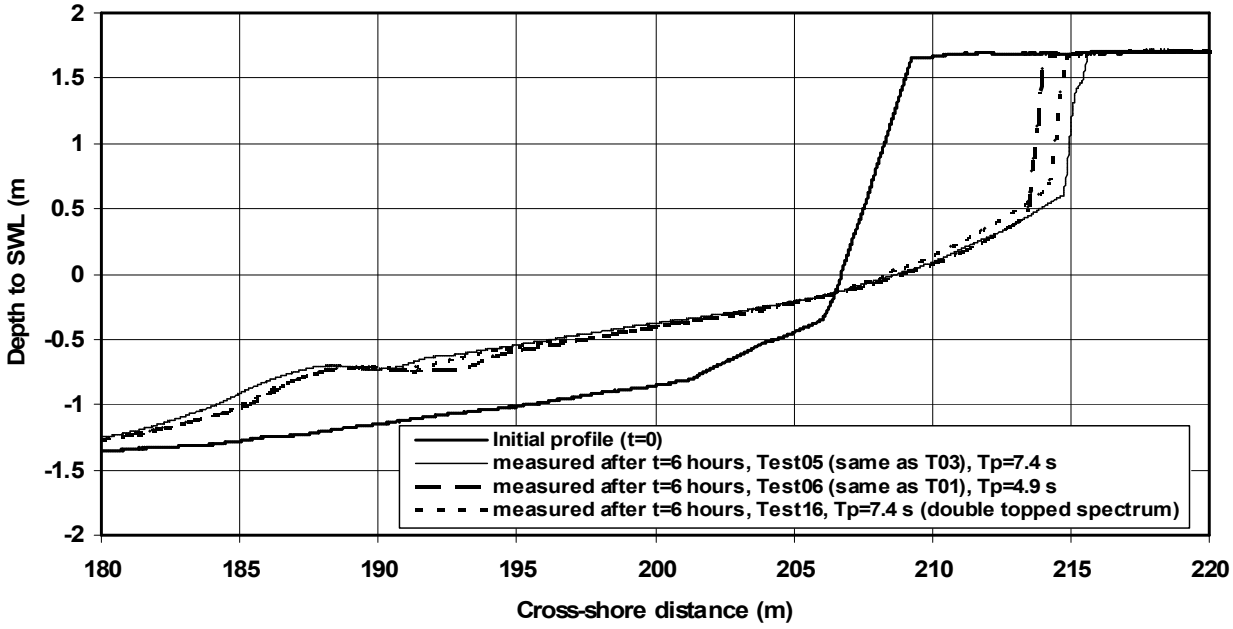

Figure 4.2 *Measured bed profiles after 6 hours for Tests T01, T03 and T16*

4.1.2 Hydrodynamic parameters for model input

The mathematical model simulations are focussed on Test T01 with the smallest wave period of T_p=4.9 s and on Test T03 with the largest wave priod of T_p=7.4 s. The incoming (offshore) significant wave height is 1.5 m. Since the **CROSMOR**-model is a model for individual waves; the wave height distribution is represented by a Rayleigh-type distribution schematized into 6 wave classes. Based on computed parameters in each grid point for each wave class, the statistical parameters are computed in each grid point. The limiting water depth is set to 0.1 m (water depth in last grid point). Based on this value (including the computed wave-induced set-up), the model determines by interpolation the number of grid points (x=0 is offshore boundary, x=L is most landward computational grid point of hydrodynamic and sand transport parameters). The effective bed roughness in the violent dune erosion zone is set to a fixed value of 0.02 m; the bed roughness outside the dune erosion zone is predicted by the model.

Figure 4.3 shows the computed significant wave heights (initial values at t=0) along the cross-shore profile for two tests T01 and T03 based on a fixed breaking coefficient γ=0.6 and a variable breaking coefficient (depending on bed slope and wave steepness). This latter approach is the default approach of the model. Measured H_{m0}-wave heights (based on spectral parameters) are also shown. Comparison of measured and computed data shows:

- computed wave heights along the bed profile are in close agreement with measured data for a breaking coefficient of γ=0.6; the computed wave heights are somewhat too small (10% to 15%) for a variable γ-factor (default approach);
- computed wave heights are somewhat too small in front of the dune face (x=205 m);
- measured wave heights show no marked influence of the wave period; the computed wave heights are slightly larger (5% to 10%) for a larger wave period.

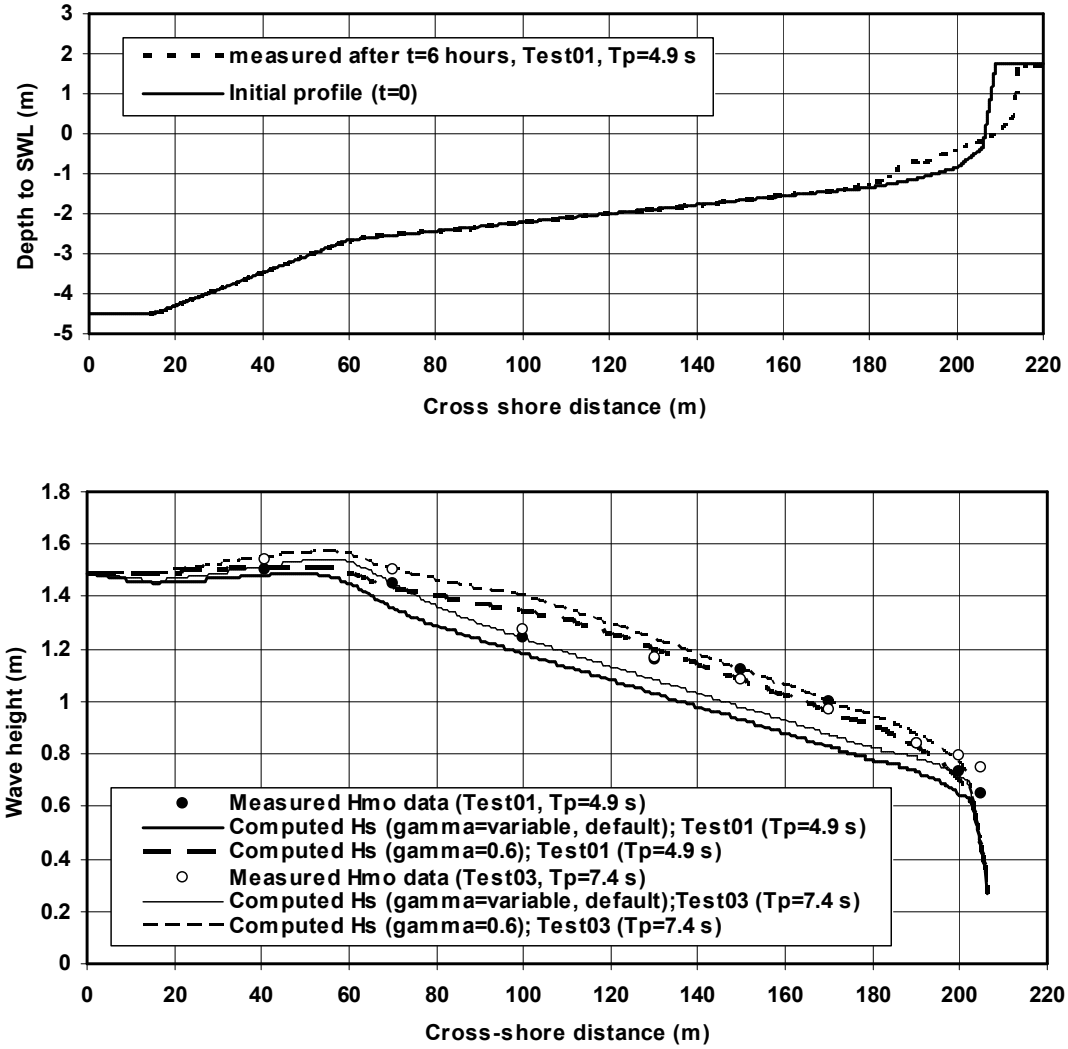

Figure 4.3 *Top: Measured bed profiles*
Bottom:Computed and measured wave heights for Tests T01 and T03 (initial values)

Figure 4.4 shows the computed significant peak orbital velocity near the bed in onshore and in offshore direction for the two tests T01 and T03. The significant value refers to the mean value of the 33% highest values. The computed results show a marked influence of the wave period on the onshore peak orbital velocity; larger values (15% to 20%) for a larger wave period. The offshore peak orbital velocity is not much affected by the wave period. The increase of the peak onshore velocity will have a significant effect on the sand transport process as this parameter is being used to determine the wave-related bed-shear stress and hence the reference concentration.
Figure 4.5 shows the computed undertow velocity along the bed profile. The computed values show a strong increase up to a value of -0.45 m/s in the shallow surf zone just in front of the dune face. A larger wave period results in larger undertow velocities in the middle surf zone due to the larger computed wave heights. Values in the range of -0.08 to -0.1 m/s have been measured in the lower portion of the water depth at x=41 m from the wave board (edge of surf zone). The computed values in this zone are somewhat smaller than the measured values.

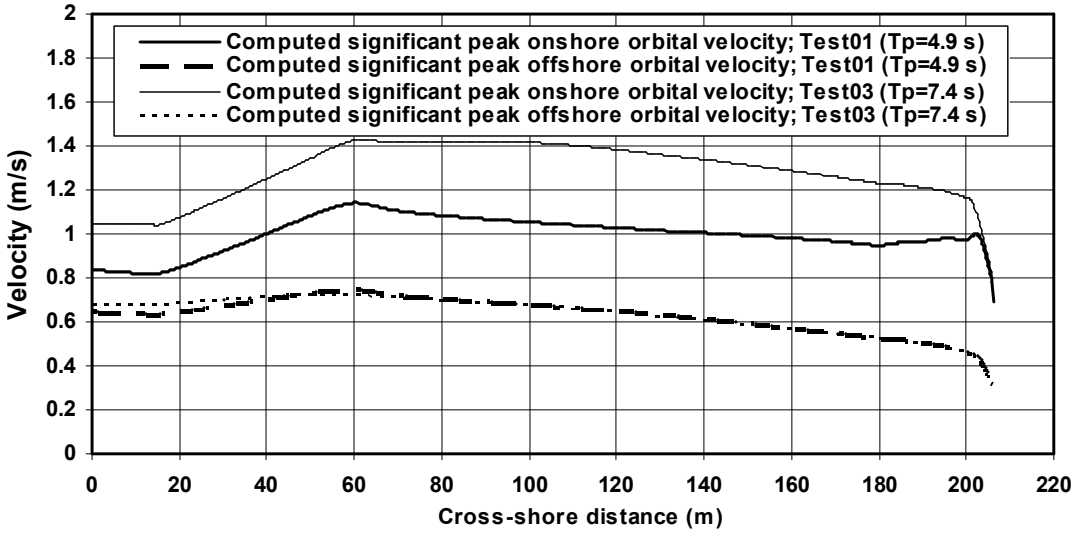

Figure 4.4 *Peak orbtial velocities near the bed for Tests T01 and T03 (initial values)*

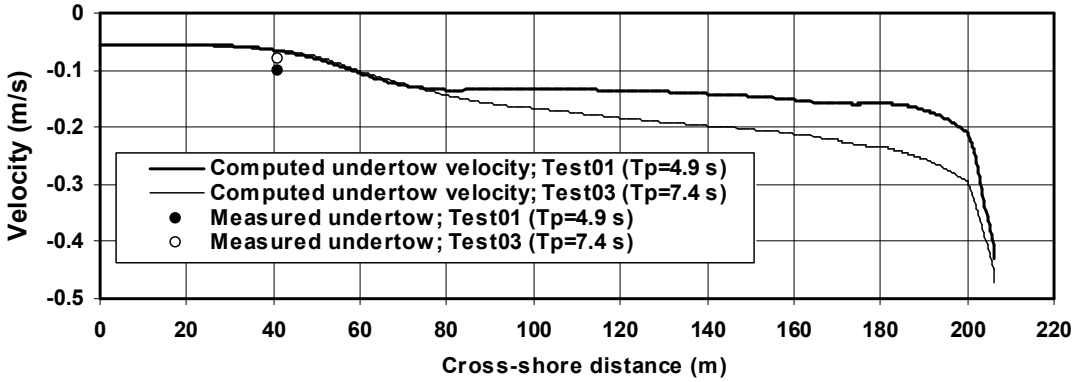

Figure 4.5 *Offshore directed undertow velocities for Tests T01 and T03 (initial values)*

4.1.3 Reference concentrations and sand transport rates of Deltaflume tests

Figure 4.6 shows the computed reference concentrations and the offshore-directed suspended sand transport rates at initial time (t=0) based on bed material diameter of 0.2 mm. Since the computed bed load transport is negligibly small, these values are not shown. The model results are shown for four cases:
a) long waves and no extra turbulence (sef=1);
b) no long waves and no extra turbulence (sef=1);
c) long waves and extra turbulence (sef=2.5);
d) no long waves and extra turbulence (sef=2.5).

The sef-factor is the suspension enhancement factor (multiplication factor) due to extra turbulence enhancing the time-averaged bed-shear stress and hence the reference concentration and the sediment mixing coefficient in the shallow surf zone. The sef-parameter has been determined by calibration. A value of sef=1 refers to the default

transport model. The best overall agreement between computed and measured bed profiles after 6 hours is found for a sef-value of about 2.5 (see **Section 3.7**). The sef-parameter is assumed to be constant in time, but this assumption basically is not correct. The sef-parameter should decrease in time as the dune erosion process will gradually diminish due to the development of a new coastal profile representative for storm conditions. The gradual decay of the sef-parameter can not be represented by the simplistic schematization used herein. Basically, the sef-parameter should be related to the wave breaking and wave collision processes (future research).

Figures 4.6A,B,C, 4.7 and **4.8** show the computed reference concentration and seaward-directed suspended transport in the shallow dune erosion zone in front of the dune face. The computed reference concentration in the swash zone in front of the dune shows an increase by a factor of about 2 (from 2 to 4 kg/m^3) when long waves are included. Inclusion of the suspension enhancement factor (extra turbulence sef=2.5) yields an increase of the reference concentration in the swash zone by a factor of about 10 (from 4 to about 50 kg/m^3). When the long wave effects are neglected the maximum reference concentration is about 20 kg/m^3. Measured concentrations up to 50 kg/m^3 have been observed in this zone, see **Figures 4.6B,C** (**Delft Hydraulics, 2006b**). It is concluded that the inclusion of extra turbulence effects on the bed-shear stress in the dune erosion zone is essential to model the near-bed concentrations correctly.

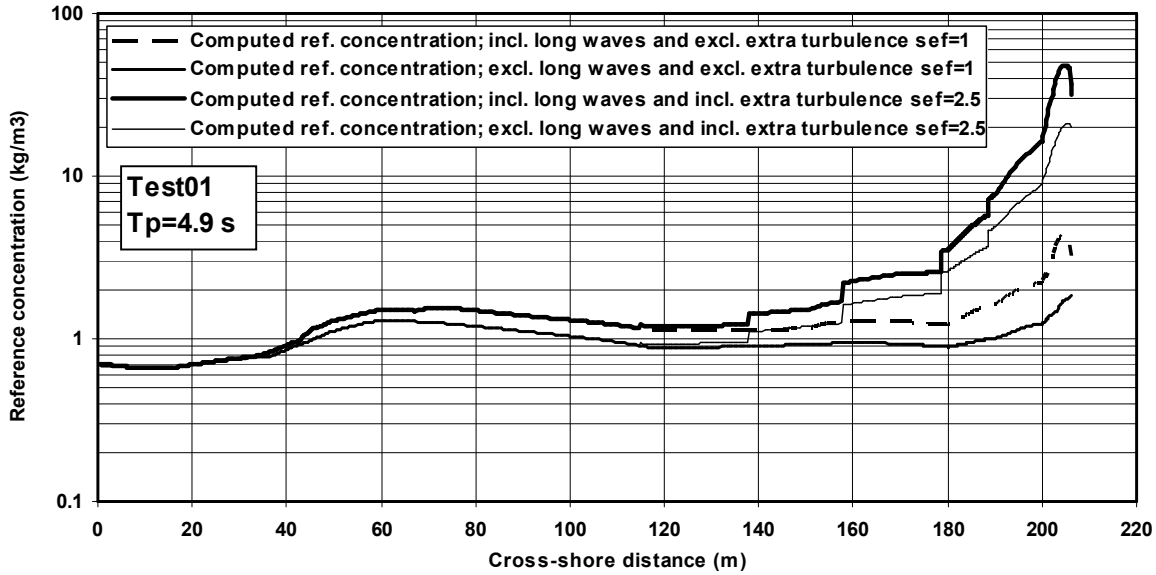

Figure 4.6A *Computed reference concentration for Test T01 (initial values)*

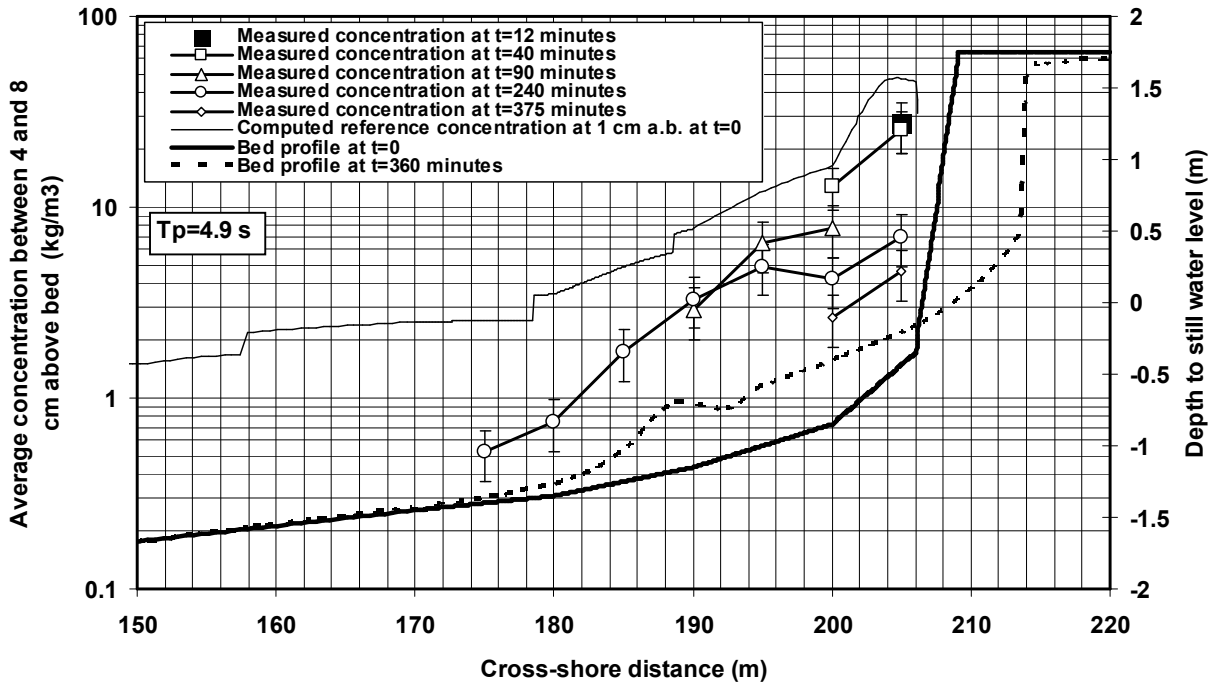

Figure 4.6B *Measured and computed reference concentration for Test T01 (initial values)*

Figure 4.6B shows measured and computed concentrations near the bed for Test T01 (T_p=4.9 s). The measured concentration is the average value of the concentrations in the lowest three measurement points (between 4 and 8 cm above the bed). Just after the start of the experiment the concentrations show a strong increase from about 0.5 kg/m^3 at 175 m to about 30 kg/m^3 at 205 m. The concentrations in the swash zone (205 m) decrease in time to about 3 kg/m^3 after 375 minutes. The computed reference concentrations (defined at 1 cm above the bed) at initial time including the effects of long waves and the extra turbulence (sef=2.5) are of the right order of magnitude in the swash zone. The computed concentrations outside the surf zone (<175 m) are much too large, because these concentrations are defined at 1 cm above the bed whereas the measured concentrations are the average values of the concentrations in the layer between 4 and 8 cm above the bed. **Figure 4.6C** show similar results for Test T03 (T_p=7.4 s). The measured and computed concentrations are somewhat larger in case of a larger wave period.

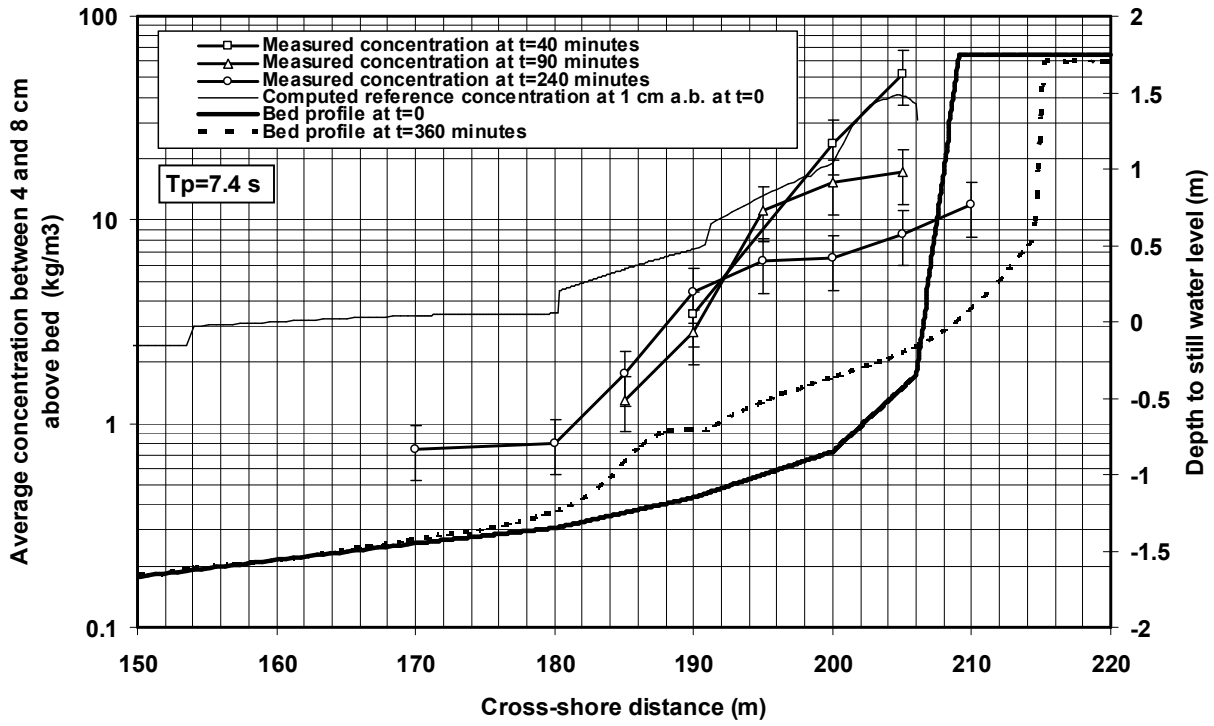

Figure 4.6C *Measured and computed reference concentration for Test T03 (initial values)*

The non-smooth distribution of the computed concentration is caused by the predicted bed roughness values which vary along the bed profile and are magnified by the sef-factor. In the case of a constant bed roughness the concentration distribution is much smoother (see **Figure 4.7** for Test T01).

The suspended sediment transport (seaward-directed) shows a similar pattern with increasing values if the long wave effects and the extra turbulence effects are included, see **Figure 4.8**. The sef-factor is used to represent the increase of the transport capacity in the zone just in front of the dune face where wave collision and breaking are the dominant processes creating a relatively large level of turbulent fluid motions. The sef-parameter is supposed to be primarily related to the wave collision effects in the shallow surf zone, which are not represented in the CROSMOR-model. Hence, the sef-parameter cannot be related to a physical model parameter, and is therefore used as an input parameter (calibration parameter).

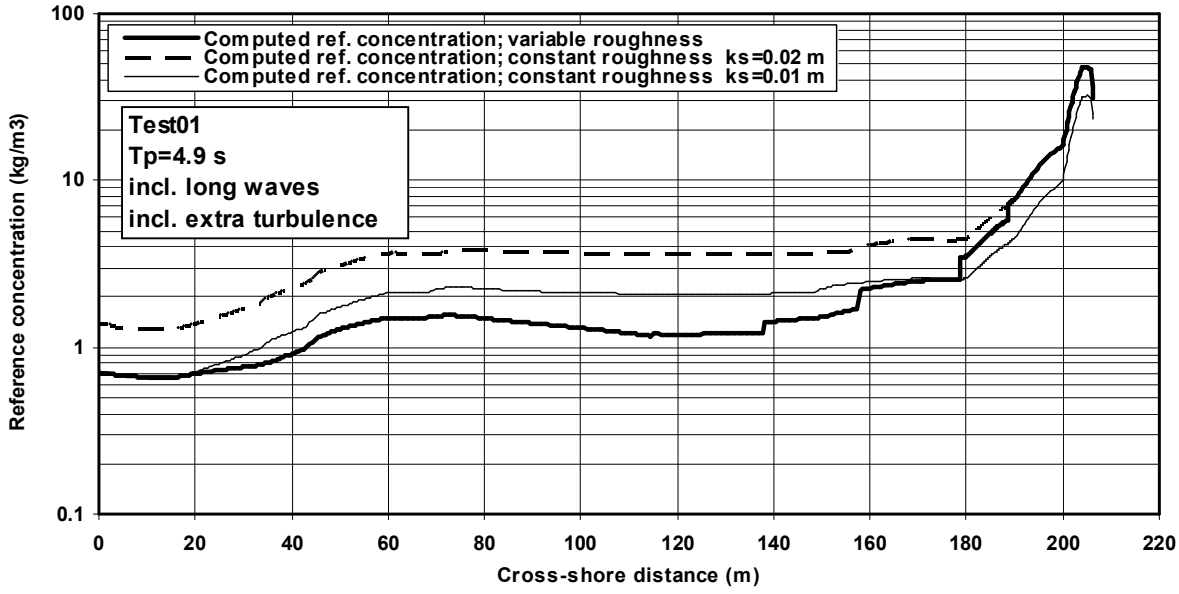

Figure 4.7 *Computed reference concentration for Test T01 (initial values); effect of bed roughness*

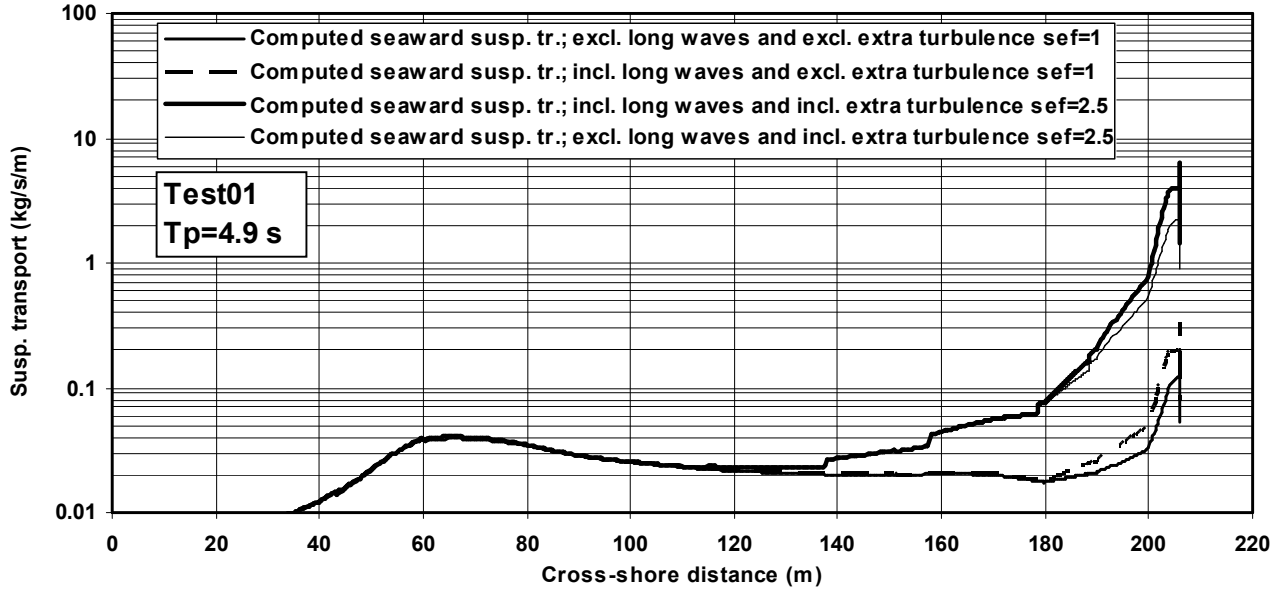

Figure 4.8 *Computed seaward suspended sediment transport for Test T01 (initial values)*

Figure 4.9 shows the effect of the wave period on the computed reference concentration and the seaward-directed suspended transport for tests T01 and T03. A larger wave period yields a larger reference concentration an hence suspended transport. The increase of the reference concentration is caused by the increase of the peak onshore orbital velocity and hence the wave-related bed-shear stress for a larger wave period. The suspended transport in the outer surf zone (x<70 m) is reduced, because the reference concentration also affects the onshore-directed wave-related suspended transport (wave asymmetry effect). This latter effect (wave asymmetry effect) is not of importance in the shallow surf zone, where the current-related suspended transport due undertow velocities is dominant.

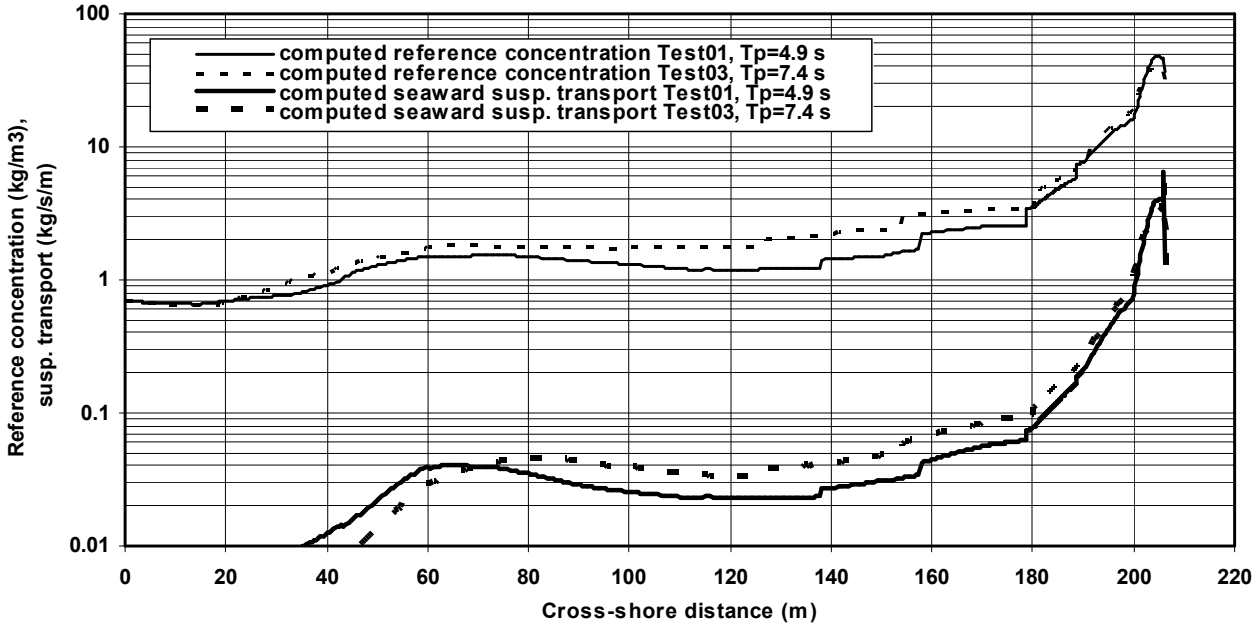

Figure 4.9 *Computed reference concentration and suspended transport (initial values) for Tests T01 and T03*

4.1.4 Simulated morphology of Deltaflume tests

Calibration

The dune erosion profiles of Test T01 have been used to calibrate the sef-parameter. The sef-parameter is the suspension enhancement factor (multiplication factor) acting on the time-averaged bed-shear stress and hence on the reference concentration and the sediment mixing coefficient in the shallow dune erosion zone; sef=1 refers to the default transport model.

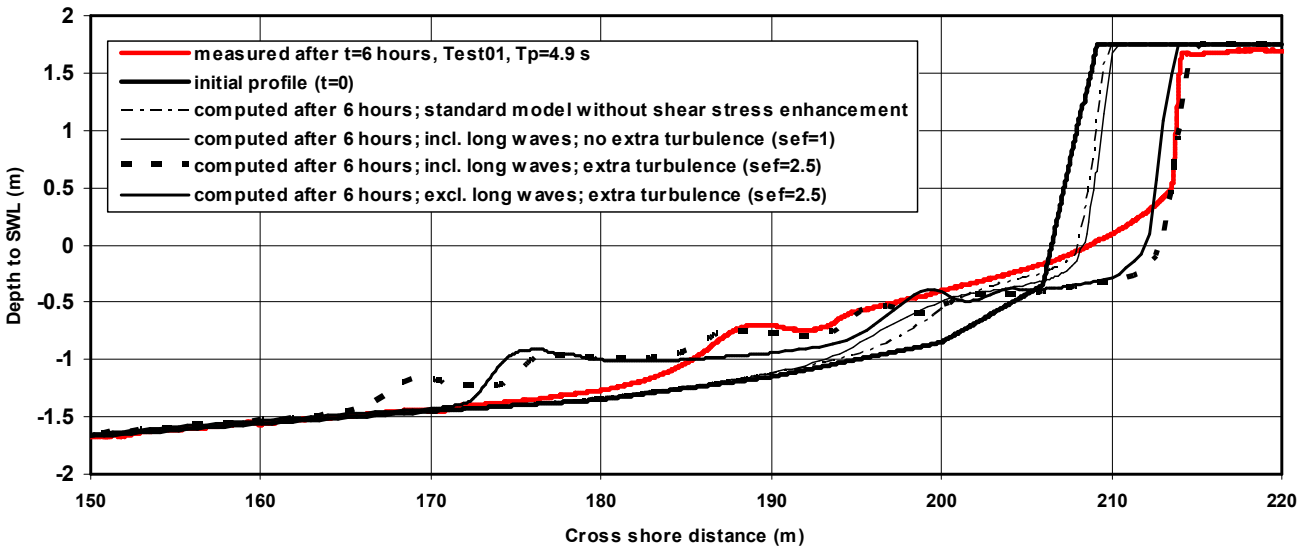

Figure 4.10A *Computed bed profiles after 6 hours for Test T01*

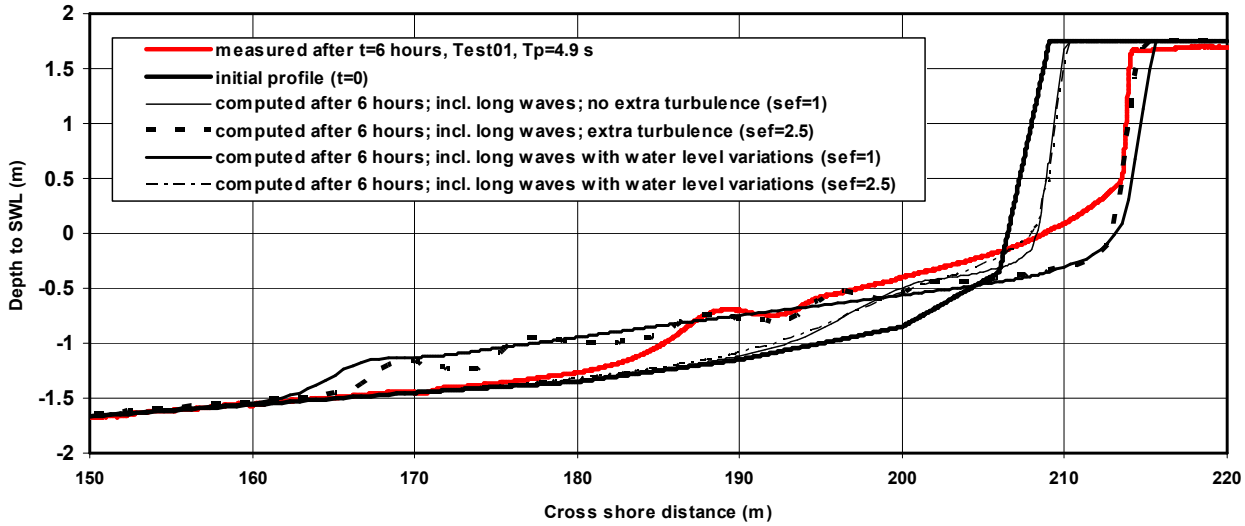

Figure 4.10B *Computed bed profiles after 6 hours for Test T01*

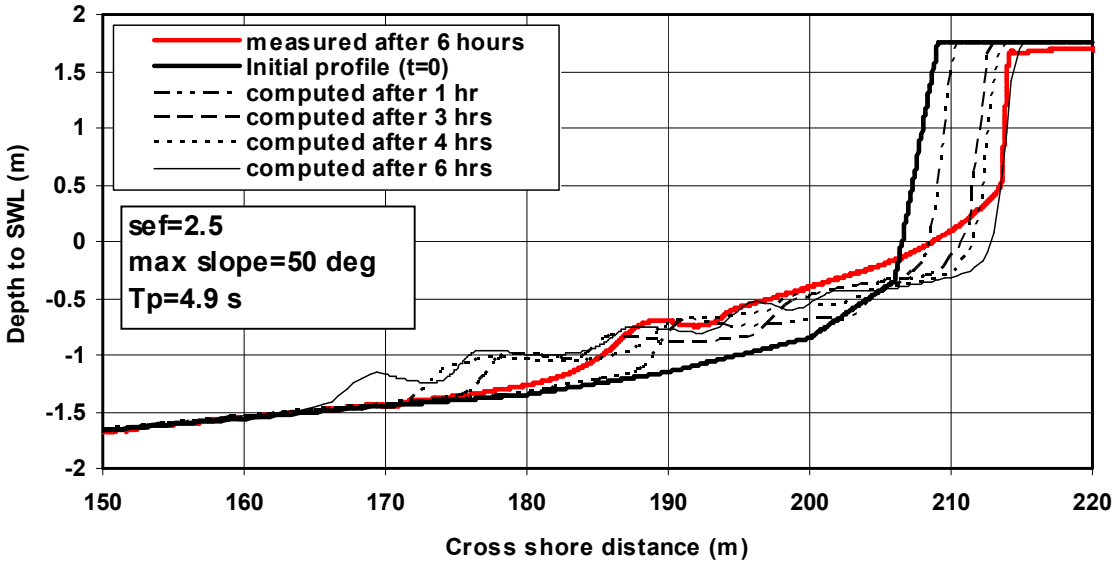

Figure 4.11A *Time development of computed bed profiles for Test T01*

Figure 4.10A shows computed bed profiles for Test T01 based on sef=1 and sef=2.5 with and without the long wave effect. The long wave effects only includes the near-bed velocity variations; the low-frequency water level variations are not included. The maximum dune face slope is set to 50 degrees (failure and sliding for slope angles larger than 50 degrees). A sef-value of 1 (default sand transport model) yields

insufficient erosion of the dune face (underestimation by a factor of about 3). Inclusion of the long wave effect increases the dune erosion only slightly (10% to 20%), see **Figure 4.10A**. **Figure 4.10B** shows similar results for the case with inclusion of the low-frequency water level variations (amplitude of 0.2 m). In the latter case the dune erosion is marginally larger (about 5%). The best overall agreement between computed and measured dune face recession (shoreline recession) after 6 hours is found for sef=2.5 with the long wave effect (on the near-bed velocities) included. It does not seem to be necessary to include the low-frequency water level variations. The erosion volume above SWL is approximately 10% too large; the erosion volume below SWL is much too large. The computed bed slope in the beach zone is too flat (tan β=0.02 with β=beach slope) compared with the obserbed bed slope in the beach zone (tan $\beta_{observed}$=0.04). The time development of the computed bed profiles (sef=2.5) is shown in **Figure 4.11A**. It can be seen that the erosion process very gradually slows down. The computed bed level profiles show small-scale bars which are generated by small irregularities in the spatial distribution of the suspended sediment transport introduced by the sef-parameter. These irregularities disappear for a smaller time step (see later).

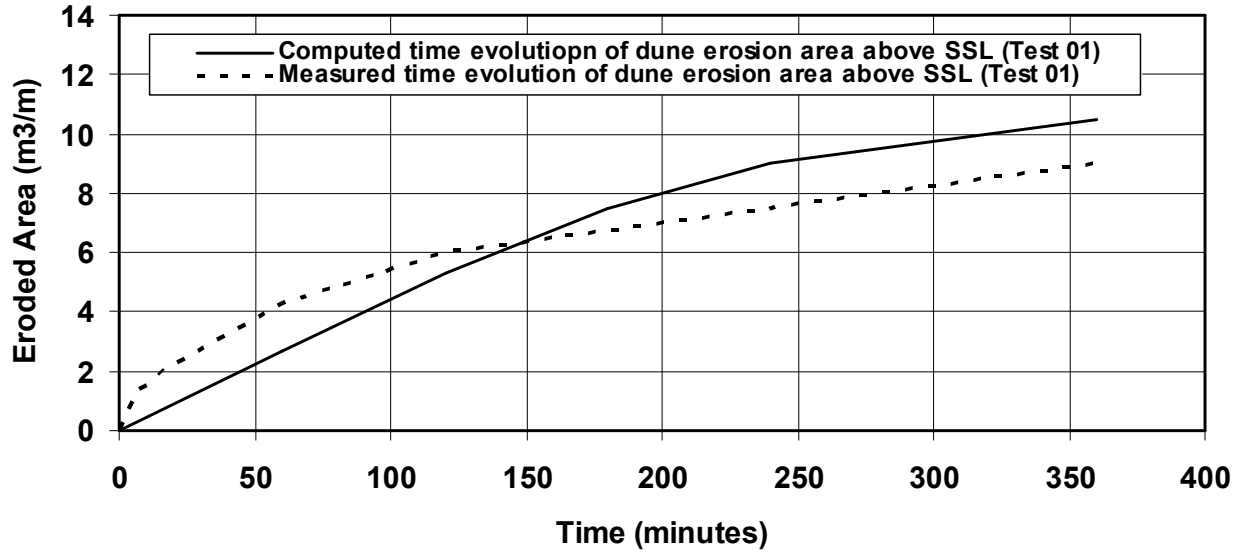

Figure 4.11B *Time development of computed and measured dune erosion area above SSL for Test T01*

Figure 4.11B shows the computed and measured dune erosion area above storm surge level (SSL) as a function of time. A significant difference between computed and measured results can be observed. The measured dune erosion area is much larger (about 50%) than the computed value in the initial phase (time<150 minutes) of the dune erosion process. This initial effect with relatively large erosion values can not be represented by the model. Almost half of the total dune erosion is produced in the first 60 minutes of the total test duration of 360 minutes (6 hours). At the end of the test duration the measured and computed values are within 15% of each other; the computed values are somewhat larger than the measured values.

Hereafter, the following effects will be studied using the data of Test T01:

- effect of time step and dune toe smoothing;

- efftec of dune face sliding and maximum dune face slope;
- effect of swash zone length;
- effect of wave breaking coefficient and roller model;
- effect of bed roughness in dune erosion zone;
- effect of bed material diameter;
- effect of wave period;
- effect of wave spectrum.

Effect of time step and dune toe smoothing

Since the bed level updating is done by using an explicit numerical solution method, the allowable morphological time step is quite small for these extreme conditions. The bed level updating method also involves a smoothing parameter. A smaller time step involves more smoothing because the smoothing procedure is applied after each time step. The influence of the time step on the computed results is shown in **Figure 4.12** for time step values of 90, 180 and 360 s. A time step of 360 s yield the largest dune erosion area; the dune erosion area is not much affected for time step values of 180 and 90 s. The smallest time step of 90 s produces a smooth bed in the offshore zone (x<200 m). Most runs of the sensitivity study are based on a time step of 180 s. **Figure 4.13** shows results for a low, medium and high value of the smoothing parameter. Small-scale bar development can be suppressed by using a medium smoothing factor. The dune erosion area is only slightly affected by the smoothing parameter.

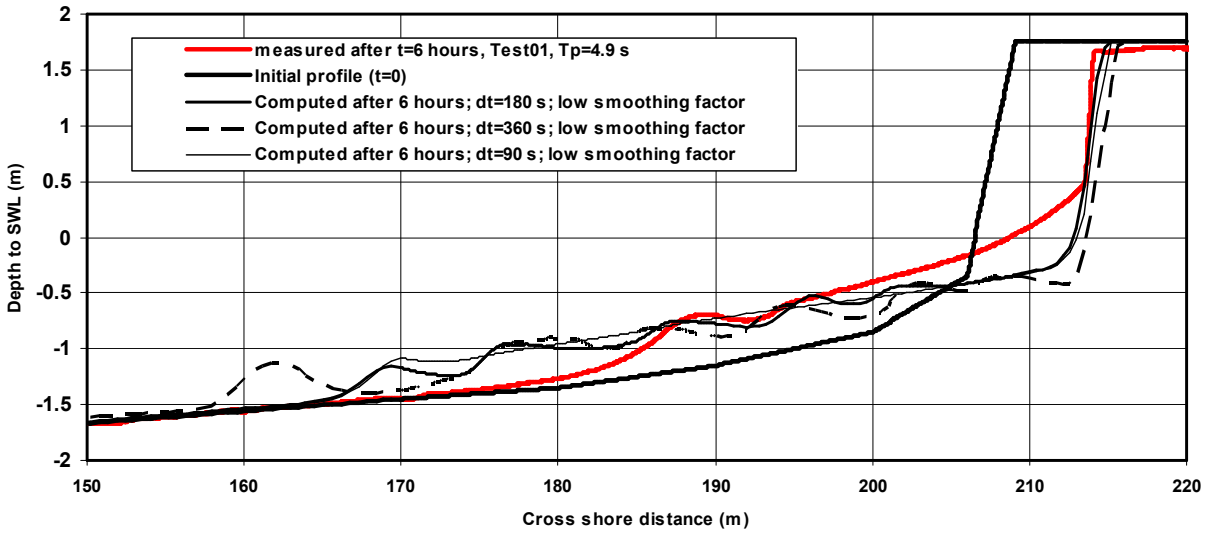

Figure 4.12 *Effect of time step value on computed bed profiles for Test T01*

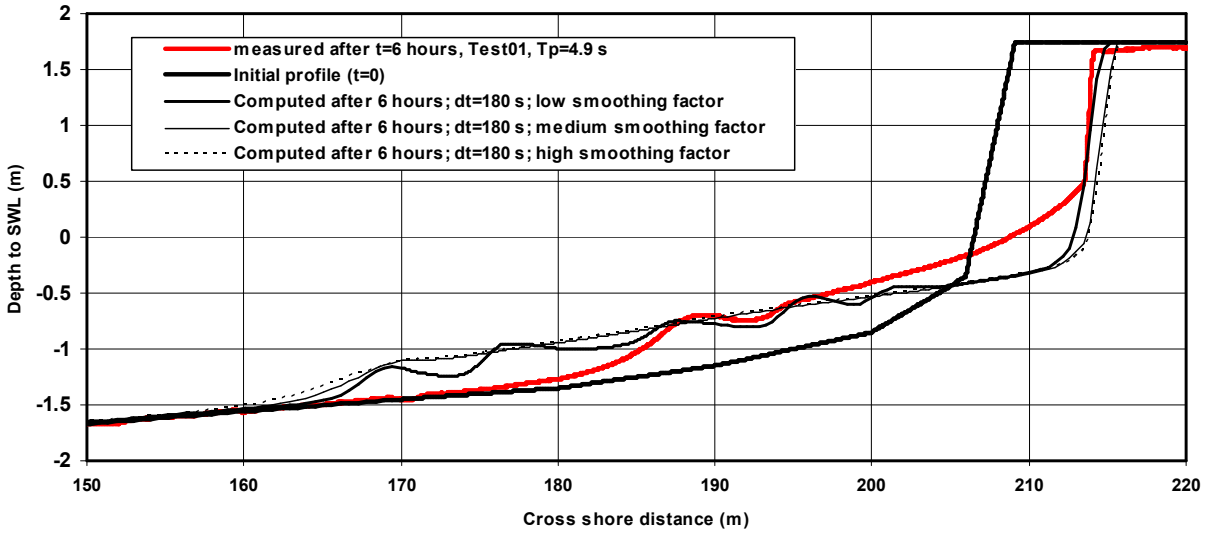

Figure 4.13 *Effect of numerical smoothing factor on computed bed profiles for Test T01*

Effect of maximum dune face slope

Figure 4.14 shows the effect of dune face sliding (time step of 180 s and low smoothing parameter). Horizontal dune erosion is largely suppressed when the dune face sliding procedure is not taken into account. In the latter case the erosion mainly proceeds in the vertical direction resulting in a large-scale scour hole. Neglecting dune face sliding, the model produces a deep scour hole at the dune face position.

Figure 4.14 also shows the effect of the maximum dune face slope on the computed bed profile. The maximum slope has been varied in the range of 30 to 70 degrees. The initial dune face slope is about 35 degrees (slope of 0.7 to 1). The dune face slope steepens during the erosion process; the observed dune face slope after 6 hours is about 70 degrees (slope of 2.5 to 1). The model can simulate the slope steepening process to some extent. Using a maximum dune face slope of 50 degrees, the dune face slope after 6 hours is steepened from the initial value of 35 degrees to a value of about 45 degrees. A smaller value (30 degrees) of the maximum dune face slope yields a dune face slope of 30 degrees after 6 hours. A larger value (70 degrees) of the maximum dune face slope yields a lower dune face slope of about 60 degrees after 6 hours. This slope is somewhat smaller than the applied maximum slope of 70 degrees, which is caused by the applied dune toe smoothing procedure reducing the maximum dune face slope, particularly for relatively steep slopes. The upper dune face slope is largely affected by the smoothing procedure in the case of a slope of 70^{o}.

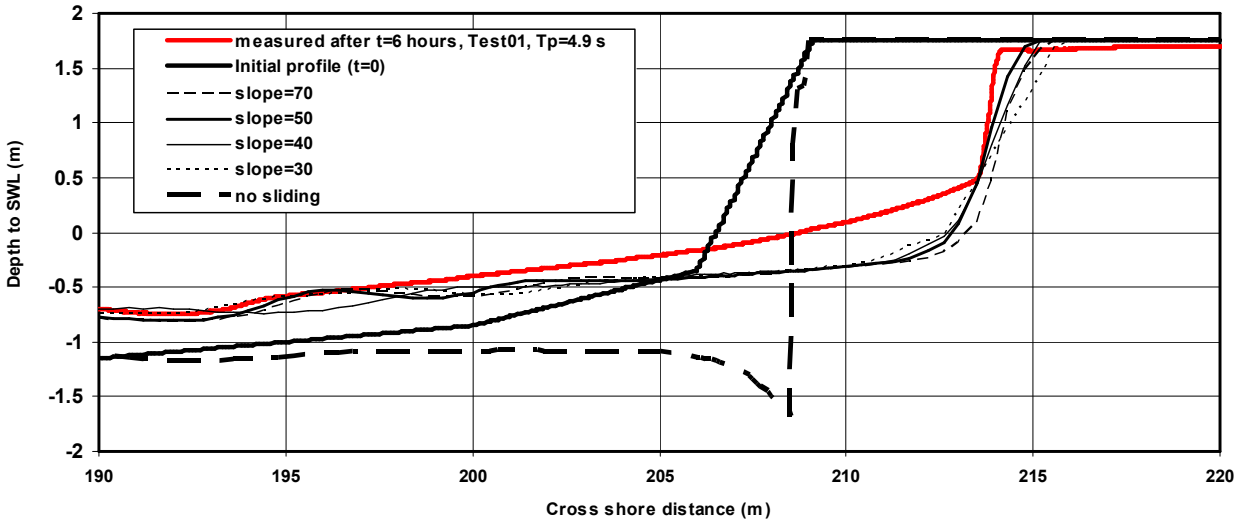

Figure 4.14 *Effect of dune face slope on computed bed profiles for Test T01*

Effect of length of dune erosion zone

Figure 4.15 shows the effect of the length of the dune erosion zone (L_s). This length scale is determined as the maximum value of 1) $L_s=6h_{L,m}$ with $h_{L,m}$= average water depth of last, five computational grid points or 2) $L_s=x_R-x_L$ with x_R=horizontal coordinate of run-up point and x_L=horizontal coordinate of last computational point. The water depth of the last computational point has been set to a value of $h_L=0.1$ m (input value) for the Deltaflume conditions. The water depth h_L is approximately equal to $0.05L_d$ for Test T01, with L_d=length of dune face (about 2.5 m). The length of the dune erosion zone is varied in the range of $L_s=3$ to 10 h_L or $L_s=0.15$ to $0.5L_d$.

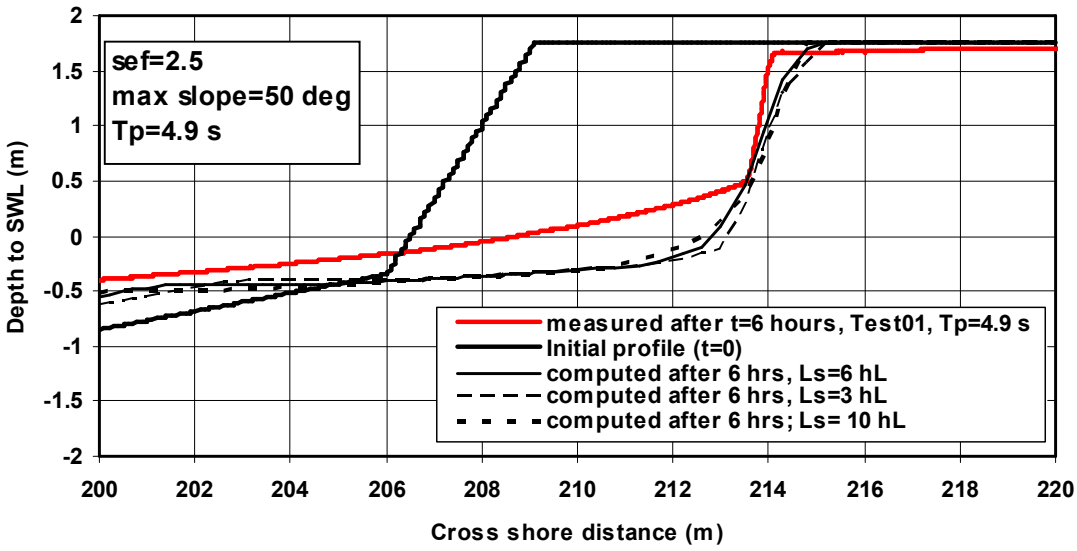

Figure 4.15 *Effect of length of dune erosion zone on computed bed profiles for Test T01*

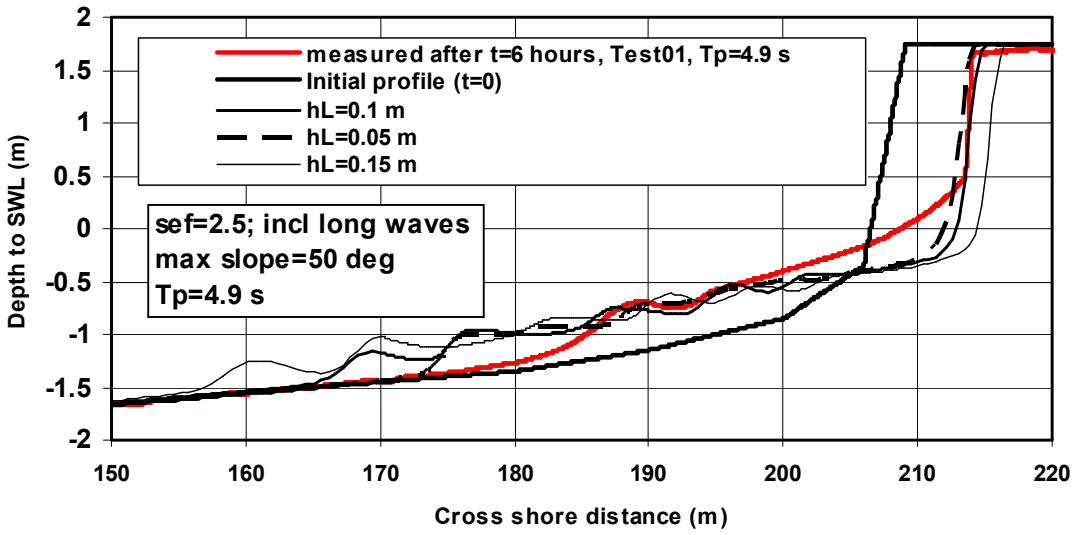

Figure 4.16 *Effect of water depth in last computational grid point on computed bed profiles for Test T01*

As can be observed in **Figure 4.15**, the length of the dune erosion zone has not much effect on the computed bed profile after 6 hours. A length of L_s=3 h_L leads to somewhat more erosion in the dune toe zone. The length of the dune erosion zone is also affected by the value of the water depth in the last computational grid point (h_L). The h_L-parameter affects the wave height and the suspended transport rate in the last grid point. **Figure 4.16** shows the effect of h_L (values of 0.05, and 0.15 m) on the bed profile for Test T01. The dune face erosion increases slightly with increasing values of the h_L-parameter.

The length of the dune rosion zone may also be affected by the type of run-up formula used. Using **Equation (3.5c)** in stead of **(3.5a)** produces similar results (not shown). Hence, the results are not noticeably affected by the type of run-up formula, provided that realistic run-up values based on observations are used

Effect of wave breaking coefficient and roller model

Figure 4.17 shows the effect of the wave breaking coefficient (either γ=variable or γ=0.6) and the inclusion or exclusion of the roller model for Test T01. The exclusion of the roller model leads to smaller undertow velocities in the shallow surf zone. The maximum undertow velocity is -0.28 m/s for the case without roller model, whereas the maximum undertow velocity is -0.45 m/s for the case with roller model (see **Figure 4.5**). Smaller undertow velocities (no roller model) yield smaller offshore-directed suspended transport rates and hence smaller erosion values.

The application of a constant wave breaking coefficient of γ=0.6 yields larger wave heights along the bed profile (see **Figure 4.3**) and hence large suspended rates resulting in an increase of the erosion rates and hence larger dune face recession. When the sef-value is reduced from 2.5 to 2, the dune erosion using γ=0.6 is almost the same as that for γ=variable (default model), as shown in **Figure 4.18**.

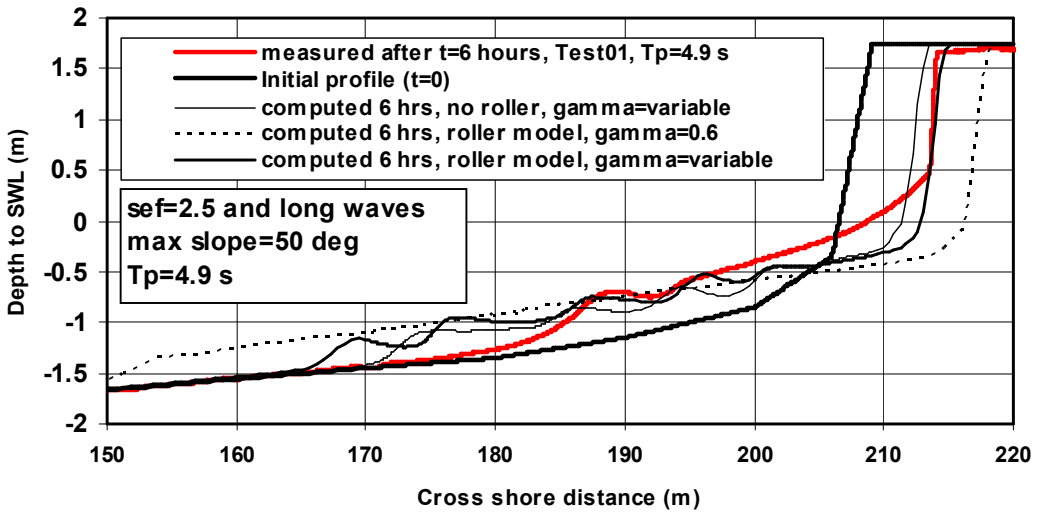

Figure 4.17 *Effect of roller model and breaking coefficient on computed bed profiles for Test T01*

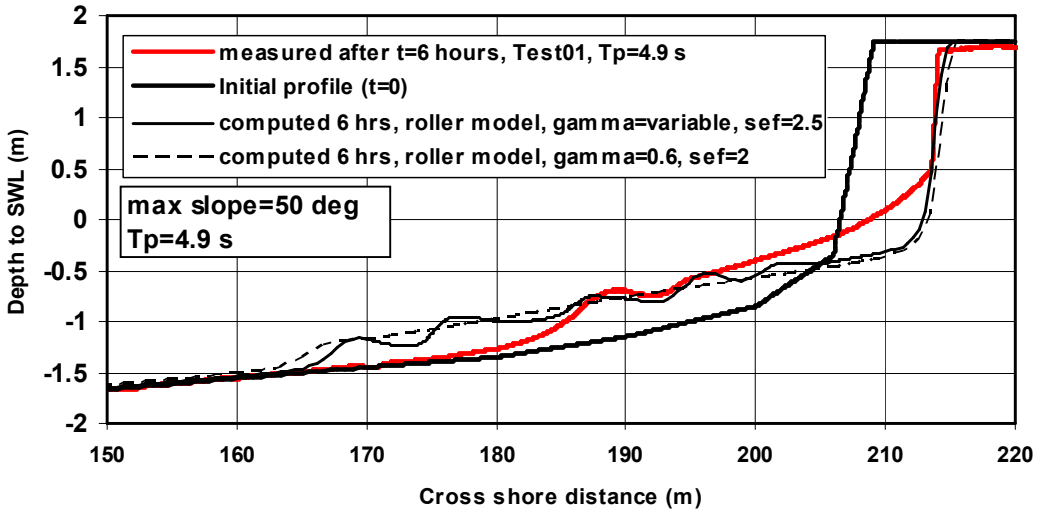

Figure 4.18 *Effect of sef-parameter and breaking coefficient on computed bed profiles for Test T01*

Effect of bed roughness in dune erosion zone

Figure 4.19 shows the effect of the effective bed roughness in the dune erosion zone. This parameter has been been varied in the range of k_s=0.01 to 0.03 m. The default value is k_s=0.02 m. The bed roughness outside the dune erosion zone is variable and predicted by the model based on the particle size and the hydrodynamic conditions. A smaller bed roughness yields smaller friction coefficients and hence smaller concentrations and transport rates resulting in somewhat less dune erosion. A larger bed roughness leads to somewhat larger dune erosion.

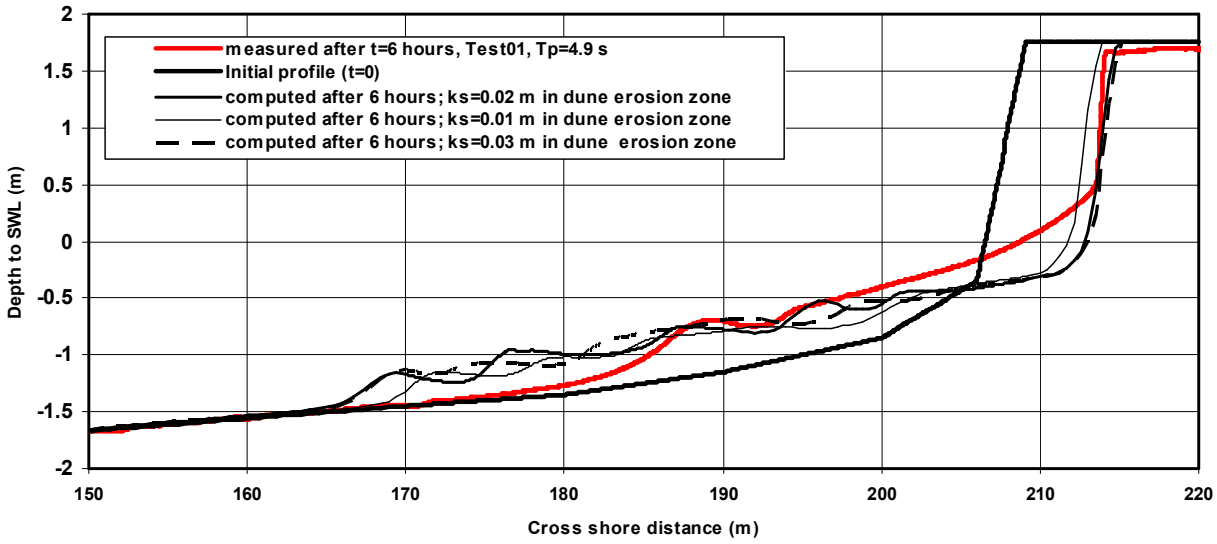

Figure 4.19 *Effect of effective bed roughness on computed bed profiles for Test T01*

Effect of bed material diameter

Based on analysis results of many bed material samples taken at various locations along the bed profile during all tests, the d_{50} of the bed material is found to vary between 0.175 and 0.225 mm for the Deltaflume experiments (**Delft Hydraulics, 2006a,b**). The mean value is d_{50}=0.2 mm.

Figure 4.20 shows the effect of the bed material diameter using d_{50}=0.15 to 0.5 mm for Test T01. A smaller bed material diameter of d_{50}=0.15 mm yields considerably larger (50%) dune erosion; a larger d_{50} value in the range of 0.25 to 0.5 mm leads to slightly smaller (10% to 20%) dune erosion values.

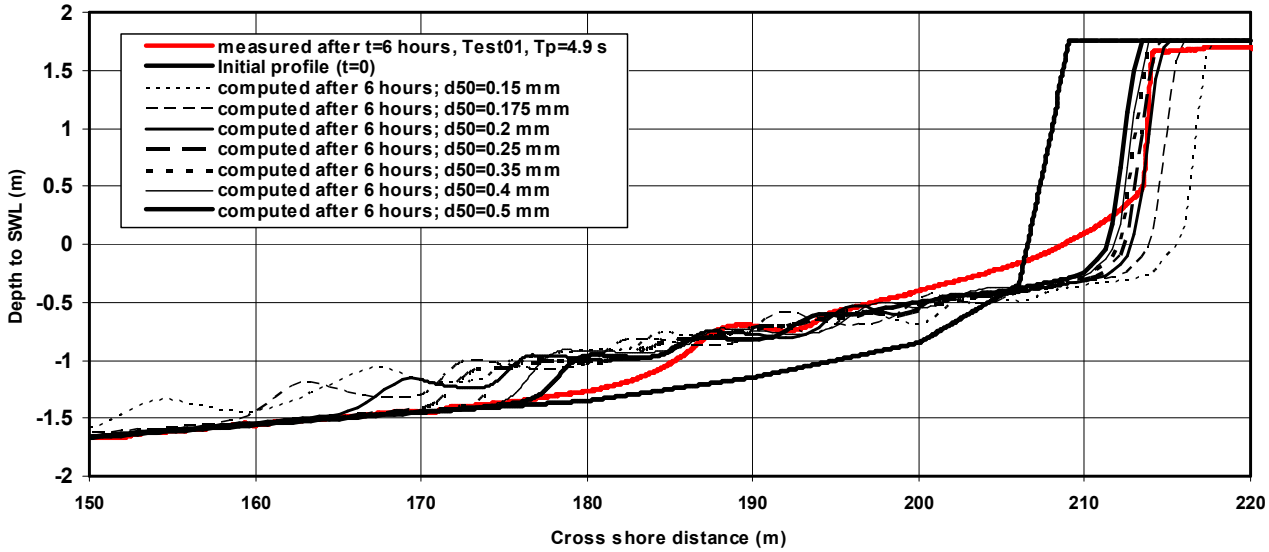

Figure 4.20 *Effect of bed material diameter on computed bed profiles for Test T01*

Table 4.2 shows the computed reference concentration at the sea boundary (x=0) and the maximum value in the dune erosion zone (x>200 m) for various bed material

diameters based on sef=2.5 and including the long wave effect. The bed roughness is constant (=0.02 m) in the dune erosion zone and variable in the outer zone depending on the bed material diameter (larger bed roughness for larger diameter). The reference concentration is affected by both the bed material diameter and the bed roughness which affects the bed-shear stress. The reference concentration decreases with increasing bed material (coarser sediment). The reference concentration increases with increasing bed-shear stress. The reference concentration at the sea boundary is minimum (order of 0.7 kg/m^3) for a bed material diameter of 0.2 mm. It increases for a smaller diameter due to the dominating diameter effect and increases for a larger diameter due to the dominating effect of the bed roughness which increases with grain diameter. In the dune erosion zone the bed is assumed to be flat with a constant effective roughness (of 0.02 m) independent of the bed material diameter resulting in an almost constant reference concentration in this zone of the order of 45 kg/m^3.

Parameter	**d_{50}=0.15 mm**	**d_{50}=0.175 mm**	**d_{50}=0.2 mm**	**d_{50}=0.225 mm**	**d_{50}=0.25 mm**	**d_{50}=0.3 mm**	**d_{50}=0.35 mm**	**d_{50}=0.4 mm**	**d_{50}=0.5 mm**
Reference concentration (in kg/m^3) at x=0 m	0.89	0.788	0.70	0.70	0.78	0.89	1.12	1.23	1.16
Maximum reference concentration (in kg/m^3) in dune erosion zone	70	56	48	44	44	44	44	44	38

Table 4.2 *Computed reference concentration as function of bed material diameter*

Effect of wave period

Figure 4.21 shows the effect of a larger wave period (T_p=7.4 s in stead of T_p=4.9 s). The incoming wave height is the same $H_{s,o}$=1.5 m. A larger wave period of T_p=7.4 s yields a larger dune face recession in good agreement with the observed value of Test T03. The increase of the erosion is caused by the influence of the wave period on the peak onshore orbital velocity; a larger wave period results in a larger peak onshore orbital velocity near the bed (see **Figure 4.4**) and hence larger bed-shear stresses, reference concentrations and suspended transport rates (see **Figure 4.9**).

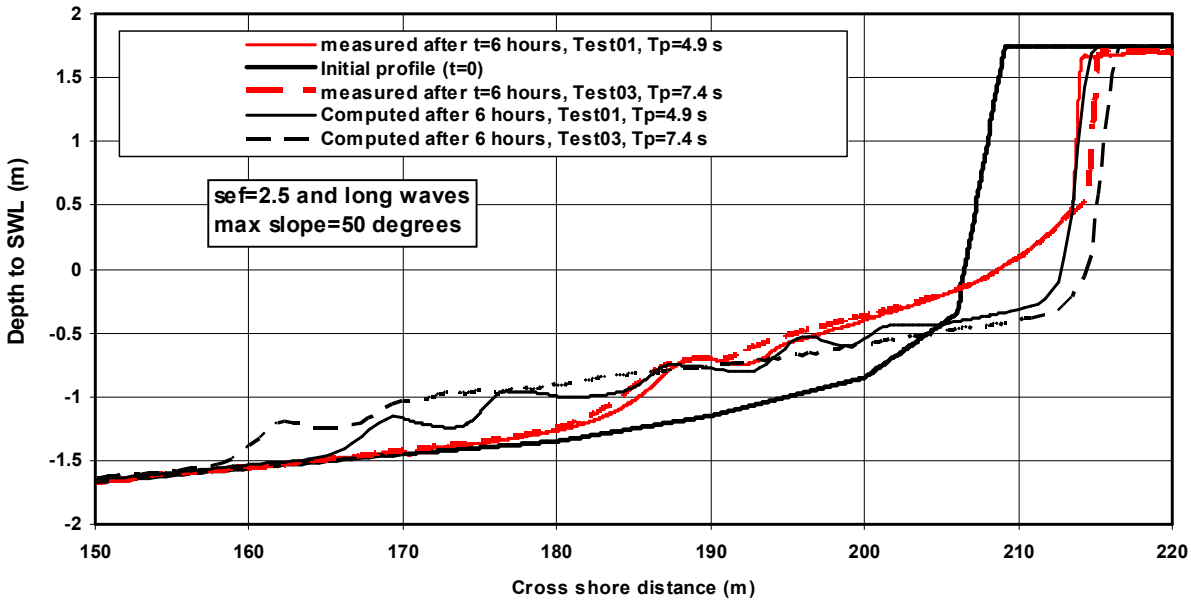

Figure 4.21 *Effect of wave period; Test T01 and T03*

Effect of wave spectrum

The effect of the wave spectrum was studied by applying a double-topped spectrum (see **Figure 4.22**) in Test T16 with T_{p1}=7.6 s and T_{p2}=4.3 s (**Delft Hydraulics, 2006a,b**). Based on the wave exceedance line (see **Figure 4.22**), the wave spectrum is schematized into 8 wave classes, as presented in **Table 4.3**. The largest wave period is assumed to be T=10 s; the smallest wave period is taken to be T=3 s. The computed significant wave height is $H_{s,o}$=1.47 m and T_s=7.4 s.

Wave height class (m)	**Mean wave height (m)**	**Wave period (s)**	**Percentage of occurrence**
<0.5	0.25	3	30%
0.5-0.75	0.625	4	15%
0.75-1.0	0.875	5	15%
1.0-1.25	1.125	6	15%
1.25-1.5	1.375	7	11%
1.5-1.75	1.625	8	9%
1.75-2.0	1.875	9	4%
2.0-2.25	2.125	10	1%
			100%

Table 4.3 *Wave spectrum of Test T16*

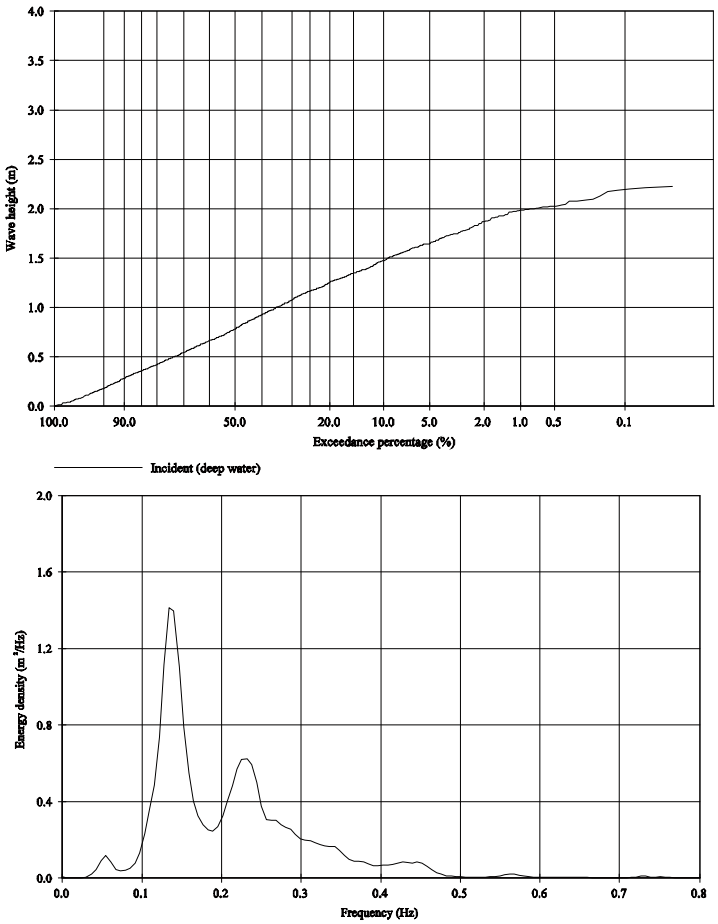

Figure 4.22 *Wave exceedance line and wave spectrum of Test T16*

Figure 4.23 shows the computed bed profile after 6 hours for Test T16 and for Test T05. A double-topped spectrum leads to a smaller dune face recession than a single-topped spectrum due to a shift of wave energy from the larger wave periods to smaller wave periods. The model prediction is in good agreement with the observed pattern. The computed horizontal dune face recession is slightly too large compared with the observed value of Test T16.

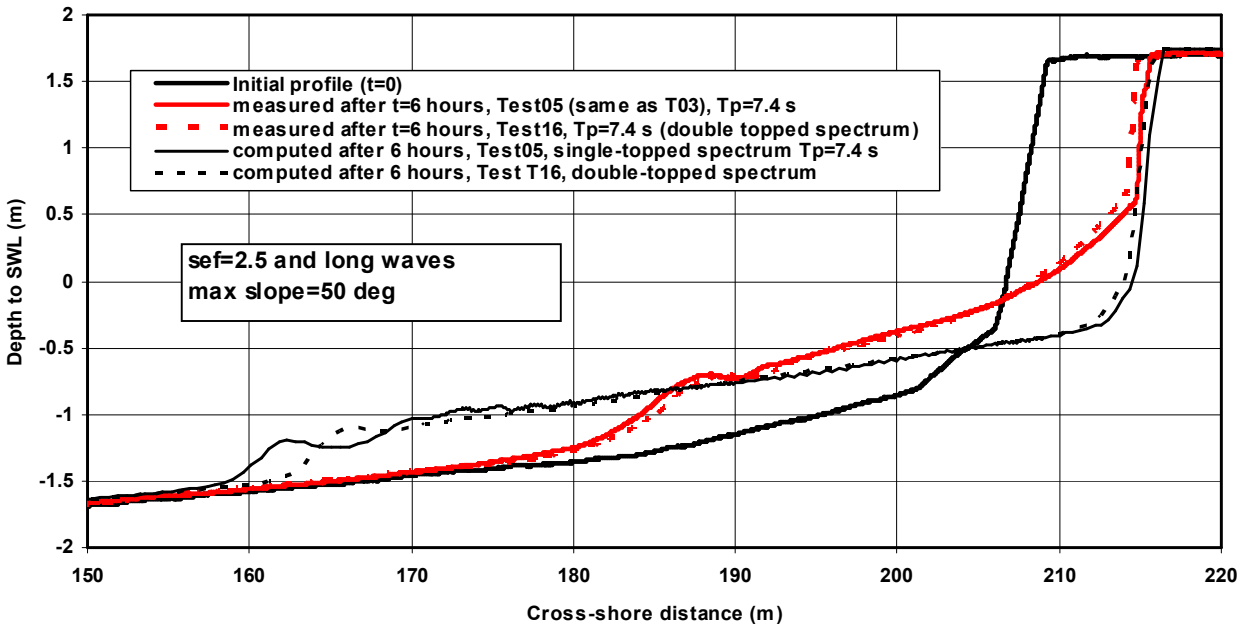

Figure 4.23 *Effect of wave spectrum on computed bed profiles; Test T05 and T16*

4.2 Modelling of small-scale laboratory data

4.2.1 Experimental results

Experiments on dune erosion have been performed in the small-scale Scheldegoot (length of 50 m, width of 1 m and depth of 1.2 m) of **Delft Hydraulics** in 2003. The bed material is sand with d_{50} of 0.09 to 0.1 mm.

The simulations are focussed on Test T01 with a significant offshore wave height of $H_{s,o}$=0.24 m and peak wave period of T_p=2.2 s. The water depth at deep water is 0.7 m. Since the **CROSMOR**-model is a model for individual waves; the wave height distribution is represented by a Rayleigh-type distribution schematized into 6 wave classes. Based on computed parameters in each grid point for each wave class, the statistical parameters are computed in each grid point. The limiting water depth is set to 0.05 m (water depth in last grid point). The maximum slope of the dune face is set to 50°. The bed roughness is predicted by the model. The bed roughness in the dune erosion zone is set to 0.005 m

4.2.2 Simulated morphology

Figure 4.24 shows measured bed profiles after 6 hours. The maximum observed dune recession is of the order of 1 m; the maximum dune erosion volume above the original dune toe level is of the order of 0.4 m^3/m after 6 hours. Simulations have been done for 2 cases:

- Case 1: including long waves and including extra turbulence sef=2.5; effective bed roughness in dune erosion zone of k_s=0.005 m
- Case 2: including long waves and including extra turbulence sef=2.5; effective bed roughness in dune erosion zone of k_s=0.01 m

Computed results are shown in **Figure 4.24**. Good results are obtained for Case 1 based on a bed roughness of k_s=0.005 m in the dune rosion zone. The computed dune erosion is much too large (factor of about 2), if the bed roughness value in the dune erosion zone is increased to k_s=0.01 m.

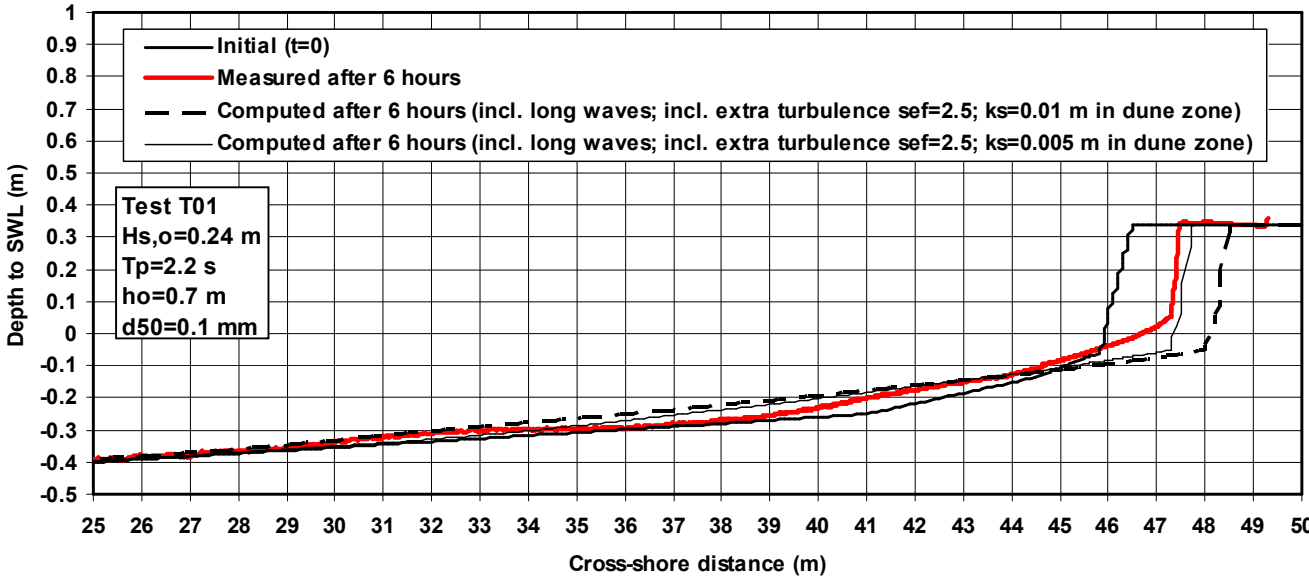

Figure 4.24 *Measured and computed dune erosion profiles for Test T01 in small-scale Scheldeflume*

5 Modelling results of field cases

5.1 Hurricane Eloise 1975, USA

The model has been used to simulate the dune erosion in Walton county (Florida, USA) due to hurricane Eloise in 1975. The hydrodynamic conditions are given in **Table 5.1** based on **Hughes and Chiu (1981), Vellinga (1986) and Steetzel (1993)**. The bed material is d_{50}=0.26 mm. The wave height distribution is represented by a Rayleigh-type distribution schematized into 6 wave classes for each wave condition. The pre-storm and post-storm bed profiles are given in **Figure 5.1**. Computed bed profiles are also shown in **Figure 5.1** for two values of the bed roughness in the dune erosion zone. The computed dune erosion above the maximum storm surge level of 2.5 m is in the range of 45 to 60 m^3/m which larger (30% to 70%) than the measured value of about 35 m^3/m.

Time (hours)	Storm Surge Level (SSL in m above MSL))	Significant offshore wave height $H_{s,o}$(m)	Peak wave period T_p (s)
0	0	0.5	5
12	2.5	3.6	11
13	2.5	3.6	11
18	0	1.0	6

Table 5.1 *Data of hurricane Eloise 1975, USA*

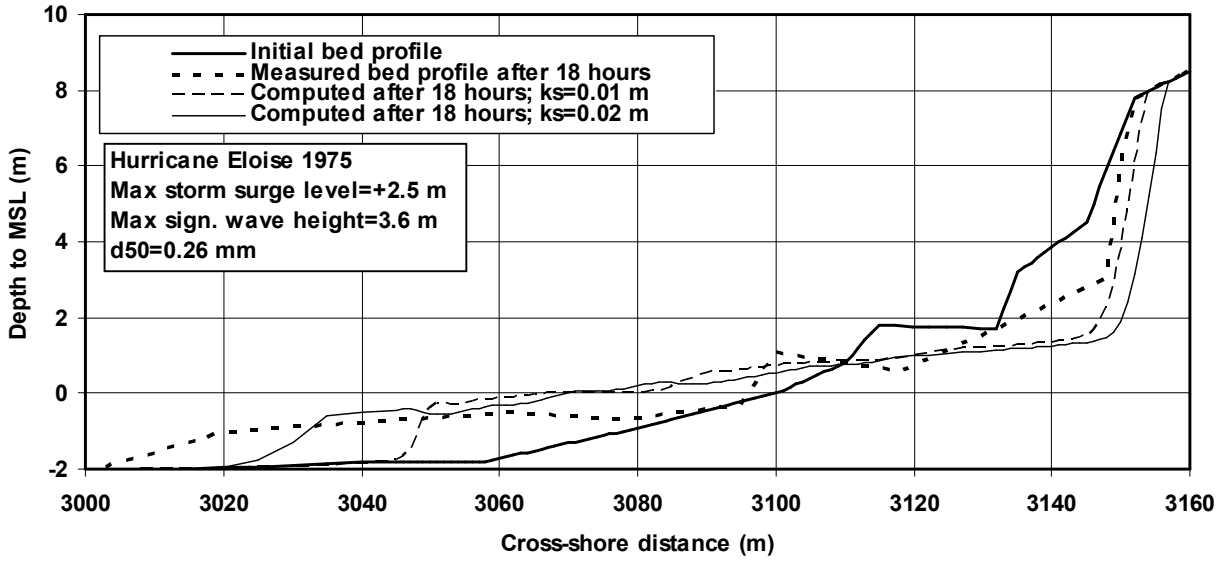

Figure 5.1 *Measured and computed bed profiles for hurricane Eloise 1975, Florida, USA*

5.2 February 1953 storm, The Netherlands

The model has been used to simulate the February-1953 storm which attacked the Dutch coast and particularly the south-west part of The Netherlands. The initial profile consists of four sections as shown in **Figure 5.2**. The beach slope is 1 to 20

and the dune slope is set to about 1 to 1 (angle of 45 degrees). The dune height is set to 12 m above MSL. The dune toe is at +3 m above MSL. The storm surge level (SSL) varies between +1.5 and +3.9 m above MSL over a period of 30 hours (storm duration), see **Table 5.2**. The maximum SSL occurs after 14 hours and remains constant for about 2 hours. The wave height at deep water varies between 4.9 and 6.3 m; the peak wave period varies between 8.8 and 10 s, see **Table 5.2**.

Measured erosion volumes in the Delfland region (south-west part of the Holland coast) are in the range of 60 to 150 m^3/m with a mean value of 90 m^3/m, which is equivalent to a dune recession of about 10 m above the dune toe level.

Model runs have been made using a bed material diameter of 0.2 and 0.25 mm. The wave height distribution is represented by a Rayleigh-type distribution schematized into 6 wave classes for each wave condition. The computed dune erosion volume above the maximum SSL varies between 100 m^3/m for 0.25 mm and 120 m^3/m for 0.2 mm, which is somewhat larger than the observed values. The maximum horizontal dune recession is about 13 m for 0.2 mm. Computed bed profiles are shown in **Figure 5.2**.

Time (hours)	**Storm Surge Level (SSL in m above MSL))**	**Significant offshore wave height (m)**	**Peak wave period (s)**
0	1.5	4.9	8.8
2.5	2.3	5.2	8.8
5	2.1	5.5	8.8
7	2.1	5.6	8.9
8	2.5	5.7	8.9
10	2.3	5.8	8.9
12	3.0	6.0	9.0
14	3.9	6.1	9.3
16	3.9	6.2	9.6
17	3.2	6.3	10.0
20	2.0	6.3	10.0
23	1.7	6.3	10.0
25	2.0	6.3	10.0
27	2.5	6.2	10.0
30	1.5	6.0	10.0

Table 5.2 *Data of February-1953 storm, The Netherlands*

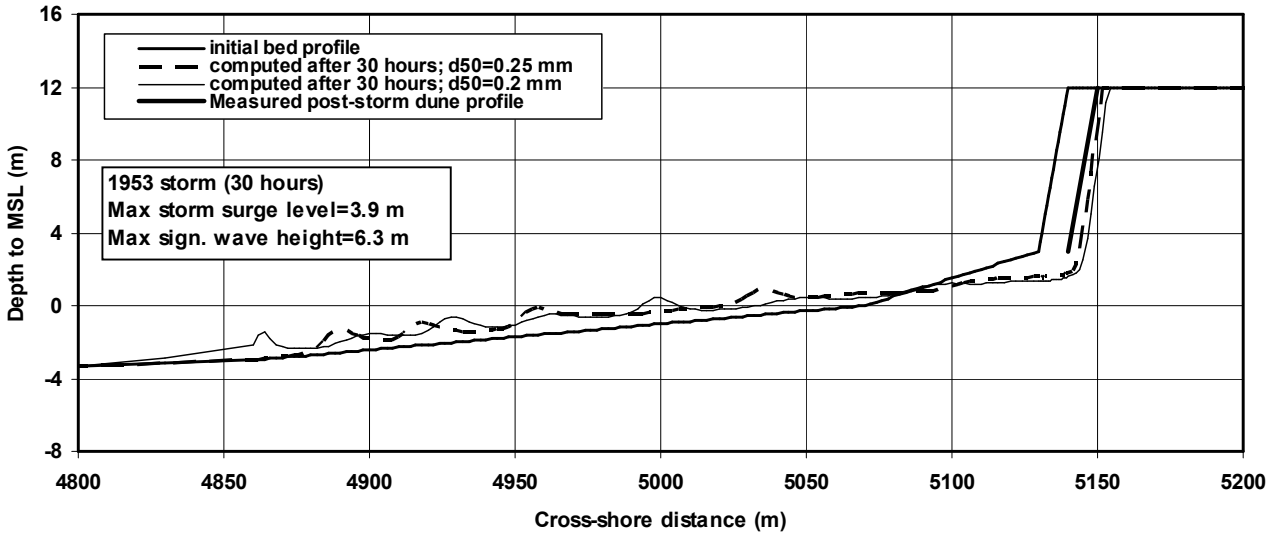

Figure 5.2 *Measured and computed bed profiles for February 1953 storm, The Netherlands*

5.3 Reference field case, The Netherlands

5.3.1 Computed results of various models

The model has been applied to a schematized Dutch field case (Reference Case) as proposed by Vellinga (1986) and given in **Table 5.3**. The initial profile consists of four sections as shown in **Figure 5.3**. The beach slope is 1 to 20 and the dune slope is 1 to 3 (angle of about 20^o). The dune height is set to 15 m above MSL. The dune toe is at +3 m above MSL. The storm surge level is set to +5 m. The duration of a standard storm is set to 5 hours. The wave height at deep water is set to 7.6 m. The peak wave period is 12 s. The forcing parameters are constant in time; the growing and decaying phases of the storm have been neglected.

The wave height distribution of the **CROSMOR**-model is represented by a Rayleigh-type distribution schematized into 6 wave classes. Input data are given in **Table 5.3**.

Parameters	**Values**
Significant wave height at deep water	7.6 m (constant)
Peak wave period	12 s
wave incidence angle to shore normal	0
water depth at deep water	30 m
Storm surge level above MSL (including tidal water levels)	+5 m
Tidal velocities	sinusoidal velocity with peak value of 0.5 m/s (period of 12 hours)
water depth at last grid point	0.25 m
Dune height above MSL	15 m
Dune face slope	1 to 3
Beach slope	1 to 20

d_{50}	0.225 mm
Time step	120 s
number of wave classes	6

Table 5.3 *Boundary conditions of field Reference Case*

Figure 5.3 shows the spatial distribution of the significant wave height at t=0 hours and the reference concentration at t=0 and 5 hours of the **CROSMOR**-model. The maximum value of the reference concentration is in the range of 80 to 100 kg/m^3.

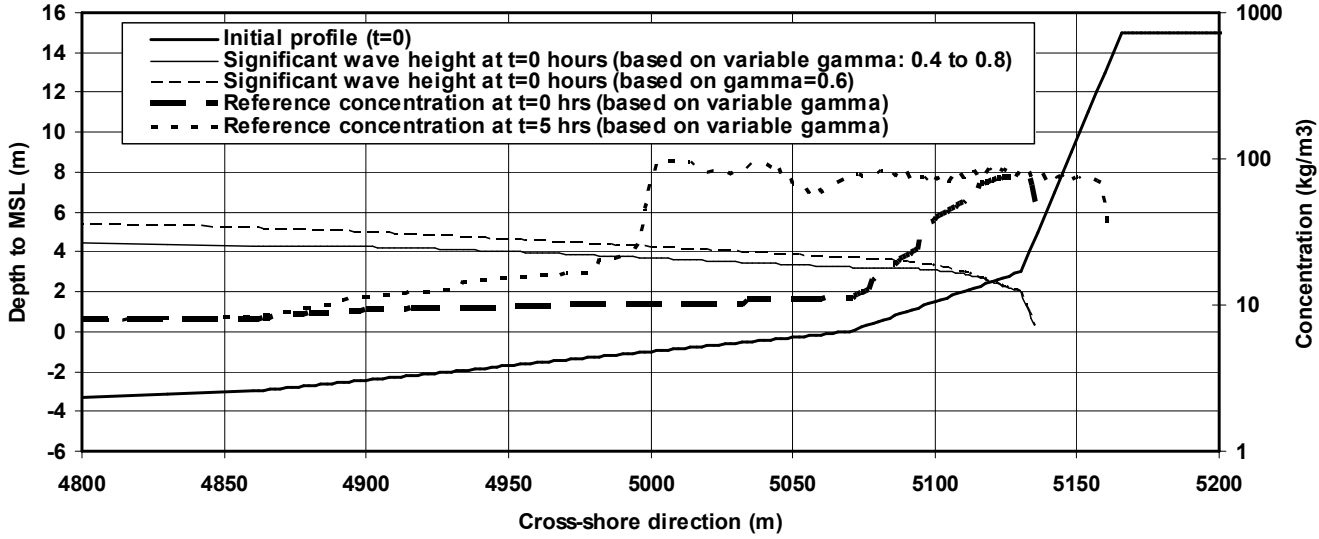

Figure 5.3 *Computed significant wave height and reference concentration of CROSMOR-model*

Figure 5.4 shows the computed bed profile of the **CROSMOR**-model after 5 hours using a variable breaking coefficient (between 0.4 and 0.8 depending on wave steepness and bottom steepness) and a constant breaking coefficient of 0.6. This latter approach yields slightly larger dune erosion values (5% to 10%) due to larger wave heights, see **Figure 5.3**. The computed hydrodynamic and transport parameters at initial time (based on variable breaking coefficient) are plotted in **Figure 5.11**. The computed bed levels of the **DUROSTA**-model (**Steetzel, 1993**) and the **DUROS**-model (**Vellinga, 1986**) are also shown in **Figure 5.4**. The computed dune erosion volumes above the storm surge level (+5 m to MSL) are, as follows:

- 300 m^3/m for **DUROS**-model,
- 170 m^3/m for **DUROSTA** and **CROSMOR**-models.

The dune recession values at storm surge level of 5 m values are: 35 m and about 25 m for **DUROSTA**-model and **CROSMOR**-model. Both mathematical models produce much smaller values than the empirical **DUROS**-model.
The discrepancy between the DUROS-model and the DUROSTA-model was also noted and studied by **Steetzel (1992)**. Based on these results (Table 2.2 from **Steetzel, 1992**), the DUROSTA-model produces about 200 m^3/m for the Reference Case which is about 30% smaller than the value of about 300 m^3/m produced by the DUROS-model. It is not clear why the DUROSTA-model results of **Steetzel (1992)** are considerably larger (200 m^3/m) than those of the present study (170 m^3/m). According

to **Steetzel (1992)**, the discrepancy between the DUROS-model and the DUROSTA-model is caused by:

- incorrect representation of the offshore wave height by the empirical DUROS-model (model is based on laboratory test results; water depth in front of the wave board is not deep water resulting in over-estimation of nearshore wave height and hence the dune erosion volume; error estimated at about 10% by **Steetzel, 1992**);
- incorrect representation of the erosion processes at the dune front (too much erosion at the dune foot and too little erosion at the dune front by DUROSTA-model) and the application of a constant porosity by the DUROSTA-model resulting in under-estimation of the dune erosion volume (porosity of dune front material is about 10% to 20% larger than that of the deposited material).

According to the present results (this study), the discrepancy between the empricial DUROS-model and the more sophisticated mathematical models (DUROSTA and CROSMOR) is also caused by the under-estimation of the initial erosion (after 1 to 2 hours) by the mathematical models, see **Figure 4.11B**.

Based on the scaling laws, the dune erosion after 5 hours in the prototype is approximately quivalent to the (initial) erosion after 1 to 2 hours in the laboratory flume. For example, Test T01 from the Deltaflume experiments in 2005 and 2006 yields a measured dune erosion area (above SSL) of 4.3 m^3/m after 1 hour (see **Tables 2.3A and 2.3B**). The wave conditions are: $H_{s,o}$=1.5 m, T_p=4.9 s, d_{50}=0.2 mm. The scaling parameters are: n_h=6, n_l=12, $n_{l,s}$=9, n_w=1.2, n_{d50}=1.12, yielding: n_A=54 to 72 and n_{TM}=2.4 to 3 according to the Vellinga-method (see Section 2.9) or n_A=55 to 72 and n_{TM}=2.7 to 4.5 according to the Van Rijn method. These methods based on the scaling laws produce a prototype dune erosion of about 230 to 300 m^3/m after 2.4 to 4.5 hours. These values are considerably larger than the initial erosion values produced by the mathematical model CROSMOR, see **Figure 4.11B**.

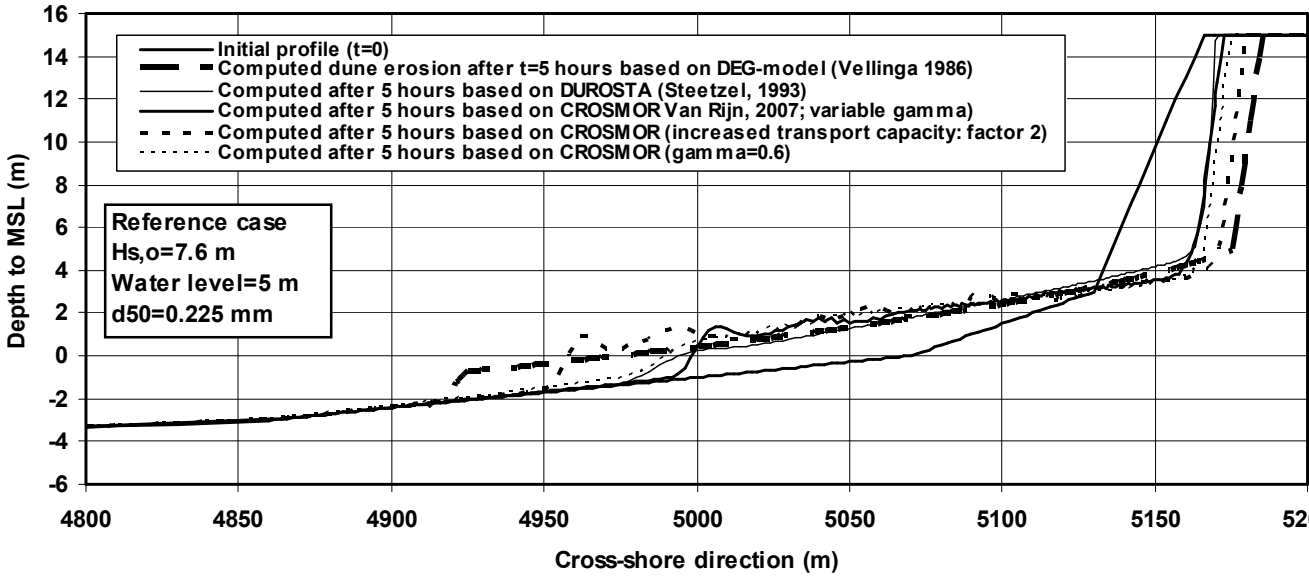

Figure 5.4 *Computed bed levels after 5 hours*

Upscaling of the laboratory results to field conditions (DUROS-model) may introduce scaling errors. Furthermore, scale errors may also be introduced by schematization of 3D field conditions to 2D flume conditions. The 2D laboratory simulation results of the 3D prototype dune erosion caused by the February 1953 storm show an over-estimation of the measured prototype dune erosion by about 30% (see Section 2.10). One of the most uncertain scaling relationships is the morphological time scale (n_{Tm}). Based on experimental research in flumes, this relationship is found to be: $n_{Tm}=(n_h)^{\alpha}$ with $\alpha=0.56$, see **Equations (2.12b)** and **(2.14h)**. The value $\alpha=0.56$ is valid for n_h in the range of 5 to 50. The experiments in the Deltaflume have a depth scale of about 6. Hence the time scale is about 2.7, which means that the erosion due to a storm of 5 hours in prototype (Reference Case) is comparable to the erosion in the Deltaflume after about 2 hours. To reduce the over-estimation effect, the exponent of 0.56 should be increased significantly to about 0.9 yielding a time scale of about 5.

As regards scaling errors, the mathematical models are more reliable. These models have been verified using field data. For example, the **CROSMOR**-model has been used to simulate the 1975 hurricane Eloise in the USA and the 1953 storm in The Netherlands. In both cases the model over-estimates the observed erosion. Hence, the model seems to produce conservative rather than optimistic results.

5.3.2 Sensitivity study based on CROSMOR-model

The **CROSMOR**-model has been used to study the effect of various key parameters on the computed dune erosion after 5 hours (duration of standard storm) for the Reference Case:

- effect of storm surge level in the range of 2 to 8 m;
- effect of offshore wave height in the range of 3.8 to 10 m;
- effect of peak wave period in the range of 9 to 18 s;
- effect of wave angle in the range of 0 to 30 degrees;
- effect of bed material size in the range of 0.15 to 0.3 mm;
- effect of increased transport capacity (factor 2 larger);
- effect of tidal velocities (peak velocity in range of 0 to 3 m/s; period of 12 hours);
- effect of rip channel;
- effect of offshore breakwater;
- effect of steeper and milder beach profile;
- effect of beach fill.

Effect of storm surge level

Figure 5.5 shows the effect of the storm surge level (in the range of 2 to 8 m above MSL) on the bed profile after 5 hours. The reference storm surge level is 5 m above MSL. The dune erosion strongly increases with increasing storm surge level. The computed dune erosion area (A_d) above SSL can roughly be represented by: $A_d/A_{d,ref}=(SSL/SSL_{ref})^{\alpha}$ with: $A_{d,ref}=170$ m^3/m, $SSL_{ref}=5$ m above MSL, $\alpha=1.3$ for $SSL<SSL_{ref}$ and $=0.5$ for $SSL>SSL_{ref}$. yielding values of about $A_{d,}=50$ m^3/m for SSL=2 m and $A_{d,}=215$ m^3/m for SSL=8 m.

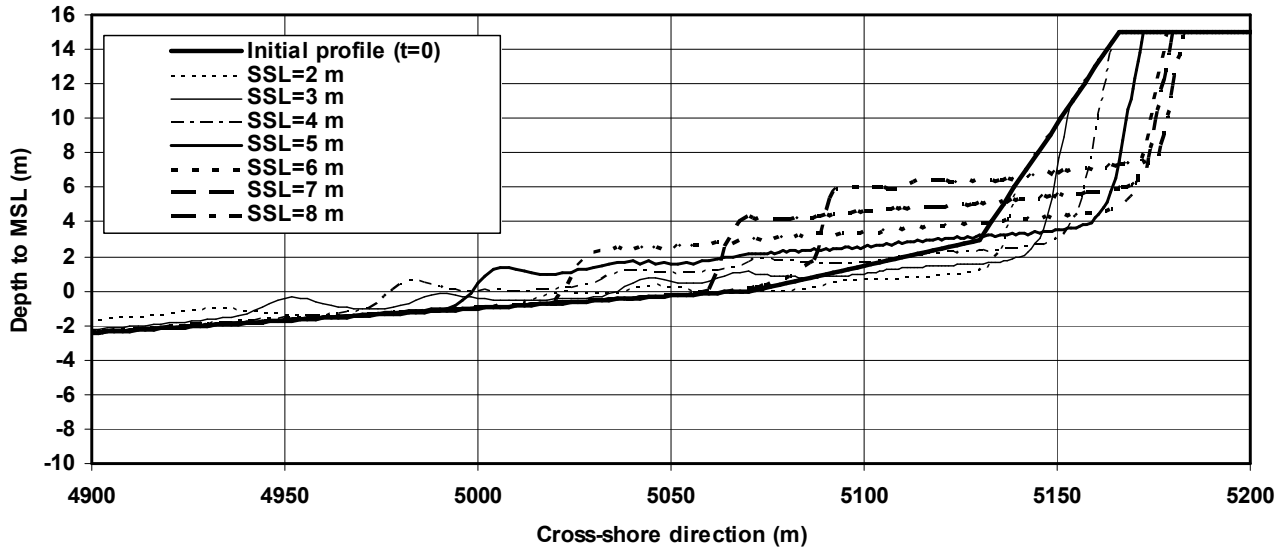

Figure 5.5 *Effect of storm surge level on computed bed profile after 5 hours for Reference Case*

Effect of offshore wave height

Figure 5.6 shows the effect of the offshore wave height (in the range of 3.8 to 10 m) on the bed profile after 5 hours. The reference offshore wave height is $H_{s,o}$= 7.6 m. The dune erosion increases with increasing wave height. The computed dune erosion area (A_d) above SSL can roughly be represented by: $A_d/A_{d,ref}=(H_{s,o}/H_{s,o,ref})^{0.5}$ with: $A_{d,ref}$=170 m^3/m and $H_{s,o,ref}$=7.6 m, yielding values of about $A_{d,}$=120 m^3/m for $H_{s,o}$=3.8 m and $A_{d,}$=195 m^3/m for $H_{s,o}$=10 m.

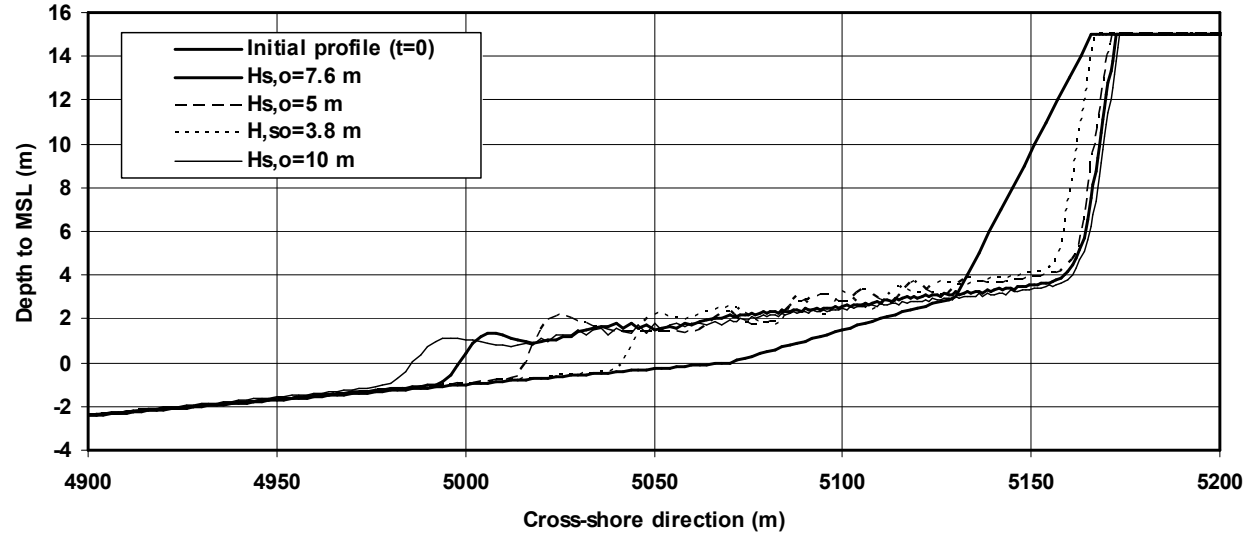

Figure 5.6 *Effect of offshore wave height on computed bed profile after 5 hours for Reference Case*

Effect of offshore peak wave period

Figure 5.7 shows the effect of the peak wave period (in the range of 9 to 18 s) on the bed profile after 5 hours. The reference offshore wave height is T_p=12 s. The dune erosion increases with increasing wave period. The computed dune erosion area (A_d)

above SSL can roughly be represented by: $A_d/A_{d,ref}=(T_p/T_{p,ref})^{0.5}$ with: $A_{d,ref}$=170 m^3/m and $T_{p,ref}$=12 m, yielding values of about $A_{d,}$=145 m^3/m for T_p= 9 s and $A_{d,}$=210 m^3/m for T_p=18 s.

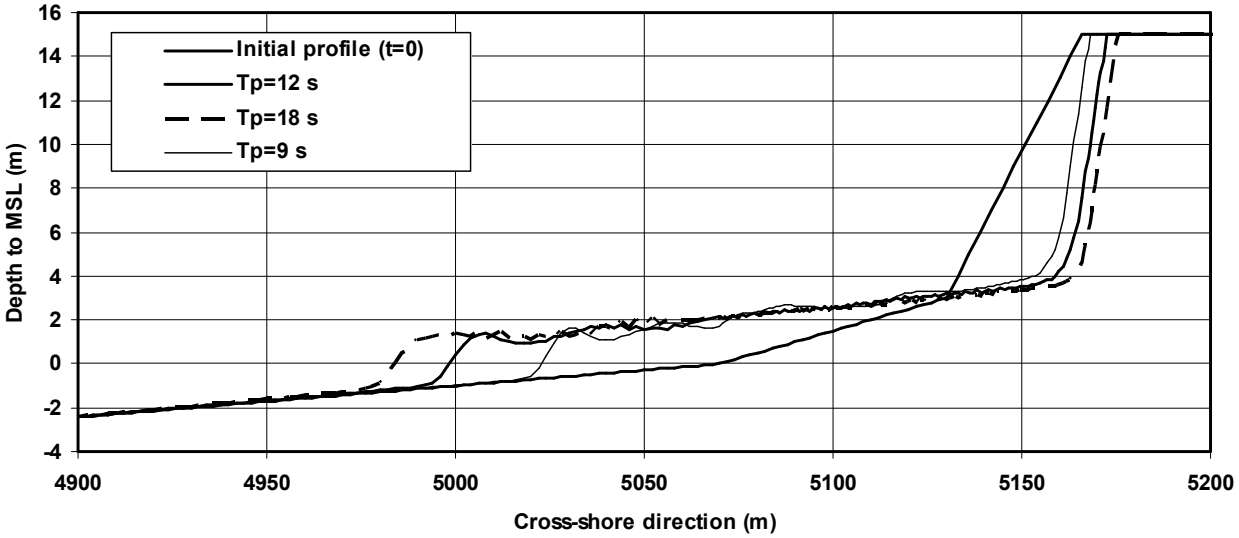

Figure 5.7 *Effect of peak wave period on computed bed profile after 5 hours for Reference Case*

Effect of offshore wave angle

Figure 5.8 shows the effect of the offshore wave angle (in the range of 0 to 30° to coast normal) on the bed profile after 5 hours. The reference offshore wave angle is α_o=0° (normal to coast). When the offshore wave incidence angle is non-zero, two adversary effects do occur: 1) oblique incident waves produce a longshore current in the shallow surf zone resulting in an increase of the transport capacity in the shallow surf zone and a larger erosion capacity and 2) oblique incident waves are refracted in the nearshore zone resulting in a decrease of the wave height and hence transport capacity in the surf zone. The longshore current scours a channel in the surf zone. The dune erosion increases for wave angles in the range of 0 to 10° and remains about constant for larger values. The computed dune erosion area (A_d) above SSL can roughly be represented by: $A_d/A_{d,ref}=(1+\alpha_o/100)^{0.5}$ with: $A_{d,ref}$=170 m^3/m and α_o =offshore wave angle to coast normal (in degrees), yielding values of about $A_{d,}$=195 m^3/m for α_o =30°.

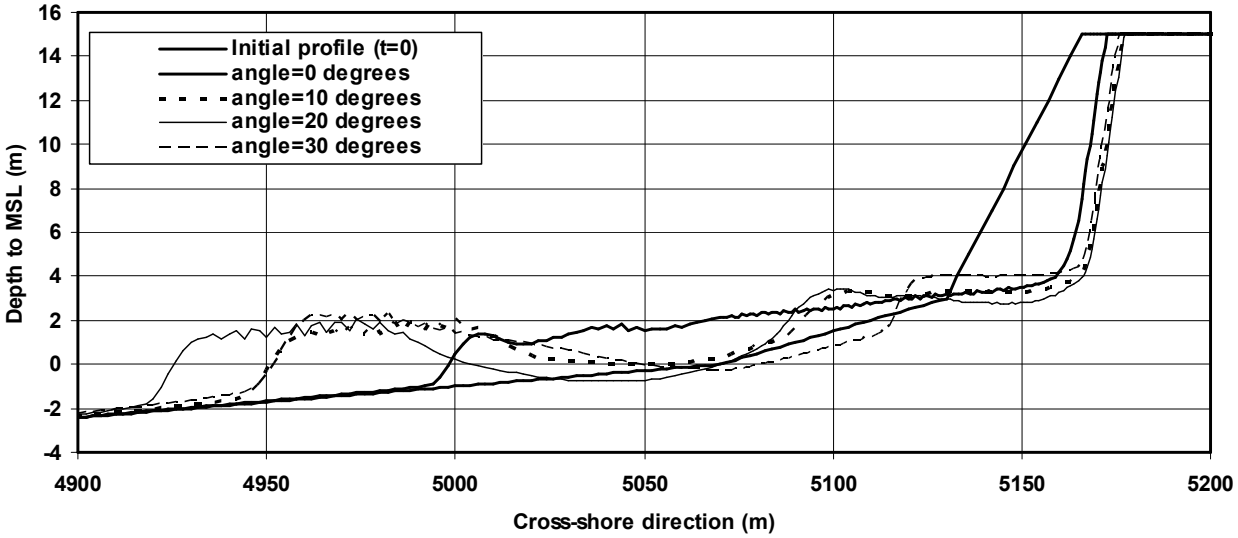

Figure 5.8 *Effect of incident wave angle (deep water) on computed bed profile after 5 hours for Reference Case*

Effect of bed material diameter

Figure 5.9 shows the effect of the bed material diameter (in the range of 0.15 to 0.3 mm) on the bed profile after 5 hours. The reference bed material diameter is d_{50}=0.225 mm. The dune erosion decreases with increasing bed material diameter. The computed dune erosion area (A_d) above SSL can roughly be represented by: $A_d/A_{d,ref}=(d_{50,ref}/d_{50})^{1.4}$ with: $A_{d,ref}$=170 m^3/m and $d_{50,ref}$=0.225 mm, yielding values of about $A_{d,}$=100 m^3/m for d_{50}=0.3 mm and $A_{d,}$=250 m^3/m for d_{50}=0.15 mm.

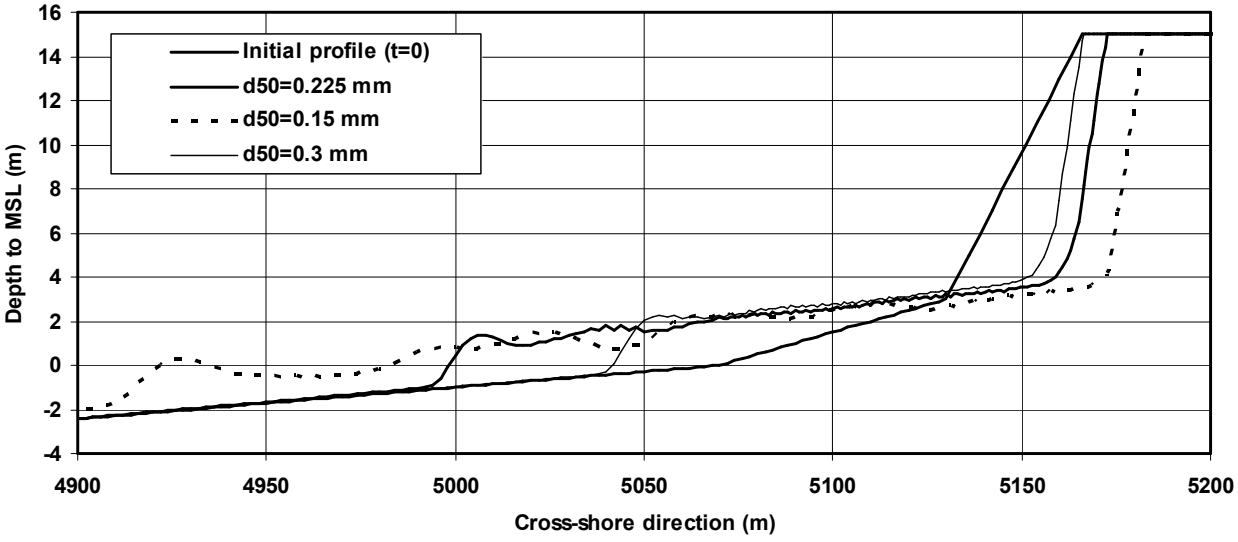

Figure 5.9 *Effect of bed material diameter on computed bed profile after 5 hours for Reference Case*

Effect of increased transport capacity

The transport capacity largely depends on the value of the reference concentration close to the bed. This latter parameter can be increased or decreased by a calibration factor. So far, the default value (=1) of the calibration factor has been used. **Figure 5.10** shows the effect of a larger reference concentration by using a calibration factor of 2. The maximum reference concentration in the swash zone increases from about

75 to 150 kg/m^3 and hence the maximum seaward-directed suspended transport increases from about 25 to 50 kg/s/m.

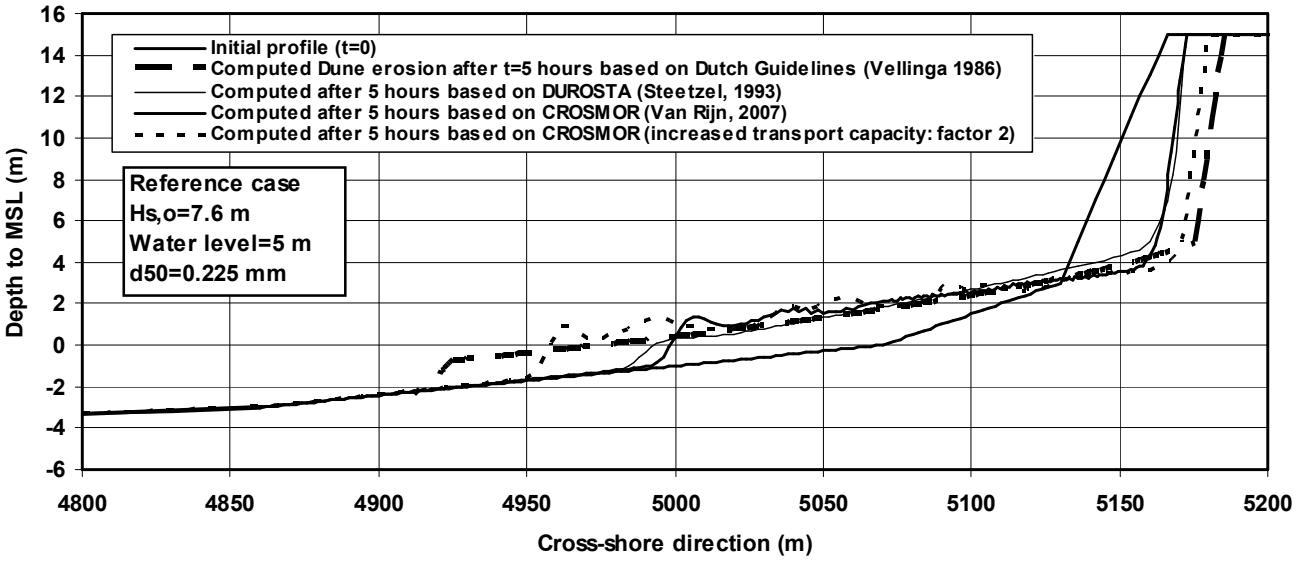

Figure 5.10 *Effect of increased transport capacity on computed bed profile after 5 hours for Reference Case*

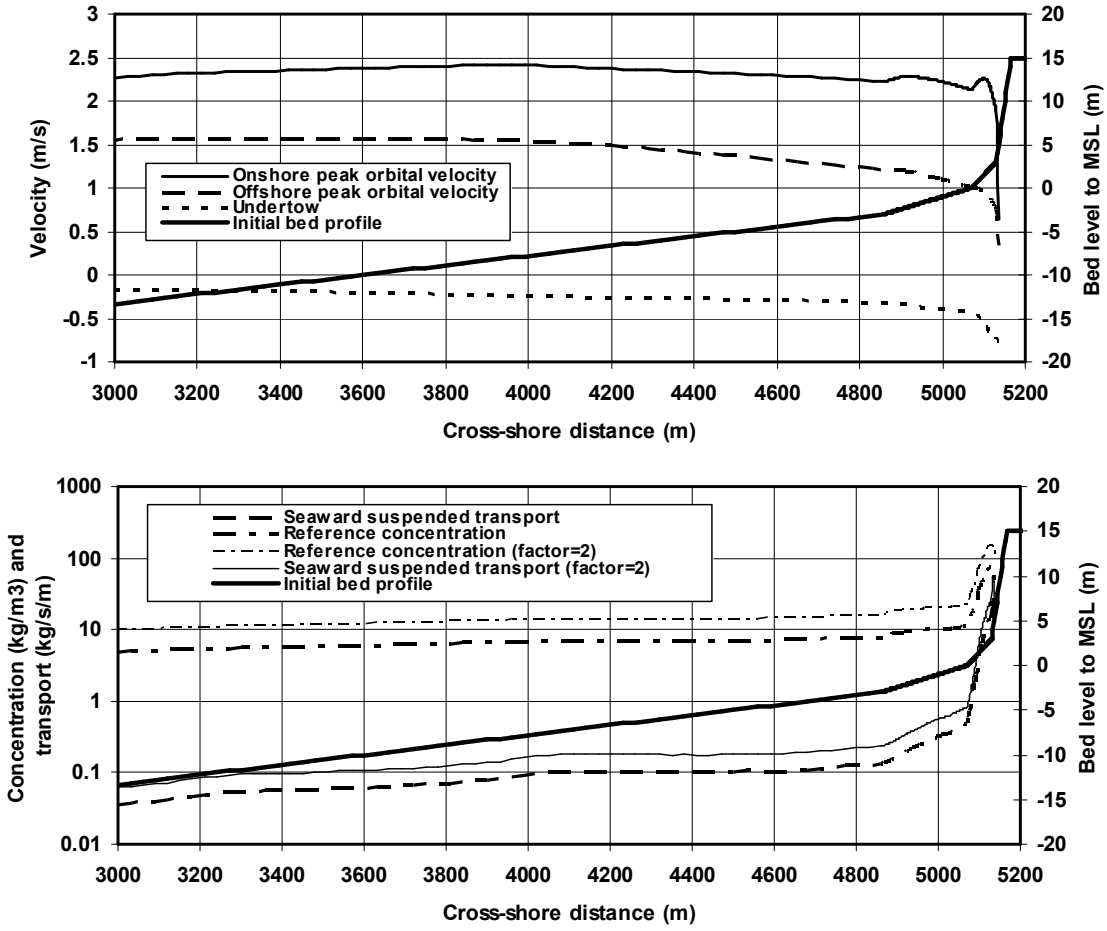

Figure 5.11 *Computed Peak orbital velocities, undertow, reference concentration and suspended transport at initial time for Reference Case*

The dune erosion area (above SLL) after 5 hours increases from about 170 m^3/m to about 270 m^3/m. This latter value is more in line with the value predicted by the Dutch Dune Erosion Guidelines (**Vellinga, 1986**). The generation of a reference concentration of the order of 150 kg/m^3 close to the bed (at 0.01 m) is equivalent to a volume concentration of the order of 10%. The concentrations close the water surface are a factor of 10 smaller (order of 10 to 15 kg/m^3) resulting in a depth-integrated suspend transport rate of about 50 kg/s/m (water depth of about 1 m and undertow velocity of about 0.75 m/s, see **Figure 5.11**). To evaluate these rather large near-bed concentrations of about 150 kg/m^3, the **TRANSPOR2004**-model (**Van Rijn, 2007a,b,c,d**) has been used to convert these values to equivalent river flow conditions (same depth of 1 m and bed material of 0.225 mm) resulting in a current velocity of about 5 m/s. Thus, a river flow of 5 m/s is required to generate the same magnitude of concentrations near the bed (about 150 kg/m^3). The maximum peak orbital velocity in the swash zone is of the order of 2 m/s, see **Figure 5.11**. Hence, it is questionable whether the breaking waves in the surf zone can generate these large concentrations of about 150 kg/m^3.

The near-bed concentrations measured in the swash zone of the Deltaflume experiments are of the order of 50 kg/m^3 (**Delft Hydraulics 2006b**). **Equation (2.9)** representing the concentration scale reads as: $n_c=(n_h)^{0.5}\ (n_{d50})^{-1}\ (n_{s-1})^{-1}\ (n_l/n_h)^{-1}$. Using: $n_h\cong5$, $n_{d50}\cong1$, $n_l/n_h\cong2$, $n_{s-1}=1$, it follows that: $n_c\cong1.1$. Based on this approach, the concentrations in protype conditions are expected to be about 10% larger than those in the Deltaflume resulting in values of the order of 60 kg/m^3. Similar values (about 75 kg/m^3) are computed by the **CROSMOR**-model (default settings). It is concluded that the mathematical model confirms the applied scaling law for the concentrations.

Based on this, it is concluded that the increase of the reference concentration by a factor of 2 leads to rather high values (> 100 kg/m^3) which donot seem to be very realistic.

Effect of tidal velocity

The model run for the Reference Case is based on a peak tidal velocity at deep water of 0.5 m/s (tidal period of 12 hours). Additional runs have been made with tidal velocities in the range of 0 to 3 m/s. This parameter has almost no effect on the dune erosion volume, mainly because the tidal velocities in the shallow surf zone remain very small (order of 0.3 m/s) due to relatively strong frictional effects. The results are shown in **Figure 5.12**.

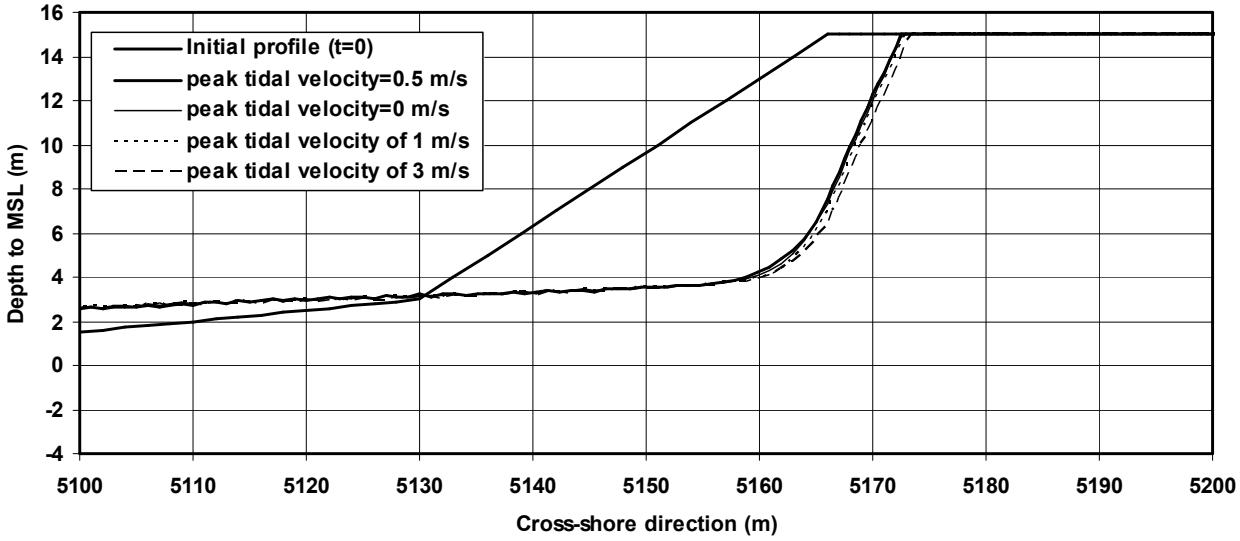

Figure 5.12 *Effect of tidal velocity on computed bed profile after 5 hours for Reference Case*

To study the effect of a deep tidal channel relatively close to the shore (often present near a tidal inlet), a run has been made with a tidal channel between x=4700 and 4900 m. The maximum depth below MSL is set to 10 m. The wave height at the seaside of the channel is taken from the Reference Case at x=4700 m, yielding a value of H_s=5 m. The peak tidal velocity is set to 2 m/s at x=4700 m.

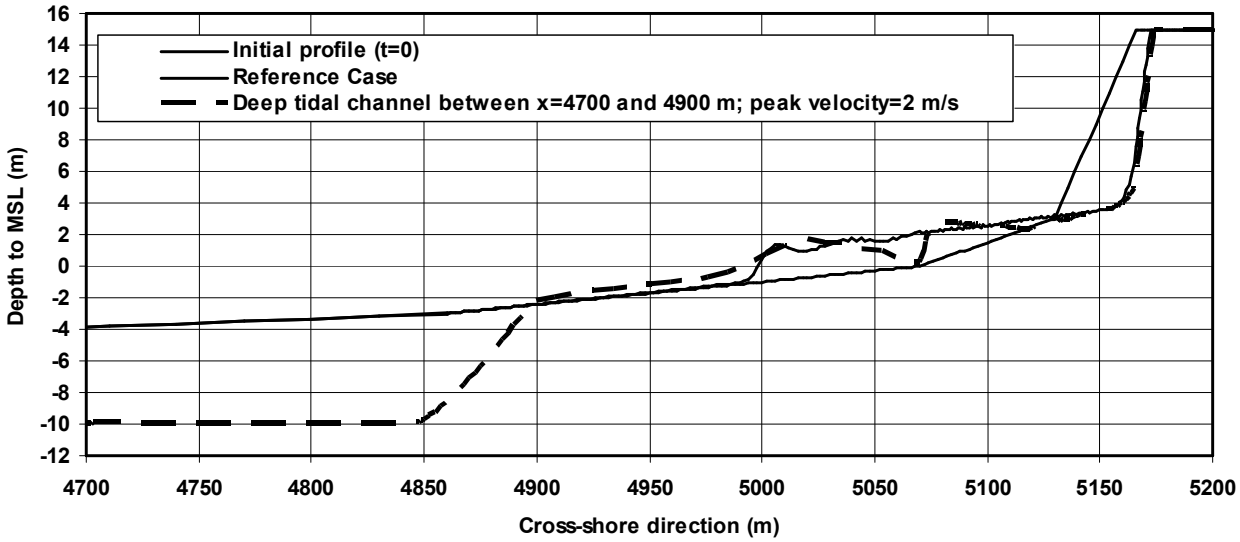

Figure 5.13 *Effect of tidal channel on computed bed profile after 5 hours for Reference Case*

Figure 5.13 shows that the dune erosion after 5 hours is increased by about 10%. The horizontal dune recession increases by about 2 m. The tidal velocities on the landward side of the channel are rapidly reduced by frictional forces (from 2 m/s at x=4700 m to about 0.9 m/s at x=5100 m and to about 0.25 m/s in last computational point at x=5135 m at initial time) and have not much effect on the transport capacity in the

dune erosion zone. The model results show an irregular bar-type pattern in the deposition zone due to bar generation processes.

Effect of horizontal nearshore terrace

To study the effect of a nearshore horizontal terrace (remains of rip channel) close to the dune front, runs haves been made with a horizontal terrace between x=4930 and 5070 m. The bottom of the terrace is set to 2 m. The terrace ends at the beach (x=5090 m) where the depth is +1 m. Using a variable breaking coefficient (between 0.4 and 0.8 depending on wave steepness and bottom steepness), the presence of a horizontal terrace reduces the dune erosion significantly as shown in **Figure 5.14**!. The sediments are not deposited on the terrace bottom (x=5075 m). The bed surface in the deposition zone is only 0.5 m higher (after 5 hours) than in the situation without a terrace. At the end of the terrace a scarp-type transition is created, which acts as a focus point for wave breaking causing a marked reduction in wave height. The wave height patterns are shown in **Figure 5.15**. At initial time (t=0 hours) the presence of the terrace reduces the wave height because the shoaling process is absent and the stable wave height on the horizontal terrace (water depth of about 7 m) is about 3 m. Strong wave shoaling is present at the end (x=5090 m) of the terrace increasing the wave height to a value which is much larger than that without the terrace. The wave height in the swash zone is not affected by the presence of the terrace. The wave heights at t=5 hours above the deposition zone and in the swash zone are strongly reduced due to intense wave breaking at the scarp-type front (x=5070 m) at the end of the terrace.

Using a constant breaking coefficent of 0.6, the dune erosion is not much affected by the terrace. The dune erosion after 5 hours is approximately the same as that for the Reference Case without the terrace based on a constant breaking coefficient (see **Figure 5.4**). The wave height in the terrace zone is much larger for a constant breaking coefficient of 0.6. According to the work of **Nelson (1985, 1987, 1994)** and **Nelson and Gonsalves, 1992**), the maximum relative wave height along a horizontal bottom is about 0.4 o 0.45.

The reduction of dune erosion due to the presence of the terrace is **not** in line with the common engineering belief that a nearshore deepened zone (or a rip channel) is a hot spot for erosion intensifying dune erosion rather than reducing it. Experiments in a laboratory flume should be done to reveal the influence of a horizontal terrace on wave height and dune erosion.

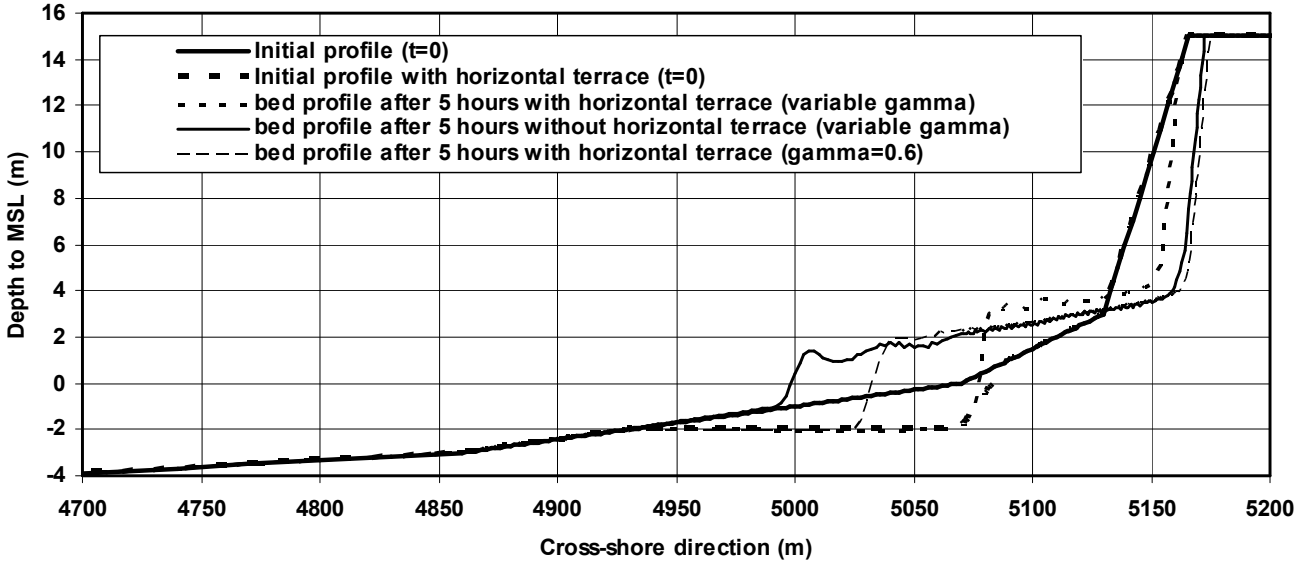

Figure 5.14 *Effect of horizontal terrace on computed bed profile after 5 hours for Reference Case*

Effect of offshore breakwater

To study the effect of an offshore breakwater, a run (based on variable breaking coefficient) has been made with an offshore breakwater at the -5 m depth contour (between x=4500 and 4565 m). The crest of the breakwater has been set to -1 m and to +1 m to MSL. The crest width is set to 35 m. A breakwater with its crest at -1 m below MSL has almost no effect on the computed dune erosion, as can be seen in **Figure 5.16**. Similarly, a natural sandy breaker bar in the outer surf zone below -1 m will hardly affect the dune erosion during a major storm with a high storm surge level. A breakwater with a crest at +1 m above MSL reduces the dune erosion considerably, because the higher waves of the spectrum will break at the breakwater. It is noted that such a breakwater is not very attractive from an aesthetic point of view as it will be visible from the beach with its crest above water.

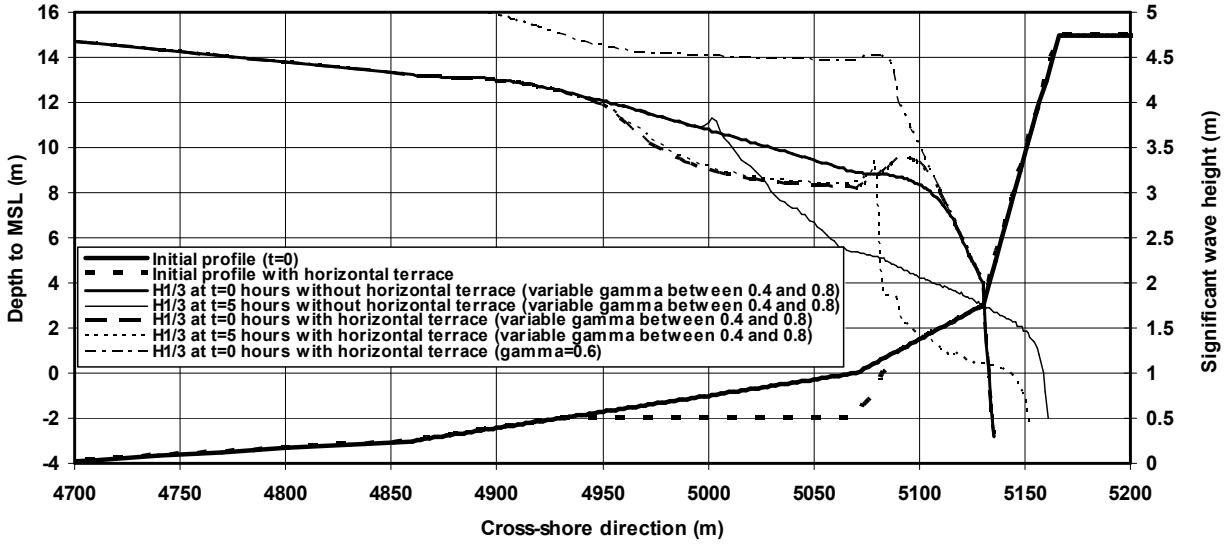

Figure 5.15 *Effect of horizontal terrace on computed significant wave height for Reference Case*

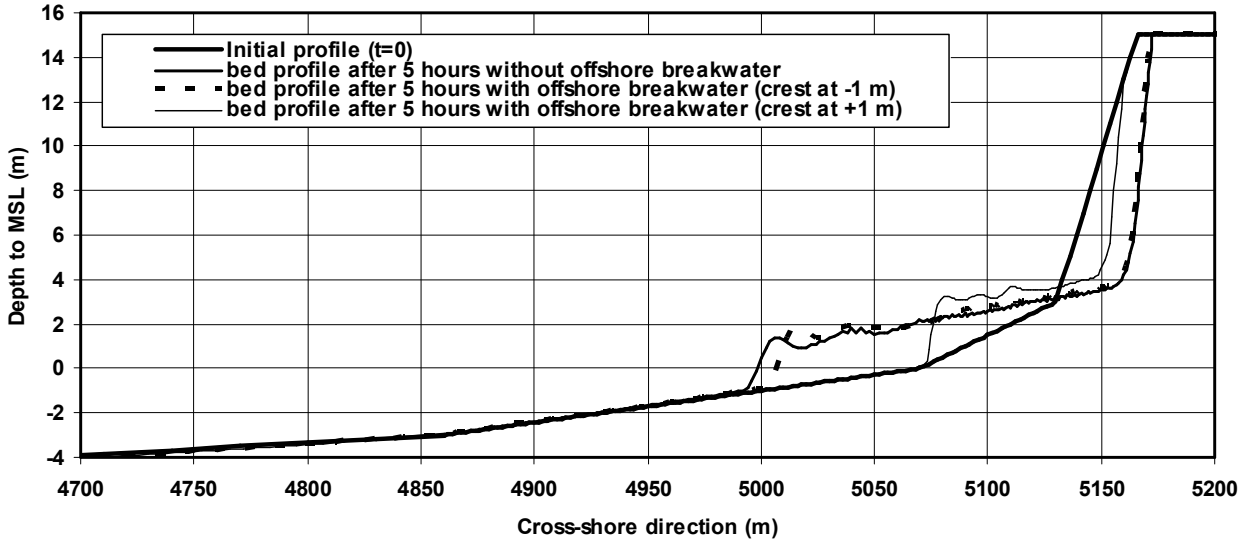

Figure 5.16 *Effect of offshore breakwater on computed significant wave height for Reference Case*

Effect of steeper and milder coastal profile

Figure 5.17 shows the effect of steep sloping and mild sloping coastal profile. The coastal slope is defined as the slope between the +3 m and -3 m contours. The coastal slope slope of the Reference Case is 1 to 45 ($\tan\beta_{ref}$=0.0222). A steeper slope (1 to 22 or $\tan\beta$=0.046) yields a 20%-increase of the dune erosion volume. To model the influence of larger maximum waves along a steep bed profile, the wave breaking coefficient has been set to γ=0.8. A milder slope (1 to 100 or $\tan\beta$=0.01) leads to a 30%-decrease of the dune erosion volume.

Effect of beach fill

Figure 5.18 shows the effect of a beach fill. The total beach fill volume is about 300 m^3/m creating a much wider, mild sloping beach (1 to 60). The beach width increases from 60 m (for Reference Case) to 160 m. The dune erosion during a major storm is considerably reduced (by about 30%).

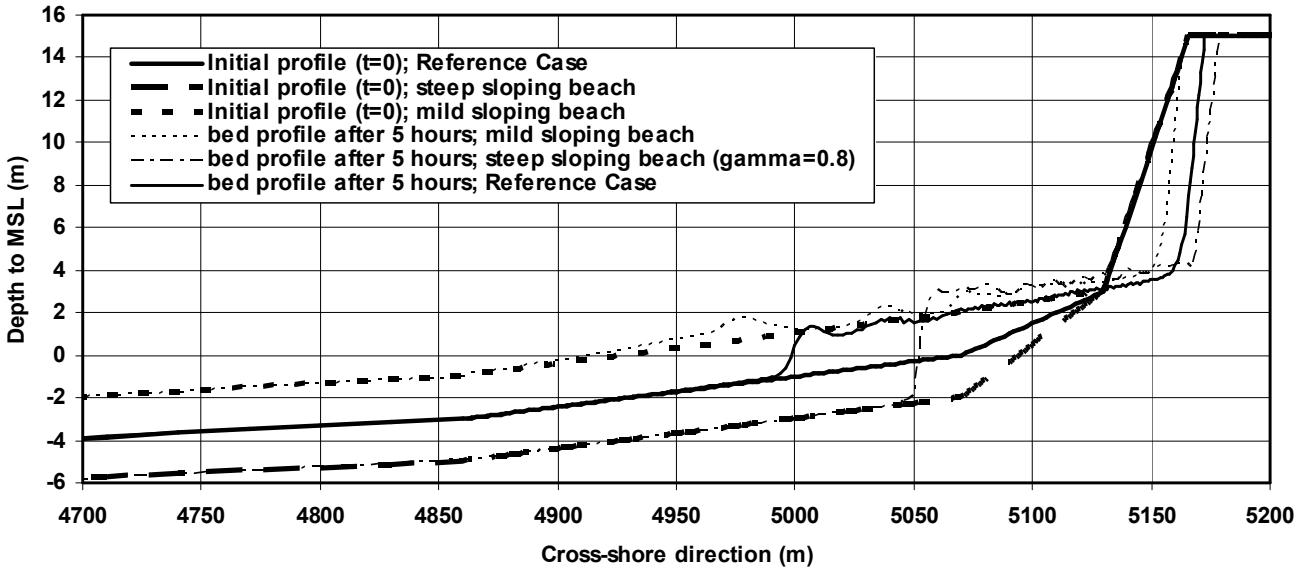

Figure 5.17 *Effect of beach profile steepness on computed bed profiles*

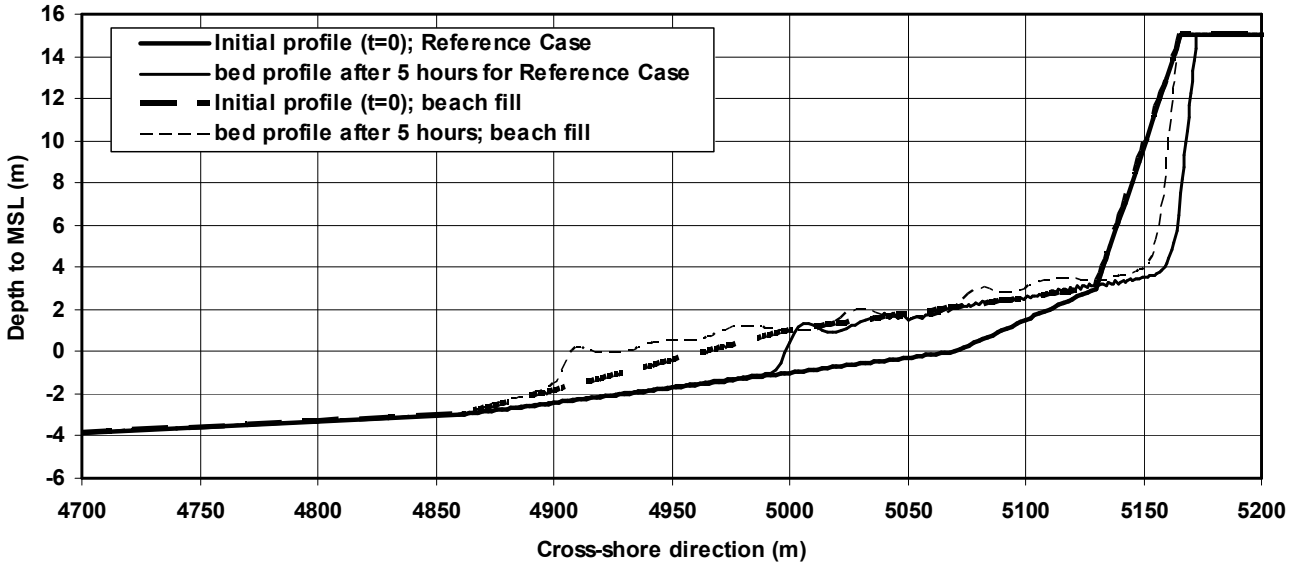

Figure 5.18 *Effect of beach fill on computed bed profiles*

5.4 Simplified dune erosion rule (DUNERULE-model)

The results of the sensitivity study of Section 5.3.2 have been used to propose a simplified dune erosion rule (**DUNERULE-model**), as follows (see **Figure 5.19** and **Section 2.11**):

$$A_{d,t=5} = A_{d,ref}\ (d_{50,ref}/d_{50})^{\alpha 1}\ (S/S_{ref})^{\alpha 2}\ (H_{s,o}/H_{s,o,ref})^{\alpha 3}\ (T_p/T_{p,ref})^{\alpha 4}\ (\tan\beta/\tan\beta_{ref})^{\alpha 5}\ (1+\theta_o/100)^{\alpha 6} \qquad (5.1)$$

with:
$A_{d,t=5}$ = dune erosion area above SSL after 5 hours (m^3/m),
$A_{d,ref}$ = dune erosion area above SSL after 5 hours in Reference Case= 170 (m^3/m),

S = storm surge level above MSL (m),
S_{ref} = storm surge level above MSL in Reference Case= 5 (m),
$H_{s,o}$ = offshore significant wave height (m),
$H_{s,o,ref}$ = offshore significant wave height in Reference Case= 7.6 (m),
T_p = peak wave period (s),
$T_{p,ref}$ = peak wave period (s) in Reference Case= 12 (s),
d_{50} = median bed material diameter (m),
$d_{50,ref}$ = median bed material diameter in Reference Case= 0.000225 (m),
$\tan\beta$ = coastal slope gradient defined as the slope between the -3 m depth contour (below MSL) and the dune toe (+3 m),
$\tan\beta_{ref}$= coastal slope gradient defined as the slope between the -3 m depth contour and the dune toe (+3 m) for the Reference Case= 0.0222 (1 to 45),
θ_o = offshore wave incidence angle to coast normal (degrees),
α_1 = exponent=1.3,
α_2 = exponent=1.3 for $SSL<SSL_{ref}$ and α_2=0.5 for $SSL>SSL_{ref}$,
α_3 =α_4=α_6=0.5 (exponents),
α_5 = exponent=0.3.

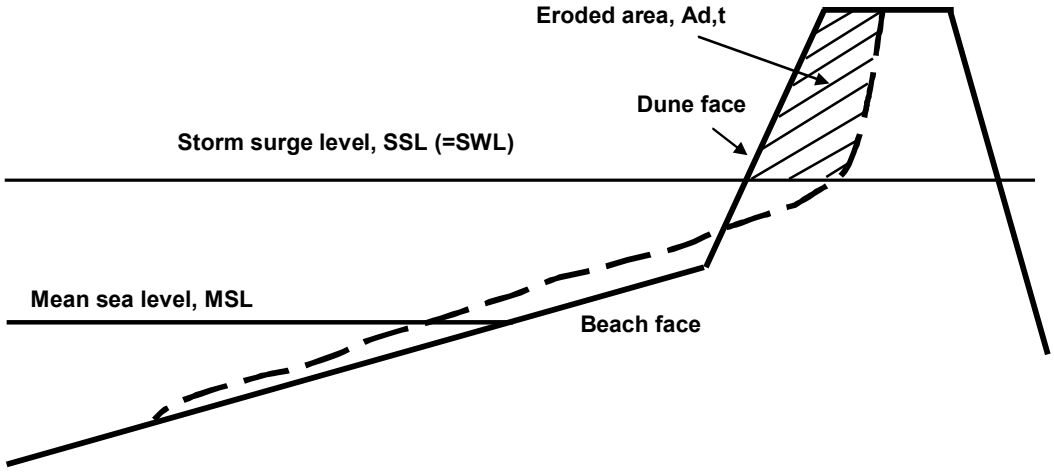

Figure 5.19 *Sketch of dune erosion*

The average horizontal dune recession (R_d) can be estimated from:

$$R_d=A_d/(h_d-S) \quad (5.2)$$

The maximum horizontal dune recession ($R_{d,max}$) at SSL can be estimated from:

$$R_{d,max}\cong 1.5\ R_d \quad (5.3)$$

with:
R_d = average horizontal dune recession (m),
$R_{d,max}$ = maximum horizontal dune recession at SSL (m),
h_d = height of dune crest above MSL (m).

The time development over 100 hours can be estimated from:

$$A_{d,t}=A_{d,t=5}\ (t/t_{ref})^{\alpha 6} \quad (5.4)$$

with:

t = time in hours (t_{ref}= 5 hours),
α_6 = exponent= 0.5 for $t<t_{ref}$ and 0.2 for $t>t_{ref}$.

Basically, the proposed method produces dune erosion values with respect to a defined Reference Case (storm with a constant storm surge level, wave height and duration of 5 hours). According to the **CROSMOR**-model the dune erosion area above SSL in the Reference Case is approximately $A_{d,ref}$= 170 m^3/m. According to the experimental values (**Vellinga, 1986**), this value is in the range of $A_{d,ref}$= 250 to 300 m^3/m. The storm surge level (SSL) above mean sea level and the bed material diameter (d_{50}) are the most influencial parameters.

As an example, the following storm values are used:
S=4 m, $H_{s,o}$=5m, T_p=10 s, d_{50}=0.0002 m, α_o=20°, h_d=15, tanβ=0.02 yielding:

A_d= 170 $(0.000225/0.0002)^{1.3}$ $(4/5)^{1.3}$ $(5/7.6)^{0.5}$ $(10/12)^{0.5}$ $(0.02/0.0222)^{0.3}$ $(1+20/100)^{0.5}$ = 115 m^3/m after 5 hours.
A_d= 82 m^3/m after 2.5 hours and 135 m^3/m after 10 hours.

R_d= 115/(15-4)=10.5 m after 5 hours; 7.5 after 2.5 hours and 12.5 m after 10 hours.
$R_{d,max}$= 16 m after 5 hours; 11 m after 2.5 hours and 19 m after 10 hours.

Equation (5.1) is most valid for dune erosion under major storms, but also yields realistic results for minor storm events. Data are taken from the storm erosion field database summarized by **Birkemeier et al. (1988)**, (see Table 3 of **Larson et al., 2004**). The data have been clustered into 10 cases, shown in **Table 5.4**. The bed material diameter at these beaches varies in the range of d_{50}=0.3 to 0.5 mm. The coastal slope is taken as tanβ=0.0222.

Field site	**Wave height (m)**	**Wave period (s)**	**Surge level (m)**	**Surge duration (hours)**	**Measured dune erosion volume (m^3/m)**	**Predicted dune erosion volume (m^3/m)**
LBI	2.6	9	1.5	14	15±7	10
AC,LB	2.6	8	1.5	14	6±5	10
LB	3.4	8	1.4	24	8±4	11
LBI	1.9	8	1.5	36	27±7	10
LB	2.1	7	1.5	36	10±3	9
NB	2.4	8	2	10	25±3	15
NB	3.6	9.5	2.5	12	27±10	24
MB,WB,JB	3.8	10.5	2	11	10±5	18
AC,LB	3.0	8	1.8	10	5±3	12
LB	1.8	10	1.5	12	7±4	9

NB= Nauset Beach, MB=Misquamicut Beach, WB=Westhampton Beach, JB= Jones Beach, LBI=Long Beach Island, AC=Atlantic City, LB=Ludlam Beach

Table 5.4 *Dune erosion volumes during minor storm events along various USA-beaches*

Equations (5.1) and (5.4) have been used to predict the dune erosion volumes at these beaches. The wave incidence angle is assumed to be zero (normal to coast). The bed material diameter is set to 0.4 mm for all cases. As an example the dune erosion at Nauset Beach is computed by using **Equation (5.1)**:

$A_{d,t=5}$ =170 $(0.225/0.4)^{1.3}$ $(2.5/5)^{1.3}$ $(3.6/7.6)^{0.5}$ $(1)^{0.3}$ $(9.5/12)^{0.5}$ =20 m^3/m after 5 hours. **Equation (5.4)** yields the dune erosion volume after 12 hours: $A_{d,t=12}$ =20 $(12/5)^{0.2}$ = 24 m^3/m. The measured value is 27 m^3/m.

The predicted dune erosion is within the variation range for 6 cases; systematically too large for 2 cases and systematically too small for 2 cases.

6 Summary, conclusions and recommendations

This report present results of scaling laws, experimental and mathematical modelling of beach and dune erosion under storm events. The mathematical model results have been used to develop a simple dune erosion rule, specifying dune erosion volumes and dune recession values.

6.1 Scaling laws and dune erosion experiments

Correct modelling of the wave dynamics, wave breaking, wave runup and the undertow basically requires the application of a non-distorted model ($n_l=n_h=1$; n_l=length scale and n_h=depth scale). Correct modelling of the mobility parameter and the suspension parameter in a non-distorted model requires for a sandy bed: $n_{d50}=n_h$ (mobility) and $n_{d50}=(n_h)^{0.5}$ (suspension) with n_{d50}=sediment diameter scale. Correct modelling of the suspended transport and morphology in a non-distorted model requires: $n_{d50}=(n_h)^{0.56}$.

According to these scaling laws, the sand diameter in a small-scale, non-distorted laboratory model should be much smaller (at leaast factor 5) than in the prototype. Assuming protype sand of about 200 μm, the model sand should be about 40 μm, which is physically problematic because cohesive forces between the particles may easily be introduced in the case of very fine sediments. Also in a large-scale flume (Deltaflume) the model sand needs to be finer than (factor 2) than the prototype sand using a non-distorted model. Larger sand diameters can be used when a non-distorted model scale is used.

Another problem of scale models is that most natural cross-shore profiles cannot be fit into a laboratory model when the length scale is the same as the vertical depth scale (non-distorted model). To overcome this, distorted models can be used. However, the distortion scale should be as small as possible ($n_l/n_h \leq 2$) to prevent the generation of scale effects. Using a distorted scale, the wave breaking and wave runup processes are overestimated, which results in overestimated erosion. This can be corrected for by using model sand with a larger diameter (d_{50}). Using relatively coarse sand based on the scaling laws, the scale effects can be reduced.

Re-analysis of the experimental results on dune erosion in flumes (work of Vellinga, 1986 and others) show that the scaling laws of Vellinga are broadly confirmed. These experiments are related to dune erosion of a schematized cross-shore profile (Reference Case) representative for the Ducth coast by a well-defined storm with duration of 5 hours (constant offshore wave height of 7.6 m). Based on the scaling laws of Vellinga (Dune Erosion Guidelines 1986), the dune erosion volume above storm surge level (+5 m) is approximately 300 m^3/m after 5 hours. The results of this study (focussing on the experimental results of the Scheldegoot and the Deltaflume) show that the dune erosion for the Reference Case is about 250 m^3/m (15% smaller).

Laboratory simulation results of the dune erosion caused by the February 1953 storm (including the time-varying storm surge level) show that the dune erosion volume for the (distorted) laboratory test is about 30% larger than the mean (observed) value for

field conditions. This result may indicate that the scaling laws based on (distorted) 2D laboratory tests produce values which are somewhat too large for 3D field conditions. Given the lack of data for extreme storm conditions, a firm conclusion on this cannot yet be given.

6.2 Mathematical modelling

Dune erosion caused by wave impact has been modelled by a cross-shore profile model (CROSMOR-model), which is based on a 'wave by wave' modelling approach solving the wave energy equation for each individual wave. The individual waves shoal until an empirical criterion for breaking is satisfied. Wave height decay after breaking is modelled by using an energy dissipation method. Wave-induced set-up and set-down and breaking-associated longshore currents are also modelled. The model has been applied to the recent Deltaflume experiments on dune erosion. The three main processes affecting dune erosion have been taken into account: the generation of low-frequency effects, the production of extra turbulence due to wave breaking and wave collision and the sliding of the dune face due to wave impact. The inclusion of low-frequency effects only marginally affects the dune erosion. The two most influencial model parameters are the suspension enhancement factor (sef) which represents the effect of extra turbulence in the dune erosion zone and the wave breaking coefficient, which determines the maximum wave height. The suspension enhancement factor (sef) is required to model the increase of the sand transport capacity in the shallow surf zone in front of the dune face, which is supposed to be primarily caused by large-scale turbulence generation due to wave collision effects. The Deltaflume test results can be reasonably well simulated by using sef=2.5 (sef=1 means no effect). The sef-parameter is assumed to be constant in time, but this assumption basically is not correct. The sef-parameter should decrease in time as the dune erosion process will gradually diminish due to the development of a new coastal profile representative for storm conditions. The gradual decay of the sef-parameter cannot be represented by the simplistic schematization used herein. This may be the cause for the overestimation of the erosion below the storm surge level. Basically, the sef-parameter should be related to the wave breaking and wave collision processes (future research).

The wave breaking coefficient (γ) varies between 0.4 and 0.8 depending on the wave steepness and local bed steepness. The dune erosion increases considerably when a constant wave breaking coefficient of 0.6 is used.

The calibrated model (based on Deltaflume results) can very well simulate the observed dune erosion above the storm surge level during storm events in small-scale, large-scale and in protoype (1975 Eloise storm in USA and 1953 storm in The Netherlands) using the same model settings. The dune erosion above storm surge level after 5 hours generally is slightly over-estimated. The erosion below the storm surge level is considerably over-estimated by the model.

Based on the results of a detailed sensitivity study, the two most influential parameters are found to be the storm surge level (above mean sea level) and the bed material diameter. Dune erosion increases with increasing storm surge level (SSL) and with decreasing bed material diameter (d_{50}). The wave period also has a marked influence. Dune erosion increases with increasing wave period. The wave spectrum has no significant effect on dune erosion.

The relative changes of the erosion parameters (erosion area above SWL) caused by variation of physical parameters such as wave period, wave spectrum and bed material size are of the same order as those caused by variation of basic model parameters (wave breaking coefficient, roller model, swash zone parameters).

Application of the **CROSMOR** mathematical model to the prototype Reference Case as defined by **Vellinga (1986)** yields a dune erosion volume of about **170 m^3/m**, which is considerably smaller than the value of about **300 m^3/m** based on the Dune Erosion Guidelines (**DUROS**-model) of **Vellinga (1986)**. The **DUROST**A-model yields a value of about 170 to 200 m^3/m for the prototype Reference Case (**Steetzel (1992, 1993)**.

The discrepancy between the DUROS-model and the more sophisticated mathematical models (CROSMOR and DUROSTA) is caused by:

- upscaling errors (using available scaling laws) of laboratory test results to prototype conditions (DUROS-model); based on the present analysis results (this study) the upscaled prototype dune erosion volume for the Dutch Reference Case is about 250 m^3/m rather than the 300 m^3/m of the DUROS-model approach;
- incorrect (too large) offshore wave height in the laboratory tests resulting in over-estimation of the dune erosion volume (DUROS-model is based on scaled laboratory test results);
- porosity of dune front material is much larger than the porosity of the deposited material, which is not properly represented by the mathematical models;
- initial dune erosion is under-estimated by the mathematical models;
- dune erosion in 3D field conditions may be systematically smaller than that under 2D flume conditions.

One of the most uncertain scaling relationships is the morphological time scale (n_{Tm}). For example, the experiments in the Deltaflume have a depth scale of about 6. Hence the time scale is about 2.7, which means that the erosion due to a storm of 5 hours in prototype (Reference Case) is comparable to the erosion in the Deltaflume after about 2 hours. To reduce the over-estimation effect, the exponent of 0.56 should be increased significantly to about 0.9 yielding a time scale of about 5.

As regards scaling errors, the mathematical models are more reliable. These models have been verified using field data. For example, the **CROSMOR-**model has been used to simulate the 1975 hurricane Eloise in the USA and the 1953 storm in The Netherlands. In both cases the model over-estimates the observed erosion. Hence, the model seems to produce conservative rather than optimistic results for field conditions.

Additional research is required to evaluate whether the DUROS-model of **Vellinga (1986)** based on the two-dimensional Deltaflume experiments significantly over-estimates the dune erosion along the Dutch coast or not.

A sensitivity study for the Reference Case shows that the most influential parameters are the storm surge level and the sand diameter. The wave period and the offshore wave incidence angle have a smaller effect. Dune erosion increases slightly with

increasing wave period and increasing wave angle (oblique waves). Tidal velocities have almost no influence on dune erosion because the tidal velocities in the shallow surf zone remain very small due to frictional effects. For the same reasons a nearshore tidal channel has almost no effect on the computed dune erosion.

The presence of an offshore breakwater can reduce the dune erosion significantly if the crest of the breakwater is situated at +1 m or higher (emerged breakwater). A beach fill has a similar effect. A horizontal terrace close to the beach (remains of a rip channel) may reduce the dune erosion.

6.3 New dune erosion rule

The mathematical model results have been used to develop a new dune erosion rule (DUNERULE-model). This dune erosion rule estimates the dune erosion with respect to a base Reference Case, which represents a storm of 5 hours duration with a constant wave height of 7.6 m (period of 12 s; normal to coast), bed material diameter of 0.225 mm and storm surge level of +5 m (above mean sea level). The computed dune erosion (above SSL) of the base Reference Case is 170 m^3/m (much lower than the erosion volume of 300 m^3/m based on Deltaflume experiments). The most influential parameters are the storm surge level (SSL) and bed material diameter (d_{50}). Dune erosion decreases for smaller storm surge levels, smaller wave heights, smaller wave periods, shorter storm duration and coarser sand. The new dune erosion rule is most valid for dune erosion under major storms, but also yields realistic results for minor storm events based on a comparison with measured data from USA-beaches.

7 References

Bijker, E.W., Kalkwijk, J.P.Th. and Pieters, T., 1974. *Mass transport in gravity waves on a sloping bottom. Proc. 14th ICCE, p. 447-465*

Birkemeier, W.A., Savage, R.J., Leffler, M.W., 1998. *A collection of storm erosion field data. Miscellaneous Paper CERC-88-9, Coastal Engineering Research Center, U.S. Army Engineer Waterways Experiment Station, Vicksburg, MS, USA*

Dally, W.R. and Osiecki, D.A., 1994. *The role of rollers in surf zone currents. Proc. 24th ICCE, Kobe, Japan*

Davies, A.G. and Villaret, C., 1997. *Oscillatory flow over rippled beds. In: J.N. Hunt (ed.), Gravity waves in water of finite depth: Chapter 6, p. 215-254. Advances in fluid mechanics, Computational Mechanics Publications*

Davies, A.G. and Villaret, C., 1998. *Wave-induced currents above rippled beds, p. 187-199. In: Physics of estuaries and coastal seas, edited by J. Dronkers and M. Scheffers, Balkema, Brookfield*

Davies, A.G. and Villaret, C., 1999. *Eulerian drift induced by progressive waves above rippled and very rough bed, p. 1465-1488. Journal of Geophysical Research, Vol. 104, No. C1*

Dean, R.G., 1973. *Heuristic models of sand transport in the surf zone. Conf. on Eng. Dynamics in coastal zone, Sydney, Australia*

Dean, R.G., 1985. *Physical modelling of littoral processes. In: Physical modelling in coastal engineering edited by Dalrymple. Balkema, Rotterdam*

Delft Hydraulics, 2004. *Model study of dune erosion: experimental results of small-scale pilot tests (in Dutch), Report H4265. Delft, The Netherlands*

Delft Hydraulics, 2006a. *Dune erosion, Product 2: large-scale model tests and dune erosion prediction method. H4357, Delft, The Netherlands*

Delft Hydraulics, 2006b. *Dune erosion, measurement report of large-scale model tests. H4357, Delft, The Netherlands*

Delft Hydraulics, 2007. *Technical Report Dune Erosion (in Dutch). Report H4357, Delft Hydraulics, Delft, The Netherlands*

Dette, H.H. and Uliczska, K., 1987. *Prototype and model evaluation of beach profile. Symposium on scale effects in modelling sediment transport, IAHR, p. 35-48*

Dette, H.H. and Uliczska, K., 1987. *Prototype investigation on the time-dependent dune recession and beach erosion. Coastal sediments, New Orleans, USA, p. 1430-1444*

Grasmeijer, B.T., 2002. *Process-based cross-shore modelling of barred beaches. Doctoral Thesis. Department of Physical Geography, University of Utrecht, Utrecht, The Netherlands*

Grasmeijer, B.T. and Van Rijn, L.C., 1998. *Breaker bar formation and migration. Proc.26th ICCE., Copenhagen, Denmark*

Houwman, K.T. and Ruessink, B.G., 1996. *Sediment transport in the vicinity of the shoreface nourishment of Terschelling. Dep. of Physical Geography. University of Utrecht, The Netherlands*

Hughes, S.A., 1983. *Movable-bed modeling law for coastal dune erosion. Journal of Waterway, Port, Coastal and Ocean Engineering, Vol. 109, No. 2, p. 164-179*

Hughes, S.A., 1993. *Physical models and laboratory techniques in coastal engineering. World ScientificPublications*

Hughes, S.A. and Chiu, T.Y., 1981. *Beach and dune rosion during severe storms. Coastal and Oceanographic Engineering Department, University of Florida, Gainsville, Florida, UFL/COEL-TR/043*

Hughes, S.A. and Fowler, J.E., 1990. *Validation of movable-bed modeling guidance. Proc. 22nd ICCE, Delft, The Netherlands, p. 2457-2470*

Isobe, M. and Horikawa, K., 1982. *Study on water particle velocities of shoaling and breaking waves. Coastal Engineering in Japan, Vol. 25.*

Ito, M. and Tsuchiya, Y, 1984. *Scale-model relationship of beach profile. Proc. 19th ICCE, Houston, USA, Vol. 2, p. 1386-1402*

Ito, M. and Tsuchiya, Y, 1986. *Time scale for modeling beach change. Proc. 20th ICCE, Taipei, Taiwan, Vol. 2, p. 1196-1200*

Ito, M. and Tsuchiya, Y, 1988. *Reproduction model of beach change by storm waves. Proc. 21st ICCE, Malaga, Spain, Vol. 2, p. 1544-1557*

Ito, M. , Murakami, H. and Ito, T., 1995. *Reproducibility of beach profiles and sand ripples by huge waves. Coastal Dynamics, p. 698-708*

Kamphuis, J.W., 1972. *Scale selection for mobile bed wave models. Proc. 13th ICCE, Vancouver, Canada, Vol. 2, p. 1173-1195*

Kamphuis, J.W., 1982. *Coastal mobile bed modelling from a 1982 perspective. Research Report No. 76, Queen's University, Kingsto, Ontario, Canada*

Kraus, N.C., et al., 1991. *Evaluation of beach erosion and accretion predictors. Coastal Sediments, Seattle, USA, p 572-587*

Kriebel, D.L. et al., 1991. *Engineering methods fore predicting beach profile response. Coastal Sediments, Seattle, USA*

Kroon, A., 1994. *Sediment transport and morphodynamics of the beach and nearshore zone near Egmond, The Netherlands. Doc. Thesis, Dep. of Physical Geography, Univ. of Utrecht, The Netherlands*

Larson, M. and Kraus, N.C., 1989. *S-beach: numerical model simulating storm-induced beach change. Report 1: empirical foundation and model development. Technical Report CERC-89-9. US Army Engineer Waterways Experiment Station, Vicksburg, USA*

Larson, M., Erikson, L. and Hanson, H., 2004. *An analytical model to predict dune erosion due to wave impact. Coastal Engineering, Vol. 51, p. 675-696*

Le Méhauté, B., 1970. *A comparison of fluvial and coastal similitude. Proc. 12th ICCE, Washington, USA, p. 1077-1096*

Longuet-Higgins, M.S., 1953. *Mass transport in water waves. Royal Soc. Phil. Trans., Vol. 245A, 903, p. 535-581*

Nelson, R.C., 1985. *Wave heights in depth limited conditions. Civ. Eng. Trans., Inst. Eng., Australia, CE27 (2); p. 210-215*

Nelson, R.C., 1987. *Design wave heights on very mild slopes. Civ. Eng. Trans., Inst. Eng., Australia, CE29 (3); p. 157-161*

Nelson, R.C., 1994. *Depth limited design wave heights in very flat regions. Coastal Engineering 23 (1,2), p. 43-59.*

Nelson, R.C. and Gonsalves, J., 1992. *Surf zone transformation of wave height to water depth ratios. Coastal Engineering, 17, p. 49-70*

Noda, E.K., 1972. *Equilibrium beach profile scale-model relationship. Journal of Waterways, Harbors and Coastal Division, ASCE, Vol. WW4, p. 511-528*

Ranieri, G., 2007. *The surf zone distortion of beach profiles in small-scale coastal models. Journal of Hydraulics Research, Vol. 45, No. 2, p. 261-269*

Steetzel, H., 1992. *Comparison DUROS and DUROSTA (in Dutch), Report H1201, Part II, Delft Hydraulics, Delft, The Netherlands*

Steetzel, H., 1993. *Cross-shore transport during storm surges. Doctoral Thesis, Delft University of Technology, Delft, The Netherlands*

Stockdon, H.F., Holman, R.A., Howd, P.A. and Sallenger, A.H., 2006. *Empirical parameterization of setup, swash and runup. Coastal Engineering, Vol. 53, p. 73-588*

Svendsen, I.A., 1984. *Mass flux and undertow in the surf zone. Coastal Engineering, Vol. 8, p. 347-365*

Van Gent, M.R.A., 2001. *Wave runup on dikes with shallow foreshores. Journal of Waterways, Port, Coastal and Ocean Engineering, Vol. 127, No. 5, p. 254-262*

Van Rijn, L.C., 1993, 2006. *Principles of sediment transport in rivers, estuaries and coastal seas, including update of 2006. Aqua Publications, Amsterdam, The Netherlands (www.aquapublications.nl)*

Van Rijn, L.C., 1997. *Cross-shore sand transport and bed composition. Coastal Dynamics, Plymouth, England, p. 88-98*

Van Rijn, L.C., 2006. *Principles of sedimentation and erosion engineering in rivers, estuaries and coastal seas. Aqua Publications, The Netherlands (www.aquapublications.nl)*

Van Rijn, L.C., 2007a. *Unified view of sediment transport by currents and waves, I: Initiation of motion, bed roughness and bed-load transport. Journal of Hydraulic Engineering, ASCE, Vol. 133, No. 6, p. 649-667*

Van Rijn, L.C., 2007b. *Unified view of sediment transport by currents and waves, II: Suspended transport. Journal of Hydraulic Engineering, ASCE, Vol. 133, No. 6, p. 668-689*

Van Rijn, L.C., 2007c. *Unified view of sediment transport by currents and waves, III: Graded beds. Journal of Hydraulic Engineering, ASCE, Vol. 133, No. 7, p. 761-775*

Van Rijn, L.C., 2007d. *Unified view of sediment transport by currents and waves, IV: Application of morphodynamic model. Journal of Hydraulic Engineering, ASCE, Vol. 133, No. 7, p. 776-793*

Van Rijn, L.C. and Wijnberg, K.M., 1994. *One-dimensional modelling of individual waves and wave-induced longshore currents in the surf zone. Report R 94-09, Department of Physical Geography, University of Utrecht.*

Van Rijn, L.C. and Wijnberg, K.M., 1996. *One-dimensional modelling of individual waves and wave-induced longshore currents in the surf zone. Coastal Engineering, Vol. 28, p. 121-145*

Van Rijn, L.C., Walstra, D.J.R., Grasmeijer, B., Sutherland, J., Pan, S. and Sierra, J.P., 2003. *The predictability of cross-shore bed evolution of sandy beaches at the time scale of storms and seasons using process-based profile models, p. 295-327. Coastal Engineering, 47*

Van Thiel de Vries, J.S.M., Van de Graaff, J., Raubenheimer, B., Reniers, A.J.H.M. and Stive, M.J.F., 2006. *Modeling inner surf hydrodynamics during storm surges. Proc. 30th ICCE, San Diego, USA, p. 896-908*

Van Thiel de Vries, J.S.M., Clarke, L.B., Aarninkhof, S.G.J., Coeveld, M., Holman, R.A., Palmsten, M.L., Reniers, A.J.H.M., Stive, M.J.F. and Uijttewaal, W.S.J., 2007. *Interaction of dune face and swash zone. Coastal sediments, New Orleans, USA*

Vellinga, P., 1986. *Beach and dune erosion during storm surges. Doctoral Thesis, Delft University of Technology, Delft, The Netherlands (Publication 372, Delft Hydraulics)*

Wang, H., Toue, T. and Dette, H., 1990. *Movable bed modeling criteria for beach profile response. Proc. 22nd ICCE, Delft, The Netherlands, Vol. 3, p. 2566-2579*

Wolf, F.C.,J., 1997. *Hydrodynamics, sediment transport and daily morphological development of a bar-beach system. Doc. Thesis, Dep. of Physical Geography, Univ. of Utrecht, The Netherlands*